THE DESIGN OF NEW CATALYSTS FOR THE PARTIAL OXIDATION OF METHANE TO METHANOL

THESIS SUBMITTED IN ACCORDANCE WITH THE REQUIREMENTS OF THE UNIVERSITY OF LIVERPOOL FOR THE DEGREE OF DOCTOR IN PHILOSOPHY BY

STUART HAMILTON TAYLOR

NOVEMBER 1994

ABSTRACT

The direct partial oxidation of CH_4 to CH_3OH would offer considerable economic advantages over the current two stage process. It would also facilitate the utilisation of natural gas reserves in remote locations.

To date, the catalytic partial oxidation of CH_4 to CH_3OH has been extensively studied, however, it has proved to be an extremely demanding reaction which has met with little success.

This study has adopted a design approach for the identification of new catalysts by considering the efficacy of single oxides for CH_4 activation, CH_3OH oxidation and O_2 isotope exchange activity.

On the basis of CH_3OH stability Sb_2O_3 was the best oxide, showing only 3% CH_3OH conversion at 500°C. The majority of oxides totally combusted CH_3OH below 400°C. MoO_3, Nb_2O_5, Ta_2O_5 and WO_3 showed high selectivity to HCHO and $(CH_3)_2O$ with low levels of CO_x throughout the range of conversion. These oxides were not considered unsuitable from the perspective of CH_3OH stability as the products HCHO and $(CH_3)_2O$ are not considered undesirable by products from a CH_4 partial oxidation process. A weak but significant correlation was observed between the combustion activity of the oxides and the oxygen exchange rate.

Using CH_4/D_2 exchange as an indication of CH_4 activation it has been shown that Ga_2O_3 was a particularly good catalyst, followed by ZnO and Cr_2O_3. A relationship between exchange activity and oxide basicity was established for the rare earth sesquioxides, MgO and CaO. This relationship indicated that CH_4 activation took place by H^+ abstraction to form a surface CH_3^- species.

From these results and literature studies of oxygen isotope exchange, dual component oxides have been formulated as catalysts for CH_4 partial oxidation. The best catalysts was Ga_2O_3/MoO_3, prepared by a physical mixing process. This catalyst showed an increased yield of CH_3OH over the homogeneous gas phase oxidation of CH_4 in a quartz chips packed reactor. This increased yield has been attributed to the development of a cooperative effect between the two component oxides. Comparison of the catalytic data with the homogeneous reaction in the empty reactor tube showed that the presence of a catalyst had a detrimental effect on the CH_3OH yield.

ACKNOWLEDGMENTS

I would like to thank the following people for their help, advice, friendship and support throughout the duration of this project;

Professor Richard Joyner and Professor Graham Hutchings,

Dr Justin Hargreaves,

fellow members of the Leverhulme Centre, both past and present,

my parents (Brian and Jean Taylor), sister (Gillian) and Vicki,

and finally the Gas Research Institute Chicago for financial support.

CONTENTS

List of abbreviations

Å, Angstrom

BET, Brunauer Emmett and Teller

ESR, electron spin resonance

GC-MS, gas chromatograph-mass spectrometer

GHSV, gas hourly space velocity

h, hour

MS, mass spectrometer

min, minutes

TCD, thermal conductivity detector

TPD, temperature programmed desorption

STY, space time yield

UHV, ultra high vacuum

wt, weight

XPS, X-ray photoelectron spectroscopy

XRD, X-ray diffraction

CHAPTER 1

INTRODUCTION

1.1. GENERAL INTRODUCTION

In recent years there has been substantial interest into the direct partial oxidation of CH_4 to produce CH_3OH and HCHO. These oxidation reactions with O_2 are represented in equations 1.1.1. and 1.1.2.

$$CH_4 + 0.5O_2 \text{ ----> } CH_3OH \qquad (1.1.1.)$$

$$CH_4 + O_2 \text{ ----> } HCHO + H_2O \qquad (1.1.2.)$$

This conversion, although appearing to be a relatively simple one, has proved to be an extremely challenging problem, receiving alot of research attention [1-7].

The driving force behind this work has been the need to discover new production routes for important chemical feedstocks. In the current economic climate crude oil is the preferred feedstock for the petrochemical industry. However, world resources of crude oil are finite and a decline in future production rates can be envisaged. On the contrary, world reserves of natural gas are large, with new discoveries being made on a regular basis. It is therefore not surprising that natural gas, which is predominantly CH_4, is viewed by many as the obvious crude oil replacement for the manufacture of chemicals.

The impetus for direct CH_4 partial oxidation to CH_3OH and HCHO is two fold, firstly to develop a more efficient and cost effective route over the existing industrial processes. The second factor is related to the locations of many large gas producing fields. It is often the case that these fields are situated in remote and inhospitable areas. The cost of transportation via pipeline are high for gases such as CH_4 and thus uneconomical. If a simple process to produce C_1 oxygenated products was feasible, CH_4 could be converted to liquid products at the site of extraction. The subsequent transport via pipelines of such a liquid product is relatively inexpensive and uncomplicated. The transport costs for liquids usually only

contribute to approximately 10% of the final product costs [5]. Table 1.1.1. shows the transport costs via pipeline.

Table 1.1.1. Pipeline transport costs over 1000 and 10000 km distances for several different products [5].

product	1000 km $ t^{-1}	10000 km $ t^{-1}
crude oil	1.2	12
methanol	2	12
liquid natural gas	8	70
natural gas		
land	12	120
submarine	20	200

1.2. CURRENT AND POTENTIAL USES FOR METHANOL.

CH_3OH has many important uses in the chemical industry, both as a feedstock and an end product. Table 1.2.1. shows the current industrial uses for CH_3OH [7].

Table 1.2.1. Current industrial uses of CH_3OH [7].

formaldehyde	31%
acetic acid	12%
solvents	11%
chlorinated hydrocarbons	9%
methyl esters	8%
amines	4%
miscellaneous	25%

The largest use by far is for the production of HCHO, used principally by the plastics industry to produce cross linking agents, phenol formaldehyde and urea formaldehyde resins. As a consequence of this transformation a direct route for the production of HCHO from CH_4 is also viewed as having substantial commercial importance, particularly considering the scale of HCHO manufacture. Further details of the current processes for HCHO production are given in section 1.3.

Another important use for CH_3OH is the manufacture of acetic acid, by a carbonylation process (1.2.1.).

$$CH_3OH + CO \text{ ----> } CH_3COOH \qquad (1.2.1.)$$

The process is a homogeneous one, catalysed by a rhodium iodide catalyst [8].

One use of CH_3OH which is becoming increasingly more important is the production of methyl tert-butyl ether (MTBE). This compound is used as an octane improving agent when added to gasoline, and has found widespread use as a replacement for lead additives. MTBE is produced in solution by using an acidic ion exchange resin.

Looking to the future it seems that CH_3OH may become an important chemical for the production of synthetic fuels. Currently gasoline transport fuels are derived from crude oil by catalytic cracking, but as crude oil supplies decline new sources of transport fuels will be required. CH_3OH may be used as a fuel in its own right, but it has certain problems associated, namely low energy density, water accumulation and a relatively high volatility. However, CH_3OH may be readily converted to gasoline range hydrocarbons by the methanol-to-gasoline (MTG) process developed by Mobil. The preliminary step is the conversion to dimethyl ether over an alumina catalyst, this product is then passed over an H-ZSM5 catalyst, which typically produces C_5-C_8 hydrocarbons [9].

Therefore, it is evident that at the present time CH_3OH is a feedstock of considerable importance, and it seems it may become even more so, as energy needs and their derived sources evolve.

1.3. CURRENT TECHNOLOGY FOR THE PRODUCTION OF METHANOL AND FORMALDEHYDE

The conventional route for the production of CH_3OH involves a two stage process via a synthesis gas intermediate. The primary process is steam reforming, usually CH_4 is used as the carbon feedstock, although naptha fractions are also suitable [10].

CH_4 is reacted with steam, the reaction is described by the simple reversible process (1.3.1.).

$$CH_4 + H_2O \rightleftharpoons CO + 3H_2 \qquad (1.3.1.)$$

This reaction is highly endothermic, with a standard reaction enthalpy of 206 kJ mol^{-1}, and the forward reaction is favoured by high temperatures and low pressures. The mixture of CO and H_2 formed by this process is called synthesis gas.

The commercial steam reforming process operates using a supported Ni catalyst. This catalyst is usually prepared by impregnation of an α-Al_2O_3, MgO or a mixture of these supports, by a Ni salt solution. The supported NiO catalyst is usually reduced in-situ as the reformer is brought on line. Typical operating conditions are 800°C and 15-20 bar, with a H_2O/CH_4 stoichiometric ratio of 3.0-3.5. The excess steam is added to suppress carbon formation on the catalyst, and promote the reforming reaction.

The second stage for CH_3OH production is carried out by passing synthesis gas over a $Cu/ZnO/Al_2O_3$ catalyst [11]. This is an endothermic process, operating at temperatures around 250°C, high pressures in the range 50-100 bar are also required to obtain acceptable equilibrium yields. In practice CO_2 is also added to the feed which produces advantageous effects, $H_2/CO/CO_2$ reaction ratios are usually 80-86/8-10/6-10. The $Cu/ZnO/Al_2O_3$ catalyst produces CH_3OH highly selectively, generally greater than 99%. The reactor exit stream usually contains between 4-7 vol.% of CH_3OH, which is removed and the gas stream recycled.

It has previously been mentioned in section 1.2. that one of the main uses of CH_3OH is for the production of HCHO. Two commercial processes are currently operated to produce HCHO [12]. The first, a CH_3OH rich process, uses a CH_3OH/air ratio of 1/1 at a slightly elevated pressure. The reactants are passed through a silver catalyst gauze maintained at 600°C, typical contact times are 0.01 s. The second process, a CH_3OH lean system, operates at around 6-9 mol.% CH_3OH in air, with temperatures in the region of 280°C. The catalyst used in this system is an unsupported ferric molybdate, with the structure $Fe_2(MoO_4)_3$.

The conversion to HCHO takes place via dehydrogenation (1.3.2.),

$$CH_3OH \text{ ----> } HCHO + H_2 \qquad (1.3.2.)$$

or by partial oxidation (1.3.3.).

$CH_3OH + 0.5O_2 \text{ ----> } HCHO + H_2O$ (1.3.3.)

The standard enthalpies of reaction for equations (1.3.2.) and (1.3.3.) were 84 and -158 kJ mol^{-1} respectively. The Ag catalysed process operates by both these routes, while the process catalysed by $Fe_2(MoO_4)_3$ operates by the latter only, via a redox mechanism. Both processes offer advantages and disadvantages over the other. The Ag process uses a notably simpler and cheaper reactor design, while the alternative process usually produces higher HCHO yields with lower quantities of CO_2. The final HCHO product from both processes is supplied as an aqueous solution.

1.4. ECONOMICS OF DIRECT METHANE PARTIAL OXIDATION VERSES CONVENTIONAL ROUTES

Early studies by Edwards and Foster in 1985 [13] compared the costs for CH_3OH production from a conventional route with those from a conceptual plant, producing CH_3OH in a one stage process. The operating conditions assumed were 100 bar, 400°C, and O_2 oxidant, with a CH_4 conversion of 10% per pass. At 100% CH_3OH selectivity the production cost was \$172 t^{-1} from the conceptual plant and \$248 t^{-1} from the conventional route. The cost of CH_3OH from the direct route was found to rise in a linear manner as the selectivity fell. It was therefore concluded that at 77% selectivity the cost for both processes was equal. A more comprehensive study has been undertaken by Geerts et. al. [14], based on results obtained by Gesser et. al. [15] and Dowden and Walker [16]. Estimates indicated that capital investment costs allied with building a plant for the direct partial oxidation process were 10% lower than those for the two stage process. The main plant costs associated with the direct route were not the reactor but the distillation units for product separation, and the larger heat exchange capacity required due to limited conversion and large recycling needs. Profitability studies, based on January 1988 prices, showed the conventional plant running at a loss of \$16.9 million per year. This somewhat surprising figure was confirmed to be accurate by Methanor, a large Dutch CH_3OH manufacturer. The profitability based on the results from Gesser et. al. [15], with 80% selectivity and 20% conversion, showed a substantially greater loss of \$51.9 million per year.

Figures calculated from the Dowden and Walker data [16], 60% selectivity at 20% conversion, showed an even greater loss of $81.9 million per year. Taking into accounts raw material costs alone Geerts et. al. concluded that the direct process must operate at CH_3OH selectivity in excess 75% if it was to be profitable. Since this study was published it has been established that the results reported by Gesser et. al. [15] were inaccurate, and the actual CH_3OH selectivity was lower.

Although both of these studies were completed several years ago and the figures may now not be considered accurate, they may still serve as a guide. The main point which has been highlighted in both of these studies is the that for a direct partial oxidation process to become a viable replacement for the conventional route high CH_3OH selectivity in excess of 70% must be achieved.

In certain geographical locations, such as Siberia and parts of the Middle East, natural gas supplies are cheap and plentiful. Under these circumstances it may become economically viable to operate such a direct oxidation process [5].

1.5. THERMODYNAMIC AND KINETIC CONSIDERATIONS FOR METHANE OXIDATION REACTIONS

The CH_4 molecule is one of the least reactive of all the hydrocarbon species. The C-H bond energy in CH_4 is extremely high, around 435 kJ mol^{-1} [17], thus in many systems harsh conditions such as high temperatures are required to activate the molecule. Consideration of the thermodynamics of the reaction of CH_4 with O_2 shows that the formation of CH_3OH is thermodynamically favourable. Table 1.5.1. shows the relevant thermodynamic parameters for CH_4 partial oxidation reaction.

Table 1.5.1. Thermodynamic parameters for CH_4 oxidation reactions.

reaction	ΔH	ΔG /kJ mol^{-1}	ΔS
$CH_4 + 0.5O_2 \rightarrow CH_3OH$	-127.1	-111.2	-48.6
$CH_4 + O_2 \rightarrow HCHO + H_2O$	-276	-290.8	16.2
$CH_4 + 1.5O_2 \rightarrow CO + 2H_2O$	-519	-543.5	81.3
$CH_4 + 2O_2 \rightarrow CO_2 + 2H_2O$	-802	-800.7	-5.1

It is also clear that the production of HCHO is thermodynamically favoured, but the large negative free energy changes for the formation of carbon oxides are predominant, and ultimately total oxidation products are favoured.

Bearing in mind the thermodynamics of these reactions the production of CH_3OH and HCHO has to be viewed as a kinetic problem and attempts have to be made to try and suppress the further oxidation of these oxygenated products.

1.6. HISTORICAL BACKGROUND TO THE PARTIAL OXIDATION OF METHANE

The partial oxidation of CH_4 to oxygenated products has now been studied over a period of approximately 90 years. One of the earliest publications was a patent in 1906 by Lance and Elworthy [18], who claimed that CH_3OH could be manufactured by oxidising CH_4 with H_2O_2 in the presence of $FeSO_4$ at a temperature of 120°C and elevated pressure. In the 1930's research into this area became more widespread with studies concentrating on CH_4 partial oxidation with O_2 at elevated pressures, in both static [19] and flow systems [20]. Generally the pressures used in these studies were 50-150 bar, with temperatures >300°C. The major difference between the two studies was that HCOOH was formed in the static reactor, a product which was not detected in the flow system. A study by Newitt and Szego [20] reported a CH_3OH yield of 51% of the CH_4 converted, although the magnitude of CH_4 conversion was not clear. Studies were also reported investigating CH_4 oxidation at ambient pressure [21-23], the primary interest of these studies was elucidation of the reaction mechanism, as production of oxygenates was less successful than studies performed at elevated pressure.

A comprehensive study of the partial oxidation of CH_4 in a flow system was reported by Wiezevich and Frolich in 1934 [24]. The optimum pressure for the production of CH_3OH was 132 bar, the flow rate of the reactants did not significantly influence the CH_3OH per pass yield. When CH_4 was used as the feed gas initial activity was observed at 500°C, but when CH_4 was substituted by natural gas this temperature was decreased. Using natural gas and 5.4% O_2 at 132 bar and

390°C, 30% of the condensable product was CH_3OH. The authors also investigated the activity of iron, nickel and aluminium catalysts. The addition of these catalysts to the reactor increased the CH_3OH yield, but no specific results concerning conversion or selectivity are available.

The use of a catalyst to improve the yield of CH_3OH was pursued further by Boomer and co-workers in 1937 [25-27]. These studies were carried out at pressures around 180 bar using natural gas with a $CH_4/C_2H_6/N_2$ composition ratio of 90/3.5/5, O_2 was the oxidant used in varying concentrations between 4.1% and 12.0%. It was shown that copper was an effective catalyst for increasing the yield of CH_3OH. Other salient features of this study showed that the yield of CH_3OH increased as the % O_2 in the feed was decreased, the effects of changing flow rate were more pronounced at low O_2 concentrations. The copper catalyst was readily poisoned by traces of sulphur, which resulted in a reduction of catalytic activity by ca. 50%. Using a CH_4 feed with 5.7% added N_2 required a much higher temperature for reaction, compared to the natural gas feed, agreeing well with the previous findings of Wiezevich and Frolich [24]. The studies by Boomer et. al. also showed that other catalysts, such as steel, silver and glass were also effective for increasing the CH_3OH yield. Under reaction conditions it was concluded that Cu_2O was formed on the copper catalyst, and it was postulated that CH_3OH was formed by the surface mechanism (1.6.1).

$$CH_4 + Cu_2O \text{ ----> } CH_3OH + 2Cu \qquad (1.6.1.)$$

The origin of carbon oxides and HCHO were suggested to have derived from gas phase reactions, the latter via a carbene intermediate.

In the 1940's research effort into the partial oxidation of CH_4 increased and so subsequently did the number of related publications. One interesting report which has been highlighted in a recent review [2] describes an industrial plant developed by Germany in Copsa Mica, Romania, during World War II. The process involved the homogeneous gas phase oxidation of natural gas mixed with O_2 in the ratio 1/3.7, this feed was mixed further with recycle off-gas in a 1/9 ratio. The reactant

mix was heated to 400°C and 0.08 vol.% of HNO_3 added, this was passed through a ceramic lined stainless steel tube maintained between 400 and 600°C. The exit gases were cooled to 200°C and HCHO removed by a water scrubber. Net HCHO yields of 35% were reported, although actual yields based on the total natural gas required for heating the reactor were 10%. Other products from the process were CH_3OH, HCOOH and carbon oxides.

The studies outlined in this section indicate the directions of early work which took place in this area of research. It is not intended to be a comprehensive historical review, indeed a considerable volume of work has been reported by Russian researchers, much of which has not been translated from the original language. These historical studies and many others have not been mentioned here, but some have been reviewed elsewhere [1,2,28].

1.7. DESIGN APPROACHES FOR THE IDENTIFICATION OF METHANE PARTIAL OXIDATION CATALYSTS

Several approaches in the area of CH_4 selective oxidation have attempted to adopt a design approach to identify new and efficient catalysts. Such an approach has been applied by Dowden et. al., through the derivation and application of a virtual mechanism [29]. By thermodynamic analysis of the target reaction and side reactions it was concluded that the functions of a suitable catalyst were dehydrogenation and oxygen insertion. Oxidation reactions all led preferentially to the production of carbon oxides. A hypothetical surface mechanism by which the preferred products were formed was proposed, and this is shown in figure 1.7.1.

It was proposed that the initial interaction of CH_4 with the surface involved dissociation to form methyl and methylene groups. One important step was the suppression of methyl and methylene dehydrogenation to carbon oxidesrelative to their migration mobility. As a consequence the generation of methyl species were favoured over the more tightly bound methylene, which may also have more labile protons facilitating dehydrogenation. These factors directed the authors to choose an oxide catalyst as opposed to a metal. It was suggested that the surface methyl bond

should be weaker than the surface oxygen bond to promote methyl migration onto the oxygen. Suitably weak dehydrogenation functions suggested included d^0, d^1, d^5, d^{10} or d^4 configurations, while the oxygen insertion properties should be those of typical n-type oxides, examples given were TiO_2, V_2O_5, Fe_2O_3, MoO_3 and ZnO. These components should be present in a single crystallographic phase with the different functional sites adjacent to allow rapid migration.

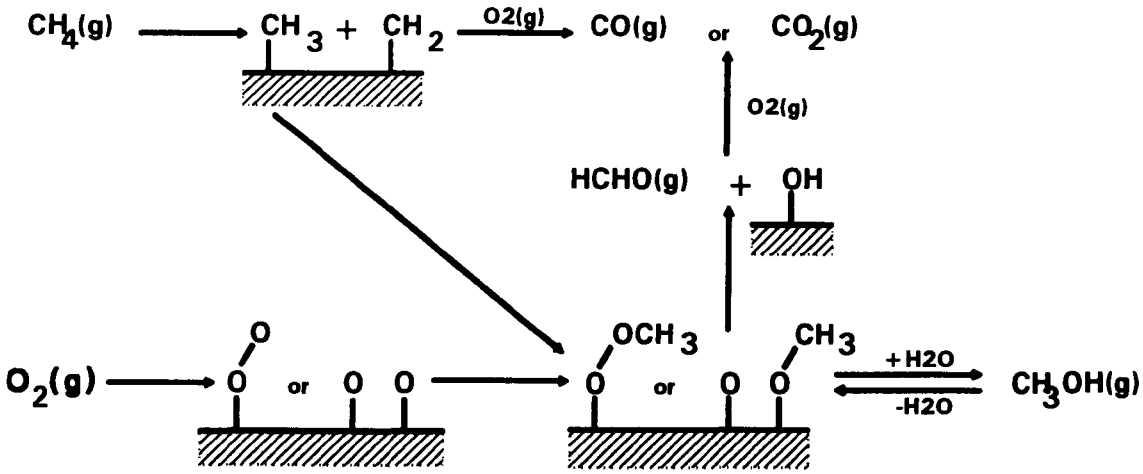

Figure 1.7.1. Virtual mechanism developed by Dowden, Schnell and Walker [29] for the design of CH_4 partial oxidation catalysts.

The rate of HCHO dehydrogenation relative to that of CH_4 was also considered, as sites for CH_4 dehydrogenation would also be active for HCHO, but CH_4 would be the slow step. The dehydrogenation of HCHO was switched to be the slow step by the addition of a hydration function to the catalyst. This function enhanced the formation of surface methylene diol, which from analogy with oxidation in aqueous solution, is relatively slowly attacked by oxidising species accepting one electron per ion. Favourable hydration components were stated to be phosphates and tungstates in conjunction with single electron oxidant transition metal ions. It was also considered that the hydration component would enhance the production of CH_3OH relative to HCHO.

It was concluded that suitable catalysts should be formulated from;

V^{5+}, Fe^{3+}, Cu^{2+} for dehydrogenation,

V^{5+}, Fe^{3+}, Zn^{2+}, Mo^{6+}, Ti^{4+} for oxygen insertion,.

all the above ions were also consistent with a dehydration function in conjunction with phosphates or tungstates.

It must be remembered that the proposed mechanism was purely hypothetical and developed on empirical evidence. No detailed catalytic data has been reported, but preliminary results based on B, Al, Cr, Mn, Fe and Ce phosphates, showed Cr^{3+} and Mn^{3+} to be the most active, Fe^{3+} exhibited intermediate activity and was the most selective but only marginally more so than Al^{3+}.

Another approach which has been developed for the direct synthesis of HCHO from CH_4 has been reported by Otsuka and Hatano [30]. CH_4 partial oxidation with O_2 was investigated over a wide range of metal oxides supported on SiO_2 in the temperature range 600-750°C. It was observed that oxides containing cations of intermediate electronegativity showed the greatest CH_4 conversion. A plot of CH_4 conversion against cation electronegativity showed a volcano type distribution. The selectivity of HCHO increased as the cation electronegativity of the supported metal oxide increased. To rationalise these observations a mechanistic pathway was proposed, figure 1.7.2.

$$CH_4 \xrightarrow[1]{\text{H abstraction}} CH_{4-x} \xrightarrow[2]{\text{O addition}} HCHO \xrightarrow[3]{\text{H abstraction}} CO,\ CO_2$$

Figure 1.7.2. Mechanistic pathway proposed by Otsuka and Hatano [30] for the partial oxidation of CH_4.

It was hypothesised that HCHO selectivity was determined by the relative rates of steps 2 and 3. The oxidative abstraction of H from CH_4 was believed to be dependent on the amount of negative charge on the oxygen, and the most active oxide had the greatest charge. On the other hand when the negative charge on the oxygen approached zero the probability of electrophilic addition of oxygen

increased. The negative charge on the adsorbed oxygen of the oxide changed according to the electronegativity of the cation, i.e. the higher the electronegativity the greater the electrophilicity of the adsorbed oxygen. CH_4 conversion was dependent on the rates of steps 1 and 2. Conversion over the metal oxides with lower electronegativity was determined by the rate of step 2, and for these oxides conversion increased as electronegativity increased. However, increasing electronegativity further, and subsequently increasing oxygen electrophilicity, decreased the ability of an oxide to abstract H from CH_4 and the rate determining step was transferred to step 1. The higher HCHO selectivity of the more electronegative oxides was therefore due to the increased rate of step 2 relative to step 3, because O addition was greater the stronger the electrophilicity of the oxygen. Based on these principles it was concluded that acidic oxides would not be successful for the oxidation of CH_4 because although high HCHO selectivity could be achieved, the process of H abstraction from CH_4 was inefficient. A range of catalysts based on B_2O_3/SiO_2 were prepared and tested. The B_2O_3/SiO_2 system was selected because it showed the highest HCHO selectivity, components added to this mixed oxide were selected on their ability to increase the rate of step 1. BeO was found to be the most effective additive, followed by MgO, these catalyst exhibited HCHO yields of 0.9% and 0.6% respectively. Otsuka and Hatano concluded that B_2O_3 mixed with moderately basic oxides were the most effective for HCHO production, which was formed by an acid-base functionality. Further catalytic results based on this approach are presented in section 1.9.

A different approach has been taken by Amir-Ebrahimi and Rooney [31], who have considered the mode of action of enzymes. The authors highlighted similarities with the process of olefin metathesis, and have developed a catalyst accordingly. Molybdenum was chosen as the central component due to its documented history for enzymic and non enzymic oxidations, and its high activity in many metathesis systems. R_4Sn (where R = Me, Bu or Ph group) activators were chosen for their performance as co-catalysts with transition metal halides. Sn was also known to be a

beneficial catalyst for the metathesis of olefins with functional groups. It was also noted that the Sn/Mo system was capable of introducing an oxygen function, for example the oxidation of propene to the unsaturated product acetone, in contrast to the majority of systems which produced allylic compounds [32].

Silica supported $MoCl_5/R_4Sn$ promoted with PCl_3 showed 80% selectivity to HCHO at 20% conversion, obtained at 700°C, using 1/1 CH_4/air at 1 bar in a flow system. Although it was not explicitly expressed, it appears that Bu_4Sn was used as the co-catalyst, both Me and Ph derivatives had a detrimental effect on HCHO selectivity. The best catalyst showed a distinctive Mo^{5+} ESR spectrum with additional signals which were attributed to F centres.

The $MoCl_5/R_4Sn/PCl_3/SiO_2$ based catalyst has also been investigated by Weng and Wolf [33]. This group were unable to reproduce the results from the earlier work [31]. Under equivalent flow conditions in the temperature range 574-675°C, 8.4% conversion and 34% HCHO selectivity was obtained. On changing the CH_4/O_2 ratio to 9/1, HCHO selectivity was increased to 60% albeit at a lower conversion of 3.4%. Experiments on the Mo/Sn and Mo/P systems showed that the former was more active, while the latter was more selective.

The approach has been extended further by using a Re based system, which was chosen because of its notable metathesis activity. An optimum HCHO yield was observed with a $Re/B/Sn/SiO_2$ catalyst, HCHO selectivities in the range 71-49% at 3-8.9% conversion were obtained. In a further paper Weng and Wolf [34] have demonstrated improved performance over their previous study by using a $MoCl_5/2Bu_4Sn/PCl_3/SiO_2$ catalyst, which gave 64.8% HCHO selectivity at a conversion of 7.4%. The role of phosphorus was postulated to be responsible for increasing the dispersion of the active phase, which was not clear, but speculated to be a tin molybdate type compound.

These studies have demonstrated that the approach appears to be a valid one, capable of producing reasonably high yields. There is generally a lack of agreement on catalytic results between the two research groups. Indeed both stress the critical

importance of the catalyst preparation, emphasising that minor differences produced catalysts with vastly different activity. What is clear however, is the complicated and careful preparation procedures were necessary to create the active catalyst. One explanation for the discrepancies in catalytic activity may be due to analytical difficulties which have been reported by Amir-Ebrahimi and Rooney [31].

Lyons and co-workers [35-37] have also used a design approach and developed a catalyst based on the activation of CH_4 by the biological enzymes Cytochrome P450 and Methane Monooxygenase (MMO). Cytochrome P450 is a heme iron catalyst [38], while MMO is a non-heme iron catalyst which incorporates a novel diiron centre [39]. Both systems effectively oxidise CH_4 to CH_3OH, and are thought to function via by a high oxidation state ferryl species capable of alkane activation.

A conceptual model has been proposed in which the redox potential of the Fe^{2+} centre was modified, to suppress the irreversible conversion to the Fe^{3+}-O-Fe^{3+} μ-oxo complex in favour of the μ-peroxo species, Fe^{3+}-O-O-Fe^{3+}. It has been suggested that via this route the formation of the ferryl species, $O{=}Fe^{5+}$, would be facilitated. Four catalysts have been prepared on these principles, these were iron perhaloporphyrins complexes, Keggin structures with iron in the framework and with proximate iron centres and crystalline iron zeolite materials.

The first three types were only tested for oxidation of C_2-C_4 alkane substrates. However, Fe-sodalite catalysts showed promising activity for the oxidation of CH_4 to CH_3OH. More specifically the catalyst was a sodalite lattice with iron, greater than 10% weight, substituted for Al^{3+} in the framework and at exchangeable sites. The most active catalysts were those which were subjected to high temperature calcination, ca. 550°C, this has been attributed to partial framework collapse, indicated by evidence from XRD and ESR studies. This process drives iron from framework sites into exchangeable positions associated with residual framework iron to create an active centre. CH_3OH selectivity was also improved when Fe-sodalite was exchanged with Fe^{3+} ions. A conceptual mechanistic pathway based on the

development of framework and extra-framework iron interactions has been proposed, this is shown in figure 1.7.3.

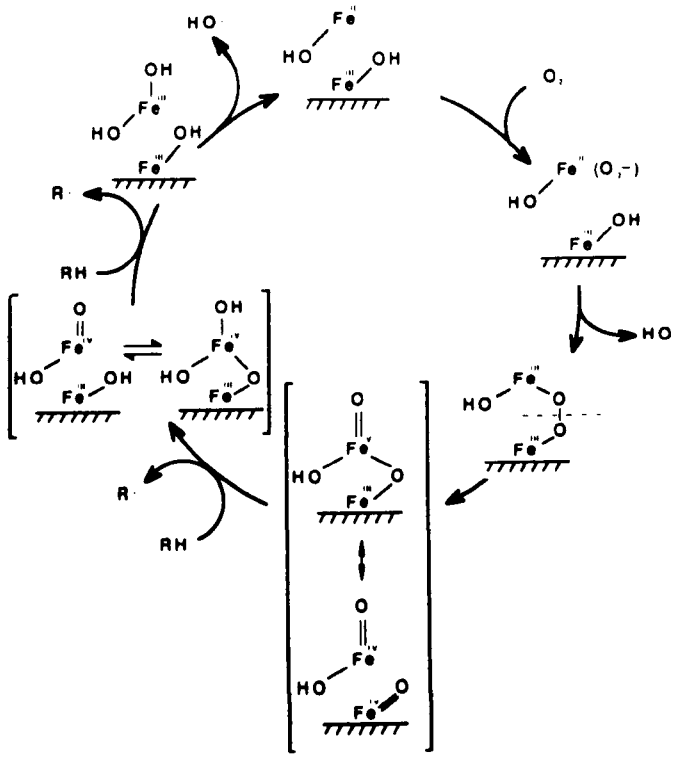

Figure 1.7.3. Conceptual mechanism proposed for CH_4 selective oxidation over Fe-sodalite [36].

We It was postulated that a surface generated ferryl intermediate was responsible for CH_4 activation, leading to the release of $CH_3\cdot$ to the gas phase. Results indicated that 70% CH_3OH selectivity at 5.7% conversion was possible using 3/1 CH_4/air at 53 bar, 416°C with a GHSV = 530 h^{-1}. Fe-sodalite calcined at 300°C, Fe-silicalite, hydroxysilicalite and SiO_2 supported iron oxide all showed poorer performance.

have also carried out a study of the Fe-sodalite system using experimental and theoretical methods [40]. Using similar flow rate conditions, the best catalytic performance was 33% CH_3OH selectivity at 3.1% conversion, obtained at 410°C and 33 bar. This proved significantly better than the empty tube. Mössbauer studies have indicated the presence of Fe^{3+} in the sodalite framework before reaction. Post reaction Fe^{2+} was identified along with small particles , <1 μm, of iron oxide, which on the basis of CH_3OH oxidation studies, was presumed to be highly

effective for CH_3OH oxidation to carbon oxides. Theoretical studies indicated that the framework $Fe^{2+/3+}$ redox couple was the most energetically favourable. Calculations also showed that CH_4 was not able to diffuse into the sodalite framework, limiting catalytic activity to the external crystallite surface.

The high activity for Fe-sodalite demonstrated by Lyons and co-workers may to some extent be a result of the elaborate reactor design used [35]. Details were not clear but the reactor has some type of by-pass facility, which allowed a portion of the reaction feed gas to by-pass the catalyst bed. Results for other catalysts such as iron silicalite and supported iron oxide are very similar to our blank tube and Fe-sodalite data.

1.8. A NEW APPROACH FOR THE DESIGN OF METHANE PARTIAL OXIDATION CATALYSTS

In the present study a new design approach has been applied for the identification of new and effective catalysts. This approach has considered the interactions between reactant and product molecules with catalytically active materials, in order to search for factors which may be indicative of, and lead to the identification of synergy (also referred to as a cooperative effect). In many catalytic systems synergy is an extremely important element, one which may be difficult to interpret although advances have been made [41].

The most promising catalysts to date for CH_4 partial oxidation have been based mainly on oxide systems [1-7], by this precedent the activation of CH_4, O_2 and CH_3OH have been examined on single metal oxides. CH_3OH activation studies have been performed, investigating the stability of this product to oxidation by O_2 (1.8.1).

$$xCH_3OH + yO_2 \text{ ----> } HCHO + CO + CO_2 + \text{etc} \qquad (1.8.1.)$$

Activation studies for CH_4 were carried out by isotopic experiments, as the exchange reaction may be considered the first indicator of catalytic activation. The reaction investigated was the exchange of CH_4 with D_2 (1.8.2.).

$$CH_4 + D_2 \text{ ----> } CH_3D + HD \qquad (1.8.2.)$$

Finally, O_2 activation which has been previously studied by the exchange reactions of gaseous isotopically labelled oxygen with the oxide. Due to the many studies already completed on this subject, and their relevance to this approach it was considered unnecessary to repeat this work. A more detailed summary of oxygen exchange activity is given in Appendix A.

By applying this three tier approach and studying these primary processes it is hoped that two component oxide systems can be developed as catalysts. It can be envisaged that oxides which are effective for activating CH_4 and O_2, but do not catalyse the oxidation of CH_3OH to carbon oxides would be the basis of an effective catalyst. It can also be reasoned that oxides which activate CH_4 and O_2 at similar rates may well be the most promising for the development of synergistic effects when the oxides are combined to produce a bi-component catalyst.

It is recognised that many renowned selective oxidation catalysts are composed of two or more component oxides, one such system is the Bi/Mo oxide catalyst for the oxidation of propene to acrolein [42]. The mechanism for this conversion is recognised to proceed by alkane activation on the Bi component, via hydrogen abstraction to give an allylic intermediate. This intermediate subsequently undergoes oxygen insertion by the Mo component in cooperation with the Bi component. It is by analogy with this type of catalyst that this study aims to develop bi-component catalysts for CH_4 partial oxidation to CH_3OH and HCHO, based on results from the activation studies of reactants and products.

1.9. REVIEW OF CATALYTIC METHANE PARTIAL OXIDATION

Two distinct approaches have been adopted for the direct partial oxidation process, these are the heterogeneous and homogeneous routes. The homogeneous gas phase partial oxidation of CH_4 takes place by a radical mechanism involving a series of rapid reactions. Many studies have investigated this route, and it is not the object of this section to review these studies, as they have been comprehensively dealt with elsewhere [2-5].

With regards to the catalytic process, one of the most widely used components has been molybdenum. The catalysts based on Mo can be categorised into two general groups, these are catalysts which have used bulk MoO_3 as the basis, and those which have used a more highly dispersed molybdenum species on a silica support.

One of the earliest studies based on MoO_3 has been reported in a patent by Dowden and Walker [16], who developed a series of two component oxide catalysts based on the principles developed by the virtual mechanism [29]. Results were reported for MoO_3/ZnO, $(MoO_3)_4/Fe_2O_3$, MoO_3/VO_2 and MoO_3/UO_2 supported on 1/3 Al_2O_3/SiO_2 with a low area of ca. 0.1 m^2g^{-1}, containing ca. 5% active oxide. Experimental conditions were 30 bar with CH_4/O_2 ratio of 97/3 in the temperature range 430-500°C. In order to maintain high selectivity to CH_3OH the reactor effluent was cooled to below 200°C within O.O3 s of leaving the heated catalyst bed, by the injection of liquid water. The most successful catalyst was based on $(MoO_3)_4/Fe_2O_3$ which showed a combined selectivity to CH_3OH and HCHO of 80% at 3.5% CH_4 conversion, yielding 869 $g(kg\ cat)^{-1}h^{-1}$ and 100 $g(kg\ cat)^{-1}h^{-1}$ of CH_3OH and HCHO respectively.

Details of unsupported two component oxides have been reported in a patent by Stroud [43] and assigned to the British Gas Corporation. It was considered that the first component should be one of variable valency. The oxides of Cu, Fe, Co, Ni, Cr, V, Sn or Bi were all considered suitable. The best catalyst was CuO/MoO_3 producing a yield of oxygenated products equal to 540 $g(kg\ cat)^{-1}h^{-1}$, at 19 bar and 485°C with a GHSV of 46,700 h^{-1}. The yield of oxygenates in this case included C_2H_5OH and CH_3CHO, as well as CH_3OH and HCHO, as C_2H_6 was a major constituent (6.1%) of the hydrocarbon feed. The presence of C_2H_6 in the reactor feed was an important factor, one indeed acknowledged by Stroud. Gesser et. al. [4] have reviewed many cases when the use of CH_4/C_2H_6 or natural gas feeds reduced the initial reaction temperature relative to pure CH_4, and enhanced CH_3OH yields. The exact mechanism for this effect was not discussed although the reduction of the reaction temperature may decrease the further oxidation of the oxygenated

products. Studies by Kastanas et. al. [44] over a silicic acid catalyst and quartz glass at 3.5 bar with O_2 have also shown that the addition of small quantities of C_2H_6 to the CH_4 feed enhanced the selectivity towards HCHO, while the selectivity towards CO was suppressed. The addition of C_2H_6 to levels above 9% resulted in increased production of CO and CO_2.

A crystalline MoO_3 catalyst has been used for CH_4 partial oxidation with O_2 by Smith and Ozkan [45]. Two MoO_3 catalysts were prepared, the first denoted MoO_3-R, exposed preferentially the (010) plane, while the second catalyst, MoO_3-C, exposed a greater number of (100) planes. Comparison of the two catalysts showed that MoO_3-C was more selective towards HCHO than MoO_3-R by a factor of 2. This structure sensitive observation was evident over the entire O_2 concentration and CH_4 conversion ranges used, although increasing the O_2/CH_4 ratio favoured the production of CO_X over both MoO_3-R and MoO_3-C. The authors proposed that Mo=O sites, residing preferentially on the (100) plane were active for selective oxidation, while Mo-O-Mo bridging sites, mainly on the (010) plane contributed to complete and sequential oxidation. In-situ laser Raman spectroscopy, TPR and $^{18}O_2$ labelling studies indicated that re-oxidation of the Mo-O-Mo sites took place by gas phase oxygen while Mo=O sites were re-oxidised by diffusion of oxygen from the oxide lattice.

The combination of Mo and Fe oxides to produce successful CH_4 partial oxidation catalysts have been previously highlighted [16], this system has also been investigated by other groups. Otsuka et. al. [46] have tested $Fe_2(MoO_4)_3$ catalysts for CH_4 partial oxidation with O_2, prepared by co-precipitation from $Fe(NO_3)_3$ and $(NH_4)_6Mo_7O_{24}$ solutions. HCHO selectivity greater than 75% was observed at a low CH_4 conversion of 0.24% at 650°C, this selectivity decreased to 30% when CH_4 conversion was 7.80% at 750°C. These studies were carried out at atmospheric pressure with a CH_4/O_2/He ratio of 1/1/2. Results indicated that HCHO was formed by the sequential oxidation of CH_3OH, this was not surprising since $Fe_2(MoO_4)_3$ is known to be an excellent catalyst for CH_3OH oxidation to

HCHO (section 1.3.). The consecutive oxidation of HCHO was the main route for the production of CO_X. The presence of abundant CH_4 had the effect of improving HCHO selectivity. As a consequence of the different product distributions in the presence and absence of the catalyst, and differences in the change of CH_4 conversion with varying residence time the authors concluded that the reaction mechanism was exclusively heterogeneous. This does seem somewhat surprising considering the high reaction temperatures employed. However, a specially engineered reactor was used which tapered from 8 mm i.d. at the inlet to 1.5 mm i.d. at the exit, which should help to minimise gas phase reactions. The same group has also investigated the activity of $Fe_2(MoO_4)_3$ using N_2O oxidant instead of O_2 [47]. The main products from CH_4/N_2O were C_2H_6 and C_2H_4, opposed to HCHO and CO when CH_4/O_2 was used.

The most studied catalysts for CH_4 partial oxidation have been those of MoO_3 supported on high area SiO_2. One of the earliest studies on this system was reported by Liu et. al. [48], who used a 1.7 wt.% Mo/SiO_2 catalyst with N_2O oxidant. A combined selectivity to CH_3OH and HCHO of 84.6% was observed at 8.1% conversion, when steam was co-fed with the reactants at 560°C. A later and more detailed publication from the same research group [49] was unable to reproduce the catalytic activity data from the earlier study. The combined yield of oxygenated products was lower with a selectivity of 78.7% at 2.9% CH_4 conversion and 570°C. Investigation of the reaction kinetics showed a rate law of the form (1.9.1),

$$-d[CH_4]/dt = k[N_2O]^1[CH_4]^0 \qquad (1.9.1.)$$

These reaction orders were valid in the partial pressure ranges 80-200 torr for N_2O and 40-250 torr for CH_4. At N_2O partial pressures below 80 torr the rate was still linear with respect to N_2O, but the reaction order was decreased. In this lower region of N_2O partial pressure HCHO selectivity was consistently 100%. ESR spectroscopy identified O^{2-} as the surface product from N_2O decomposition and it was concluded that this species was responsible for the non-selective oxidation reactions. O^- species were also identified, formed from the interaction of N_2O with

a surface Mo^{5+} species. These species were proposed as the active sites for selective oxidation by the abstraction of hydrogen from CH_4 to produce methyl radicals. These radicals subsequently reacted with $Mo^{5+}O^-$ sites to produce the surface methoxide anion, resulting in the production of HCHO and CH_3OH.

Khan and Somorjai [50] also investigated silica supported Mo catalysts for the partial oxidation reaction with N_2O oxidant. In a series of similar experiments they were able to reproduce the catalytic activity data of Liu et. al. [49]. However, fundamental differences were apparent in the reaction kinetics. The rate of CH_3OH formation at 540°C was found to be zero order with respect to N_2O and first order with respect to CH_4 and H_2O, while the HCHO production rate was zero order with respect to all reactants. The activation energy for CH_3OH formation was 172 ± 11 kJ mol^{-1} up to 520°C. The Arrhenius plot for HCHO production showed two distinct linear regions, with activation energies 344 ± 17 kJ mol^{-1} below and 168 ± 8 kJ mol^{-1} above 540°C. These observations were interpreted as indicating that below 540°C HCHO and CH_3OH were derived from parallel routes. While above 540°C HCHO was produced from a CH_3OH intermediate.

The role of co-fed H_2O in both of these studies was an important factor. The specific role of H_2O in the reaction mechanism was not clear, but thermal and radical quenching can be envisaged. One suggestion from Khan and Somorjai for the function of H_2O was that it prevented the deposition of carbonaceous material, as in its absence coking was evident on the catalyst.

The Mo/SiO_2 system has also been investigated using O_2 rather than N_2O as the oxidant. One such study was performed by Spencer [51]. The major reaction products were HCHO, CO and CO_2; traces of CH_3OH and H_2 were also detected. At low conversions HCHO was produced with 71% selectivity. The best catalyst was MoO_3/Cab-O-Sil prepared by physical milling of the components, catalysts prepared by impregnation also proved to be active but were less selective. The effects of impurities were also investigated, and it was demonstrated that sodium levels as low as 300 ppm had a detrimental effect on both conversion and

selectivity. A more recent publication by Spencer et al [52] investigated more closely the role of Na in these catalysts. From kinetic analysis the authors suggested that Na retarded the direct oxidation of CH_4 to HCHO and CO_2, whilst promoting the further oxidation of HCHO to CO. It was also proposed that the initial CH_4 activation took place on a Mo-O· surface radical species, generated thermally at the reaction temperature. Molybdenum in the +5 oxidation state was referred to as an important species in several steps of the reaction scheme.

The influence of additives and the nature of the support for Mo catalysts was investigated by MacGiolla Coda et al [53]. Over the temperature range 500-600°C with N_2O, MgO or TiO_2 supports resulted in the sole production of carbon oxides. Under the same conditions with a Spher-O-Sil (porous silica) or Cab-O-Sil (fumed silica) support HCHO was produced. The same group [54] also prepared a range of catalysts in which the support was first treated with Cu or Na, before impregnation to different Mo loadings. A 2 wt.% MoO_3 catalyst on the untreated support showed 100% HCHO selectivity at 500°C. Increasing the Mo loading on this support produced a marked decrease in HCHO selectivity. The addition of Cu to the support had a three fold effect, firstly it appeared to modify the form of the supported Mo phase, as the 15 wt.% material showed no evidence for characteristic crystalline MoO_3, which was detected in the absence of Cu. Secondly a new route for HCHO formation was developed, and finally, TPR results showed that a more easily reduced molybdenum phase was formed. It was proposed that this may have taken place in the following manner (1.9.2.).

$$Cu^0 + MoO_3 \text{ ----> } Cu^{2+} + MoO_2 + O^{2-} \quad (1.9.2.)$$

Experiments with Na impurities on the support reiterated that generally Na was destructive towards HCHO. It has to be noted that Cu containing supports were prepared by impregnation from a $CuCl_2$ solution, which may well have introduced residual chloride to the catalyst, possibly exerting an influence on the reaction.

Another study by the same group [55] studied the effects of a more comprehensive range of dopants. The Cab-O-Sil support was impregnated with solutions of Cr, Co,

Fe, Ag, Na and V, to produce 2 wt.% loadings. These silica materials showed low activity for CH_4 conversion, and only the V impregnated catalyst exhibited any selectivity towards HCHO when N_2O was used as the oxidant. Under the same conditions the addition of Mo to the majority of the supports resulted in the production of HCHO. In the case of the 2 wt.% V_2O_5 catalyst the addition of Mo depressed HCHO selectivity whilst increasing CH_4 conversion, as a consequence rates of HCHO production were increased. Using O_2, comparison of a 7 wt.% MoO_3 catalyst with the Na doped analogue, showed that Na had detrimental effects on CH_4 conversion and HCHO selectivity; a conclusion which was in good agreement with earlier studies [52,54]. On the contrary, when N_2O was used, the effects were less systematic, although under CH_4 rich conditions the production rate of HCHO was approximately doubled. From the data presented it is difficult to identify which oxidant was the more suitable for this reaction, but it was clear that important differences existed in the reaction mechanisms.

The influence of oxidant, Mo loading and silica support for MoO_3/SiO_2 catalysts with respect to CH_4 partial oxidation has also been investigated by Banares et al [56]. A series of catalysts with MoO_3 wt.% loadings ranging from 0.5-16.2 were prepared, these corresponded to surface concentrations ranging from 0.3 to 3.5 Mo nm^{-2}. Significant differences in activity and selectivity were observed depending on the oxidant used. With N_2O, CH_4 and oxidant conversions were considerably lower when compared to data obtained using O_2, also HCHO selectivity was higher for O_2 compared with N_2O, clearly indicating that O_2 was the preferred reactant. The catalytic differences were ascribed to the differing oxidising power of N_2O and O_2 for the regeneration of catalytic sites. It was proposed that the reaction operated by a Mars van Krevelan mechanism, and the re-oxidation of the catalyst was less effective by N_2O. The intense blue colour, indicative of partially reduced MoO_3, and the presence of reflections attributed to a MoO_2 phase in the XRD pattern of the used N_2O catalyst were presented as evidence to support this view.

Investigations into the effect of loading showed that the yield of HCHO was maximised around 1 Mo nm^{-2}, irrespective of the oxidant employed. Raman, XPS and XRD studies indicated a uniformly distributed Mo species interacting strongly with the silica surface. Loadings below 0.8 Mo nm^{-2} formed a highly dispersed molybdate phase, whilst above this loading the structure of crystalline MoO_3 was detected.

Barbaux et al [57] have concentrated on characterising a range of supported Mo catalysts, and correlating the results with catalytic activity data. Studies revealed three different molybdenum species, which were dependent on the loading. Loadings in the range 1-5 wt.%, showed a uniformly distributed phase, interacting strongly with the support, this was identified as silicomolybdic acid (SMA). From 5-10 wt.% loadings, a polymolybdate species was also observed which appeared to be covering the SMA, but not the support. At loadings of 15 wt.%, SMA was no longer detected, and crystalline MoO_3 was identified. Microreactor studies carried out at 597°C with N_2O showed that over the 1-5 wt.% MoO_3 catalyst HCHO was a major product. HCHO selectivity was related directly to the concentration of SMA. Co-feeding H_2O with the reactants enhanced HCHO selectivity but depressed CH_4 conversion. CH_3OH was not detected under these conditions, which were not dissimilar to those used in previous studies with this catalyst, which did detect CH_3OH as a major product [49, 50]. Molybdenum loadings above 5 wt.% were not active for HCHO production, but did exhibit some selectivity towards coupling products. Replacing N_2O oxidant with O_2 produced CO_X over all catalyst in the presence or absence of co-fed H_2O.

Similar results to those obtained by Barbaux have been reported by Kasztelan et. al. [58] who correlated activity for CH_4 partial oxidation by N_2O with the amount of silicomolybdic acid detected on the silica support. The most active catalyst had the highest concentration of SMA. In this case the concentration of SMA was dependent on the pH of the preparatory molybdenum solution, rather than the level of Mo loading. Although the correlation has been established it should be noted that the

catalyst performance was poor, the highest CH_3OH and HCHO combined selectivity was only 9% when CH_4 conversion was 2.6% at 500°C. These results indicate that the SMA phase may not be the major component responsible for oxygenate formation.

Smith et al [59] have also investigated the nature of the surface species on the MoO_3/SiO_2 catalyst. Results also identified the presence of three surface Mo species. Below 2 wt.% MoO_3 a silicomolybdic species was present, characterised by Raman spectroscopy and a broad maximum in TPR studies. Interestingly Banares et al [56] found no evidence for this species on their catalysts. As the loading was increased a surface coordinated polymeric molybdate was identified. At loadings above 3.5 wt.% crystalline MoO_3 was again detected, with the polymolybdate species coexisting up to the highest loading examined at 9.8 wt%. The activity of the catalyst was again found to be dependent on the Mo loading. A large decrease in the CH_4 conversion was observed at 5 wt.% MoO_3, which corresponded to the emergence of an appreciable amount of crystalline MoO_3 on the surface. The catalyst with the lowest loading, 0.5 wt.%, was the best, this catalyst had the most dispersed silicomolybdic phase. It was proposed that the silicomolybdic species has associated with it terminal Mo=O sites, which were responsible for the selective oxidation to HCHO. Increasing the loading increased the number of Mo-O-Mo bridging sites at the expense of the terminal Mo=O sites. It was these Mo-O-Mo sites which were implicated in increasing the non selective oxidation to carbon oxides.

There has been general agreement between these studies for the type of molybdenum species identified at different loading regimes. However, there is some uncertainty towards the nature of the phase present at low loadings.

The preparation method of the MoO_3/SiO_2 catalysts differs between studies and it would be expected that surface Mo species would also differ. One important factor which often does not receive full attention is the pH of the heptamolybdate solution

used for impregnation. The Mo species in solution is dependent on the equilibrium (1.9.3.).

$$7MoO_4^{2-} + 8H^+ \rightleftharpoons Mo_7O_{24}^{6-} + 4H_2O \qquad (1.9.3.)$$

At pH 6 $Mo_7O_{24}^{6-}$ is predominant with Mo in an octahedral environment, while MoO_4^{2-} tetrahedra are formed at pH 11. Solutions with pH 1 showed the hydrated polymeric oxyanions with predominantly Mo in an octahedral environment. The impregnation pH also affects the net surface charge of the support. Ismail et al [60] have identified the Mo species present on the SiO_2 support after impregnation to 8 mol % loadings at varying pH and calcination temperature. At pH 6, MoO_3 islands and particles were present with Mo in tetrahedral and octahedral coordination respectively. MoO_3 particles were again identified at pH 11. In contrast, catalysts prepared at pH 1 showed a highly dispersed silicomolybdate, $SiMoO_x$ phase.

A recent report by Banares et. al. [61] has investigated the effect of the addition of alkali metal cations to the MoO_3/SiO_2 catalyst with respect to the selective oxidation of CH_4 to HCHO. The catalysts prepared were doped with Na, K and Cs, active loadings were on a molar basis and were equal to 1477 ppm Na/2.4% MoO_3/SiO_2. Microreactor, in-situ Raman and TPR studies were carried out and showed that in the absence of the metal cations Mo was present as an isolated oxide species. The addition of Na, K and Cs resulted in the formation of new alkali molybdate surface compounds which decreased both CH_4 conversion and HCHO selectivity. The activity for CH_4 partial oxidation over the Mo/SiO_2 catalyst correlated with the number of molybdenum oxide species.

The mechanism of CH_4 partial has been investigated using $^{18}O_2$ isotope tracer techniques [62]. Based on evidence from this study Banares et. al. suggested that oxygen incorporated into the HCHO molecule originated from lattice oxygen of the catalyst. It was also suggested that re-oxidation of the catalyst took place via gas phase oxygen in accordance with a Mars van Krevelan mechanistic cycle. The oxygen pathways during CH_4 partial oxidation over MoO_3/SiO_2 have also been investigated by Mauti and Mims [63], who employed oxygen isotope exchange and

steady state oxygen isotope transient techniques. On the contrary to the findings of the previous study [62] it was concluded that no information on the oxygen source for HCHO or CO_X could be obtained from these experiments, as a consequence of the substantial and rapid oxygen exchange between these products and the catalyst. The HCHO molecule was a stable product, even after participating in this multiple exchange process. It was therefore proposed that exchange may take place via interaction with a Mo=O site, forming the reversible surface acetal species shown in figure 1.9.1.

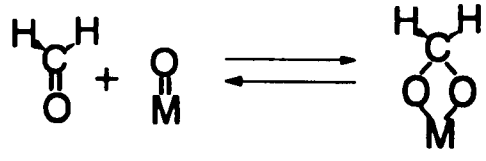

Figure 1.9.1. Surface acetal species formed by HCHO leading to a multiple oxygen exchange process [63].

However, it was clear that this exchange was predominantly due to the Mo phase, which utilised lattice oxygen from the SiO_2 support.

Catalysts based on vanadium have also been extensively used for this reaction. One of the earliest studies was reported by Somorjai and co-workers using a V_2O_5/SiO_2 catalyst [64].

Spencer and Pereira [65] also observed that V_2O_5 supported on SiO_2 was active for the production of HCHO from CH_4/O_2. At low conversions high HCHO selectivities were observed, trace quantities of CH_3OH were also produced under some conditions. HCHO decomposition studies showed that at the onset of conversion CO was the only product, while at higher conversion CO_2 was also formed, the authors concluded that a sequential oxidation mechanism was operating. Comparison with the Mo based catalyst showed that the V material was more active. Studies by Kennedy et al [55] have shown that HCHO yields under CH_4 rich and lean conditions were dependent on the V_2O_5 loading. Optimum yields were obtained when the loading was in the range 1-4 wt.%, throughout this range HCHO selectivity remained constant, and therefore the yield was influenced by the

relationship of loading with CH_4 conversion. TPR studies showed that all catalysts after the first reduction treatment exhibited V species in an oxidation state intermediate between +3 and +4. Subsequent TPR demonstrated that 2 and 0.5 V_2O_5 wt.% catalysts were re-oxidised more easily than the 7 wt.% catalyst. It was postulated that materials with loadings greater than 4 wt.% were less active due to the slower V re-oxidation rate, while catalysts below 1 wt.% loading did not possess sufficient extractable oxygen. Therefore it was only catalysts with loadings between 1-4 wt.% V_2O_5 which were able to sufficiently satisfy both of these criteria for an active catalyst.

Chen and Wilcox [66] have investigated the V_2O_5/SiO_2 system under somewhat different reaction conditions. Typical feed composition was $CH_4/N_2O/O_2/H_2O$ with the ratio of 25/65/2/8, experiments were performed at atmospheric pressure with contact times of 2.2 s. TPR indicated the presence of a single V species throughout the 1-8 wt.% range of loadings. Characterisation by XRD indicated that no well defined crystalline phases of V were present. The main reaction products were CH_3OH, CO and CO_2, the authors suggested that HCHO was formed at levels below the sensitivity of the analytical system. CH_4 conversion was increased when N_2O was used as the sole oxidant, and decreased in the case with O_2 alone, demonstrating that N_2O was the more active oxidant. It has been suggested that the increasing size of the V_2O_5 oxide ensemble, which increased in parallel with the loading, may offer an explanation for the decrease in CH_3OH selectivity. The reason given that larger ensembles, which possessed more active oxygen, were responsible for the combustion reactions.

A study by Kartheuser and Hodnett [67] has observed a relationship between the dispersion of V_2O_5 supported on SiO_2 and the selectivity for HCHO. The dispersion was measured by a method which involved passing a 1000 ppm NO and 20,000 ppm NH_3 gas mixture over the catalyst at 200°C and measuring the N_2 evolved. According to Miyamato et. al. [68] the initial burst of N_2 was associated with the V=O species, and was produced by the surface reaction (1.9.4.).

$$NO + NH_3 + V{=}O \text{ ----> } N_2 + H_2O + V\text{-}OH \quad (1.9.4.)$$

The dispersion was calculated by the following equation (1.9.5.).

$$\text{Dispersion} = (\text{mol } V{=}O_{surf}/\text{mol } V_2O_5) \times 100\% \quad (1.9.5.)$$

The maximum V_2O_5 dispersion was 27% observed at a V loading of 1 wt.%. At constant CH_4 conversion this catalyst showed a maximum HCHO selectivity of 28% and a maximum HCHO production rate of 1900 μmol (g cat)$^{-1}h^{-1}$. It was suggested that higher HCHO selectivity was observed over the smaller V_2O_5 particles because further HCHO oxidation was reduced, as a consequence of fewer active oxygen sites on these particles compared to the larger V_2O_5 particles. This suggestion was similar to that which has been made by Chen and Wilcox [66] over the same catalyst, whilst using N_2O oxidant.

Mechanistic information on the V_2O_5/SiO_2 catalyst has been provided by Kartheuser et al [69], using a temporal analysis of products (TAP) reactor. It was shown that oxygen interacted with the catalyst to produce a species with active lifetimes between 5-60 s. The interaction of CH_4 with the surface was very weak, exhibiting very short lifetimes. It was the surface oxygen species which activated the CH_4 molecule, forming methyl radicals. These radicals reacted further with the catalyst, extracting lattice oxygen which was incorporated into the HCHO molecule. These steps are represented by the following reaction scheme (1.9.6., 1.9.7.).

$$CH_4 + O^-_{(ads)} \text{ ----> } CH_3\cdot + OH_{(s)} \quad (1.9.6.)$$

$$CH_3\cdot + {}^{16}O_{(latt)} \text{ ----> } HCH^{16}O + H\cdot \quad (1.9.7.)$$

A recent report by Koranne et. al. [70] has studied the involvement of oxygen in the partial oxidation of CH_4 over V_2O_5 based catalysts. The oxygen exchange capability of V_2O_5/SiO_2 with gaseous O_2 was low in the absence of CH_4, but when CH_4 and O_2 were present simultaneously the rate was increased by a factor of ca. 4. This increase was attributed to a redox mechanism which operated when CH_4 was present, but not in its absence. It was concluded that oxygen associated with the catalyst was involved in the production of HCHO, CO and CO_2. However, the contribution from oxide lattice oxygen to the formation of these products could not

be determined due to the considerable secondary oxygen exchange of these products. These conclusions were similar to those which were derived earlier, concerning the involvement of lattice oxygen in the selective products from CH_4 oxidation over MoO_3/SiO_2 [63].

The effect of oxide loadings for Mo and V have been investigated on an active precipitated silica support [71], by Miceli et al [72]. Loadings in the range 0.2-4.0 wt.% and 0.2-5.3 wt.% have been used for MoO_3 and V_2O_5 respectively. Specific reaction rates decreased steadily with respect to those of the bare silica as the MoO_3 concentration was increased, the opposite effect was observed for V_2O_5. Generally, increasing the loading enhanced HCHO selectivity over the Mo catalyst, whilst selectivity was suppressed by the further addition of V_2O_5. Surface models were proposed for the MoO_3/SiO_2, V_2O_5/SiO_2 and SiO_2 systems. The model indicated that SiO_2 exposed two kinds of site, reduced sites capable of activating O_2 and strained siloxane bridges effective for activating CH_4. The addition of MoO_3 partially masked the active reduced sites for O_2 activation causing a detrimental effect on the HCHO yield. The addition of V_2O_5 also partially masked the reduced sites but consequently new reducible sites were created which were also active.

The studies based around supported Mo and V oxides have employed both O_2 and N_2O oxidants, from a commercial point of view the use of O_2 would be more favourable on basis of expense. Several studies have taken steps to elucidate the reaction pathways for the partial oxidation of CH_4. Kinetic analysis of experiments by Spencer et al [51,52] concluded that the MoO_3/SiO_2 catalyst oxidised CH_4 to the primary products HCHO and CO_2, via parallel reaction pathways through a common activation step. CO was produced by subsequent oxidation of HCHO, which may be further oxidised to CO_2. CO_2 may also be produced in these systems by the water gas shift reaction.

The reaction pathway over V_2O_5/SiO_2 catalysts seemed to follow a somewhat different reaction scheme [65]. At atmospheric pressure with O_2, the process followed a sequential reaction pathway, HCHO was a primary product which was

further oxidised to CO and finally CO_2. A microkinetic simulation has been carried out by Amiridis et al [73], to describe the reaction mechanisms over both catalytic systems. The nature of these mechanisms suggest that careful engineering of the reactor geometry could reduce further oxidation of the selective product over V_2O_5/SiO_2. Whereas, the CO_X yields from the MoO_3/SiO_2 catalyst may be inherently produced from CH_4 by a direct route, with little scope for any improvement A General comparison between the V and Mo supported systems indicated that the V_2O_5/SiO_2 exhibited higher activity, while the MoO_3/SiO_2 showed higher oxygenate selectivity.

The extensive research on V and Mo supported catalysts has indicated that SiO_2 was an excellent support for the partial oxidation reaction. SiO_2 alone has also been used as a catalyst for this reaction. Kasztelan and Moffat [74] showed that HCHO could be produced directly from CH_4 over a commercial Grace-Davidson 400 grade silica. HCHO selectivity was 10% at 0.7% CH_4 conversion at 514°C and ambient pressure with O_2 oxidant. When O_2 was replaced with N_2O, HCHO was no longer produced, the major product was CO. The activity of various silicas has been investigated by Kastanas et. al. [75] who demonstrated that Cab-O-Sil (fumed silica), Ludox silica gel and silicic acid were all active catalysts for HCHO formation. Reaction conditions were 620°C with elevated pressure. These Si based catalysts showed similar activity trends to those of the empty reactor tubes, which were constructed from Vycor and quartz glass. The activation energy for HCHO formation was independent of the catalyst used. From these observations the authors concluded that HCHO was produced solely by gas phase reactions. In contrast, the activation energies for the production of CO and CO_2 were dependent on the catalyst used, and resulted from surface reactions, possibly by further oxidation of HCHO. One important feature of this study was the presence of C_2H_6 in the hydrocarbon feed, this impurity is known to enhance HCHO selectivity in this reaction [43,44].

A comprehensive range of silica catalysts has been studied for CH_4 selective oxidation by Parmaliana et. al. [76], these included precipitated, extruded, fumed and gel silicas. Catalysts were tested in a batch reactor with an external recycle, experimental conditions were 520°C at 1.7 bar pressure with a CH_4/O_2 ratio of 2/1. Precipitated silicas Si4-5P and F5 (ex Akzo) were the most active, producing a HCHO STY at least 3 times greater than extruded or sol-gel silicas. Fumed silica was a poor catalyst relative to the other forms. Tableting the Si4-5P silica at 100 bar reduced activity slightly, as did increasing the level of Na impurities above the initial background concentration. Acid washing the silica decreased the Na content but no improvement in the HCHO yield was observed. However HCHO yield was improved by a factor or 2 by pre-treating the catalyst at 1000°C. The activity of precipitated SiO_2 is clearly an important observation, and it has been discussed earlier in this section with particular reference to supported Mo and V catalysts [71].

A report by Sun et al. [77] has obtained high HCHO space time yields over fumed silica and silica gel catalysts. A maximum HCHO STY of 812.9 g(kg cat)$^{-1}$h^{-1} was obtained over the silica gel catalyst at 780°C and ambient pressure when a space velocity of 560,000 l(kg cat)$^{-1}$h^{-1} and CH_4/air ratio 1.5/1 were used. By comparison the maximum HCHO STY over precipitated SiO_2 obtained by Parmaliana et. al. [76] was 17.9 g(kg cat)$^{-1}$h^{-1}, but reaction conditions were vastly different. C_2H_6 was also a major reaction product detected by Sun et. al. [77], HCHO and C_2H_6 selectivities were 28.0 and 31.6% respectively. As would be expected an increase in the residence time was accompanied by a decrease the selectivity to HCHO and C_2H_6, with an increase in CO_X. The authors have proposed that the formation of HCHO was via a surface methoxy complex and not by a gas phase process via methyl radicals. This proposal was based on observations that both HCHO and C_2H_6 were primary products, and activation energies for CH_4 conversion, HCHO and C_2H_6 production were all different, indicating that they were formed by different mechanistic pathways. The proposed reaction mechanism

also showed that CH_4 was activated by dissociative chemisorption on siloxane defect sites of the dehydroxylated surface. This chemisorption process could lead either to the formation of the methoxy group which decomposed to form HCHO, or to a methyl radical which was released to the gas phase preferentially forming C_2H_6.

A recent study by Kobayashi et. al. [78] has investigated the effect on the partial oxidation of CH_4 by doping a high area silica with 3d transition metal ions. Experiments were performed with a space velocity of 120,000 $cm^3(g\ cat)^{-1}h^{-1}$ and a CH_4/O_2 ratio of 19/1 at 600°C. In all cases the catalysts were prepared with a metal ion/Si ratio of 1/2000, which was equivalent to 0.05 atom %. Although bare SiO_2 showed some activity for HCHO production the addition of the metal ions enhanced the HCHO yield in all cases. This effect was most pronounced by the addition of Fe^{3+}, which increased the HCHO STY by an order of magnitude over SiO_2. The activity of these catalysts has been attributed to highly dispersed atomic forms of the promoting ions, as studies using the simple oxides only produced CO_X products. It was proposed that the highly dispersed atomic Fe acted as an important redox centre for HCHO formation.

Chun and Anthony [78] have looked at a diverse range of catalysts, under high pressure conditions of 48 bar. The materials studied included SiO_2 and TiO_2, mixed and single oxides of Fe, Mo, Cu, V and Sn, Ag/gamma-Al_2O_3, Pyrex beads and V_2O_5. Under conditions of almost complete oxygen conversion, the product distributions were not dramatically altered by the nature of the catalyst. The reaction temperatures in the presence of the catalyst were higher than for the homogeneous reaction, with CH_3OH selectivities critically lower than the empty tube. Chun and Anthony suggest that homogeneous reactions in the void volume of the catalytic bed were significant with respect to the heterogeneous reaction. The oxide surface was also responsible for inhibiting free radical homogeneous reactions. It appears in this study that the type of catalyst had little influence on the reaction products, it has to

be remembered that high pressures were used which would enhance the contribution from gas phase reactions.

Other oxides which may be used as catalyst supports beside SiO_2 have also been studied for the partial oxidation of CH_4. Parmaliana et. al. [76] have shown that using a CH_4/O_2 mixture at 1.7 bar the oxides gamma-Al_2O_3, MgO, TiO_2 and ZrO_2 all produced CO and CO_2 as the major reaction products, with low selectivity to C_2H_6 over MgO and ZrO_2. In the same study SiO_2 did produce HCHO in substantial quantities. A similar conclusion has also been made by Kastanas et. al. [75] who only observed combustion products from CH_4/O_2 mixtures over gamma-Al_2O_3 and MgO. Studies using N_2O oxidant have also shown that CO and CO_2 were the sole products from CH_4 oxidation over MgO and TiO_2 [53]. However, despite these previous observations HCHO has been produced over MgO from CH_4/O_2 at 750°C in relatively high space time yields [80]. This study demonstrated a selectivity switch from the CH_4 oxidative coupling product C_2H_6 and CO to the oxygenated product HCHO. This switch in the selective products was accomplished by increasing the GHSV of the reactant feed. Below 10% O_2 conversion selectivity towards HCHO was significant, but as O_2 conversion increased HCHO selectivity decreased while that of C_2H_6 and CO increased. The switch in selectivity was rationalised by considering the possible reactions of methyl radical intermediates. It was proposed that the concentration of such gas phase radicals decreased linearly as the GHSV was increased, and since the rate of C_2H_6 production was proportional to the square of the radical concentration, production declined. Whereas, at low oxygen conversion there was a relatively high O_2 partial pressure in the catalytic bed and subsequently the oxidation of methyl radicals became the dominant process generating HCHO.

A more comprehensive investigation of the selectivity switch from HCHO to C_2H_6 has been undertaken by Sinev et. al. [81] over a series of phosphate catalysts using O_2 oxidant at 725°C. The catalysts investigated were Fe, Zn and Zr phosphates and the selectivity switch was effected by increasing the O_2 partial pressure in the

reactant feed. Results reported for the Fe-phosphate system showed that below $P(O_2)$/KPa of 7, HCHO was the most selective product. Increasing the O_2 pressure above this value resulted in a decrease of HCHO selectivity accompanied by an increase in CO and C_2H_6 selectivity. Increasing the reaction temperature also increased C_2H_6 selectivity at the expense of HCHO in the same manner as the O_2 partial pressure dependence. Sinev et. al. concluded that the experimental observations indicated a common intermediate for the production of C_2H_6 and HCHO. This intermediate was the methyl radical. This proposed reaction scheme implies that HCHO formation could be a purely gas phase process, but the authors concluded that further heterogeneous reactions did contribute to the formation of HCHO as different $HCHO/C_2H_6$ ratios were observed over different catalysts under the same conditions.

The most selective of the phosphate catalysts investigated by Sinev et. al. [81] was based on Fe. A more detailed study of this catalyst for CH_4 partial oxidation by O_2 has been made by Zhen et. al. [82]. When H_2O was co-fed as a reactant the Fe-phosphate catalyst produced HCHO and HCOOH with selectivities of 29.5% and 70.5% respectively, at 600°C and 0.67% CH_4 conversion. Increasing the temperature to 680°C increased the yield of these products, as CH_4 conversion was increased to 3.7% while the selectivity of HCHO and HCOOH decreased to 25.1% and 17.9%. In the absence of H_2O, HCHO was the major product with a selectivity of 68.4% at 600°C, but CH_4 conversion was decreased approximately 2.5 fold to 0.27%. From evidence indicated by infrared studies it was suggested that CH_4 was oxidised by a mechanism involving dissociative chemisorption producing surface methyl and methylene radicals and hydroxyl groups.

The selectivity switches form oxygenated to coupled products over MgO [80] and phosphate catalysts [81] during CH_4 partial oxidation were dependent on the reaction conditions. A similar selectivity switch has been demonstrated by Sojka et. al. [83], however the switch was produced by chemical modification of a ZnO catalyst and not by changing reaction conditions. Studies performed over ZnO in the

temperature range 500-850°C using a reactant feed ratio of 1/1 CH_4/air, only produced CO and C_2 hydrocarbons. Doping ZnO with equimolar quantities of Cu^{1+} and Fe^{3+} produced a switch in selectivity to HCHO. The production of HCHO was attributed to the introduction of the redox couple $Cu^{1+/2+}$ and $Fe^{2+/3+}$, and the Lewis acid function of Fe^{3+}. These functions were suggested to operate by trapping methyl radicals at surface sites, which were subsequently oxidised by surface oxygen to form a surface methoxide species. Transfer of a hydride ion to the dopant redox couple facilitated the desorption of the HCHO product.

A Cu/Fe catalyst system has also been developed by Anderson and Tsai [84] using a zeolite catalyst with N_2O oxidant. The catalyst was based on Fe-ZSM5, which was a analogue of ZSM5 with Fe^{3+} substituted into the framework lattice replacing Al^{3+} ions. The best catalyst was one which was first exchanged with Cu^{2+} to produce Cu-Fe-ZSM5. Reactions were carried out with a CH_4/N_2O ratio of 4/1 in the temperature range 237-342°C. A maximum combined selectivity to CH_3OH and HCHO of 79.0% was obtained at 0.25% CH_4 conversion and 237°C. The oxygenate selectivity decreased to 56.2% while CH_4 conversion increased to 1.12% when the temperature was raised to 342°C. A Cu^{2+} exchanged ZSM5 catalyst only produced CO_X even at low CH_4 conversion. Anderson and Tsai assigned the catalyst performance to the development of synergy between the Cu and Fe functions.

Other catalysts for CH_4 partial oxidation based on zeolitic materials have also been investigated by other groups [36,40]. Kowalak and Moffat [85] have examined the activity of highly acidic mordenites. N_2O was used as the oxidant and activity investigated between 350-425°C. Over the H-form of the mordenite (H-mordenite) carbon oxides were not formed below 400°C, the main reaction products were the coupling products C_2H_6, C_2H_4; C_3 and C_4 products were also formed, while CH_3OH was produced with a selectivity of 10% which decreased to 1% at 425°C. The product distribution over a fluorinated mordenite (F-mordenite) was similar to that over H-mordenite, although CH_4 conversion was greater. F-mordenite was

more acidic than the H-form, the Hammett acidity function was measured at -13, which is in the superacid region. The authors suggested that the increased CH_3OH yield over F-mordenite was due to the presence of superacid sites, and that the activation of CH_4 took place by protonation to form the pentacoordinate carbocation, shown below (1.9.8.).

$$CH_4 + H^+ \text{----}> CH_5^+ \text{----}> CH_3^+ + H_2 \qquad (1.9.8.)$$

A zeolite catalyst based on molybdenum and ultrastable (USHY) zeolite has been prepared and tested by Banares et al [86]. Catalysts were synthesised using different Mo precursors and modes of activation. CH_4 oxidation by O_2 showed some HCHO selectivity, approximately 6%, at low conversion. The most selective catalyst was an 8 wt.% Mo variant synthesised by impregnation. The reaction was limited to MoO_3 crystallites located on the external surface of the zeolite, although characterisation techniques indicated that Mo ions were located within the framework cavities. The catalytic activity correlated with the degree of Mo dispersion on the external surface.

One of the most successful catalyst systems for the production of HCHO directly from CH_4 has been reported by Otsuka et. al. [87] in an extension of the design approach outlined previously [30]. The most active catalyst was a mixed oxide with the composition 1/2/2 Fe/Nb/B, denoted as FeNbBO. Analysis of the catalyst by XRD identified the phases $FeNbO_4$, $FeNb_{11}O_{29}$ and B_2O_3. Otsuka et. al. suggested the $FeNbO_4$ phase was responsible for CH_4 activation and oxygen insertion leading to the formation of HCHO. The B_2O_3 phase improved HCHO selectivity by reducing the further oxidation of HCHO and by reducing the direct combustion of CH_4. Over FeNbBO at 870°C and atmospheric pressure with a CH_4/O_2 reactant mixture HCHO was produced with a selectivity of 61.6% at 2.15% CH_4 conversion. This equated to a HCHO STY of 1210 $g(kg\ cat)^{-1}h^{-1}$, which is the highest reported HCHO yield for any catalyst in the direct conversion process.

The use of a double layered bed for CH_4 partial oxidation, consisting of Sr/La_2O_3 and MoO_3/SiO_2, has been described by Sun et. al. [88]. The reasoning behind such

an approach was that the first bed (1 wt.% Sr/La_2O_3) was selected to provide a flux of methyl radicals to the MoO_3/SiO_2 bed, which converted the radicals to HCHO. Reactions were carried out at atmospheric pressure with air oxidant. The addition of the Sr/La_2O_3 bed to the MoO_3/SiO_2 bed had a detrimental effect on the HCHO selectivity, for example at 630°C HCHO selectivity was decreased from 100% to 3.3%, however, the CH_4 conversion was increased substantially from 0.08% to 8.2%. These changes in conversion and selectivity resulted in the HCHO STY increasing from 37.9 $g(kg\ cat)^{-1}h^{-1}$ to 129.0 $g(kg\ cat)^{-1}h^{-1}$. Increasing the space velocity also had a beneficial effect on HCHO yield as the radical flux to the MoO_3/SiO_2 bed was increased. When the double layered bed was replaced with a mixed bed of the same composition the catalyst performance was poor, and the HCHO STY was decreased by nearly two orders of magnitude.

Other novel approaches which have been reported using oxide catalysts have included studies by Wada and co-workers, who have reported the use of ultra violet radiation to enhance oxygenate production from CH_4 over MoO_3/SiO_2 [89], ZnO and MoO_3/ZnO [90] catalysts. Studies were performed at 190-220°C for MoO_3/SiO_2 and 227-277°C for ZnO and MoO_3/ZnO, with a $CH_4/O_2/He$ reactant ratio of 3/1/10 at atmospheric pressure. In the presence of UV radiation the MoO_3/SiO_2 and MoO_3/ZnO catalysts produced HCHO as the major reaction product with traces of CH_3OH, no carbon oxides were produced. When the UV source was removed neither catalyst showed any activity. ZnO was also inactive in the absence of UV radiation, but when it was irradiated the yields of CO and CO_2 were greatly in excess of HCHO and CH_3OH, which were only detected in trace quantities.

An interesting approach to the problem of maintaining high selectivity to the less thermodynamically stable products during CH_4 partial oxidation has been presented in a modelling study by Lund [91]. The use of a novel reactant swept catalytic membrane reactor (RSCMR) has been proposed. The design consisted of two concentric tubes, the inner tube was porous and contained the catalyst bed, whilst

the outer tube was swept in the reverse flow direction by the reactant feed. Partial oxidation products formed in the inner tube were allowed to escape through the porous walls and were carried off by the reverse flow of reactants, thus preventing their further oxidation in the catalyst bed. Using results from MoO_3/SiO_2 and V_2O_5/SiO_2 catalyst published by Spencer [51,65] it was predicted that by using the RSCMR HCHO selectivity could be improved by up to a factor of 4 over the traditional plug flow reactor.

The study mentioned above by Lund was only a model study, but if such a reactor could be developed practically, it appears a promising prospect. Although novel reactor design may help to enhance the yields of HCHO and CH_3OH, ultimately if a direct route from CH_4 was to become economically viable then under current circumstances the discovery of more efficient catalysts are required.

The studies outlined in this section have shown that a wide range of catalysts have been tested for the partial oxidation of CH_4. One feature which is evident from many of the studies is the inverse relationship between CH_4 conversion and the selectivity to CH_3OH and HCHO. Many studies have reported high oxygenate selectivity, up to 100% in several cases, but CH_4 conversion was low, subsequently per pass yields were low. Although this was the case relatively high STY have been obtained over some catalysts when the contact time was reduced to a minimum.

It is clear from the studies presented in this review that the reaction mechanism for this transformation is complex, and although claims have been made for purely surface mechanisms it appears more likely that both heterogeneous and homogeneous reactions are involved. This seems a likely assumption particularly considering the high reaction temperatures which have to be employed.

CHAPTER 2

EXPERIMENTAL DETAILS

2.1. METHANOL OXIDATION EXPERIMENTS

2.1.1. REACTOR DESIGN

CH_3OH oxidation studies were carried out in a conventional liquid feed microreactor, the design of which is shown schematically in figure 2.1.1.1.

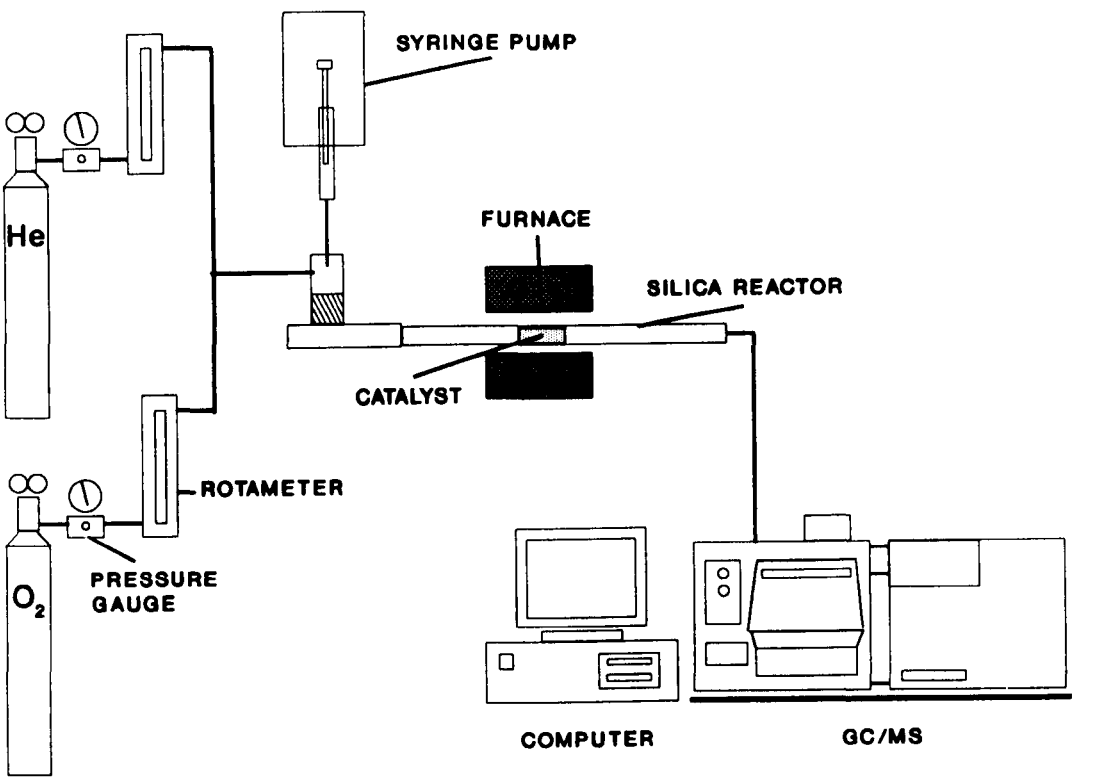

Figure 2.1.1.1. Microreactor design for CH_3OH oxidation studies.

The reactor was constructed from a fused silica tube, with internal diameter of 8 mm, fitted with a ground glass cone and socket joint to facilitate removal. He (99.995%) and O_2 (99.5%) were used as diluent and reactant respectively. Gas flow rates were regulated by Brooks needle valve flow controllers. To ensure accuracy of operation, in-line pressure regulators were used to maintain a constant 2 bar pressure gradient across the flow controllers. In-line rotameters, calibrated for 0-

100 ml min^{-1} He and O_2, gave an approximate indication of the flow rates, which were determined accurately using a bubble flow meter placed at the reactor outlet. CH_3OH (BDH Analar grade) was injected to a Pyrex vaporiser via a syringe driven by a Razel syringe pump. The vaporiser was maintained at 120°C by heating tape. Pulsing effects from the pump were reduced by packing the vaporiser chamber with silica wool. CH_3OH vapour was subsequently swept through the reactor tube by the gas stream.

The catalyst bed was secured in place between two silica wool plugs. Heating was supplied by a block furnace with a 50mm uniform heated zone, capable of maintaining temperatures in the range 100-520°C. Reaction temperatures were measured using a thermocouple placed in intimate contact with the furnace and the external surface of the reactor tube. The temperature was controlled by a Eurotherm 308 unit. Reactor lines after the catalyst bed were trace heated to 120°C by heating tape, to prevent condensation of reactants and products.

Reactor effluent was analysed on-line using a Gas Chromatograph-Mass Spectrometer (GC-MS), further details of which are given in sections 2.1.2. and 2.2.3.

2.1.2. GAS CHROMATOGRAPH-MASS SPECTROMETER ANALYSIS SYSTEM

The GC-MS analysis system was developed in conjunction with Varian. The GC was a Varian 3400 model, the chromatograph was specifically designed to effectively separate light gases and oxygenated products, which included CH_4, O_2, CO, CO_2, HCHO, CH_3OH and $(CH_3)_2O$.

The valve configuration of the GC is shown in figure 2.1.2.1.

The GC was fitted with two Valco gas sampling valves. The injection valve, V1, had 10 ports and was He flushed to minimise air leaks, whilst V2 had 8 ports and was mounted in a heated block. Two columns were used for separation. The first was a Megabore Poraplot GS-Q (30m x 0.53mm i.d.), and the second a Megabore

GS-Molesieve (30m x 0.53mm i.d.). The Megabore columns were selected for their high performance and low column bleed characteristics.

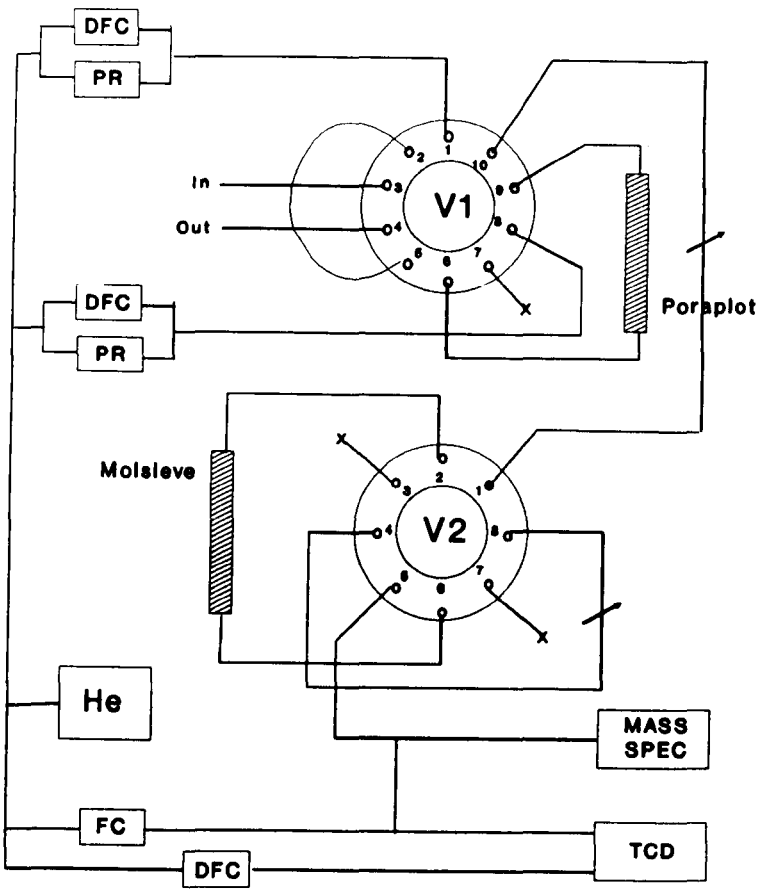

Figure 2.1.2.1. Valve and column configuration used on the GC-MS system. Key: FC=flow controller; DFC=digital flow controller; PR=pressure regulator.

Helium was used as the carrier gas, flow rates were regulated by mass flow valves. When analysis was not being performed the Poraplot column was back flushed at a high rate to remove any heavy contaminants which may have been introduced.

The operation of the GC can be represented can be by the simplified diagram shown in figure 2.1.2.2.

The reactor effluent was injected onto the Poraplot column via the 10 port valve. Light gases such as O_2, N_2 CO and CH_4 passed directly through this column with no interaction and on to the Molesieve. As soon as these light gases passed onto the Molesieve column the flow path through the 8 port valve was diverted, by-passing the Molesieve and trapping the light constituents. In the by-pass configuration CO_2 eluted from the Poraplot column directly to the detectors. The 8-port valve was then

switched again to restore flow through the Molesieve and O_2, N_2, CO and CH_4 were separated. After these compounds eluted the Molesieve column was again by-passed and the compounds CH_3OH, HCHO, H_2O and $(CH_3)_2O$, which were separated by the Poraplot column, eluted directly to the detectors.

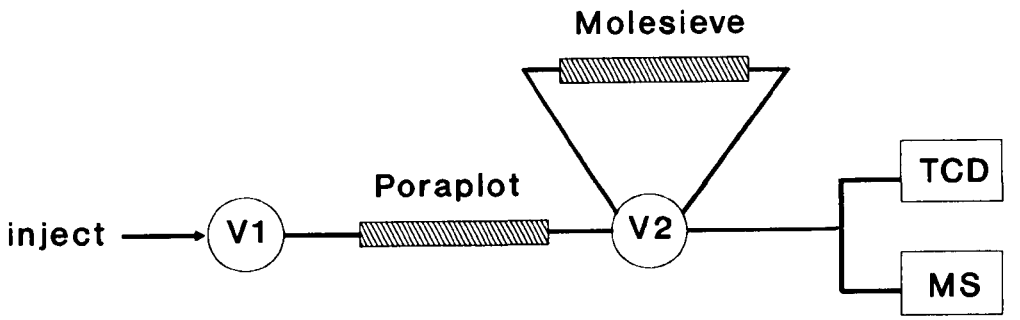

Figure 2.1.2.2. Simplified representation of the column and valve configuration of the GC.

The need for such an elaborate separation system was two fold. Firstly, it was not possible to use one column to separate all the expected reactants and products, which ranged from light non-polar compounds to highly polar compounds such as H_2O and CH_3OH. Secondly it was necessary to prevent certain constituents from entering the Molesieve column, where they would be irreversibly adsorbed. This second aspect was especially critical as this process would lead to loss of resolution and eventual column deactivation. With timed valve switches and a temperature programmed regime it was possible to separate all the components with a single injection.

The detectors used on the system were a thermal conductivity detector (TCD) and an interchangeable mass spectrometer (MS), these detectors were configured in parallel. The column effluent was split in a 9/1 ratio by a fused silica Y-piece, the majority flow was to the TCD. The split ratio was achieved by the restriction of a fine capillary tube, which introduced the column effluent to the MS vacuum manifold.

2.1.3. MASS SPECTROMETER DETECTORS

Two different mass spectrometers were used in the course of these studies, these were an ion trap and a quadrupole MS. These units were interchangeable and had to be used independently, since both were housed on a common vacuum manifold. Effluent from the GC was introduced to the manifold through a fine capillary, passing through a heated transfer line.

The ion trap MS was a Varian Saturn model with a scan range from 10 to 650 atomic mass units, at unit resolution. During analysis the manifold temperature was maintained at 220°C, typical analysis parameters were 10 μs ionisation time, with a filament current of 25 μA and a multiplier voltage of 1800 ev. Under these conditions the MS was relatively insensitive, compared to maximum achievable performance, but was still more than adequate for the concentrations encountered in these studies. Data were collected by computer operating at 1 scan per second. The software allowed peak areas to be quantified, and also provided positive identification by matching mass spectra to entries in a standard NIST mass spectral library.

The quadrupole mass spectrometer was supplied by Hiden and operated over a range of 0-200 atomic mass units at unit resolution. It was possible to monitor 16 channels simultaneously, covering partial pressure ranges from $1x10^{-4}$ to $1x10^{-10}$ torr for any mass in the scan range. Data acquisition was extremely rapid and under normal operation all mass channels were scanned in approximately 0.2 s. When the quadrupole MS was used the vacuum manifold was maintained at room temperature. Data were recorded by computer using the Hiden mASSYT software package.

The need for two mass spectrometers arose from the large degree of cross ionisation demonstrated by CH_4 in the ion trap mass spectrometer. CH_4 cracking patterns with this instrument showed a m/e base peak at 29, as opposed to the expected peak at m/e 16. Considerable effort was applied to solve this problem, but a satisfactory solution could not be attained with the ion trap instrument. For this reason the

quadrupole MS was used for CH_4/D_2 exchange studies, details of which are given in section 2.2. Experiments investigating CH_3OH oxidation, and CH_4 partial oxidation (section 2.3.) were performed using the ion trap MS.

2.1.4. EXPERIMENTAL PROCEDURE

The catalysts employed in these experiments were used in the form they were supplied, without chemical pre-treatment. Before use catalysts were pelleted to a 0.6-1.0 mm uniform particle size range. This was achieved by pressing the materials under 10 tons pressure, in a 5 cm die for 3 minutes. The resulting disc was passed through 1.0 mm and 0.6 mm standard stainless steel sieves. The catalyst bed was packed to a length of 10 mm. This was measured when the bed was secured in place, and resulted in a bed volume of ca. 0.5 cm^3.

The syringe pump setting for the CH_3OH feed was 2.0, using a 5ml Hamilton syringe this equated to a gaseous CH_3OH flow rate of 6 ml min^{-1}. O_2 and He flow rates were set to 25 and 70 ml min^{-1} respectively. These conditions produced a gas hourly space velocity (GHSV) in the region of 12,000 h^{-1}.

This GHSV and the $CH_3OH/O_2/He$ ratio of approximately 1/4/12 was maintained throughout the series of experiments to screen catalysts for CH_3OH oxidation activity.

Once flow rates were stabilised and heating tapes maintained at the correct temperature, the reactor furnace was set to 100°C, and the system allowed to equilibrate for 1 hour. No catalysts showed any activity for CH_3OH oxidation at this temperature, and six analysis injections were made to determine the composition of the reactant feed. The furnace temperature was then increased to the next set-point, allowing 30 minutes stabilisation time, before the first injection was made. Catalytic activity was investigated in the temperature range 150-520°C, increments were either 25 or 50°C, depending on the activity shown by the catalyst. GC-MS analyses were made until steady state operation was reached, and 3 sets of consistent analysis data were obtained.

The TCD and MS were calibrated directly for O_2, CO, CO_2 and CH_3OH, response factors [92] were used to calculate quantities of $(CH_3)_2O$, $HCOOCH_3$ and HCHO. At low levels of CH_3OH conversion the % conversion was calculated on the basis of products detected, in accordance with equation 2.1.4.1.

$$CH_3OH\ Conv. = \frac{nC_n}{CH_3OH_{in}} \times 100\% \qquad (2.1.4.1.)$$

Where,
C_n = volume % of products containing carbon, with n carbon atoms per molecule,
CH_3OH_{in} = volume % CH_3OH in the feed gas.

This method proved more accurate than calculating the conversion based on CH_3OH peak area by difference, as it did not rely on the small difference between two large values. Higher levels of conversion, approximately >5%, were calculated by CH_3OH peak area difference, shown in equation 2.1.4.2.

$$CH_3OH\ Conv. = \frac{CH_3OH_{in} - CH_3OH_{out}}{CH_3OH_{in}} \times 100\% \qquad (2.1.4.2.)$$

Where,
CH_3OH_{out} = volume % CH_3OH in reactor effluent.

The differences in calculated CH_3OH conversions >5% were minor between the two methods, but for consistency the latter was used. Product selectivities were calculated in the form shown by equation 2.1.4.3.

$$Selectivity = \frac{nC_n}{\Sigma nC_n} \times 100\% \qquad (2.1.4.3.)$$

Carbon mass balances were calculated for selected results to act as a calibration check. Unfortunately % O_2 levels were outside the linear range of the detectors, so accurate O_2 mass balances could not be obtained.

2.2. METHANE/DEUTERIUM EXCHANGE EXPERIMENTS

2.2.1. REACTOR DESIGN

The microreactor for CH_4/D_2 exchange experiments is shown in figure 2.2.1.1. Gas flow rates were regulated by Brooks 5850TR mass flow controllers. To provide optimum flow stability Brooks high performance pressure regulators ensured a

constant inlet pressure was maintained on the mass flow units. He (99.995%) and CH_4 (99.0%) were fed directly to the catalyst bed, whilst H_2 (99.99%) and D_2 (99.7%) were fed to a 4-port Valco valve fitted with 1/16" connections. The flow path through the valve could be switched, introducing pulses of D_2 to the catalyst.

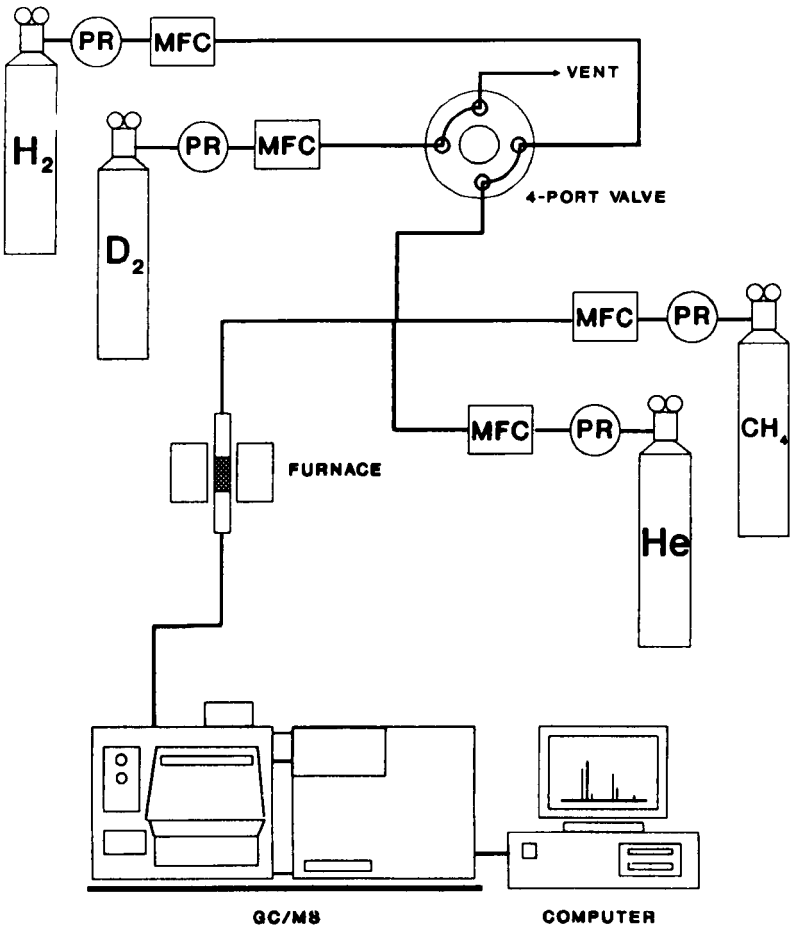

Figure 2.2.1.1. Microreactor design for CH_4/D_2 exchange studies. Key: MFC=mass flow controller; PR=pressure regulator.

The 4-port valve was switched by a 2-way actuator, driven by compressed air. The timing and duration of valve switches were controlled by a Syrelec electronic timing device. The use of compressed air to actuate the valve was chosen in preference to electrical actuators, because switching at higher speeds could be achieved. This configuration was designed so that under normal operation the catalyst was conditioned under a flow of He, CH_4 and H_2. D_2 was only used for actual exchange experiments. The reactor was made from 6 mm o.d. fused silica tubing

approximately 70 mm in length. Heating was by a furnace with a uniform heated length of 25 mm. Temperatures were regulated by a Eurotherm controller via a thermocouple mounted in the furnace a few mm below the reactor tube.

The reactor was built from 316 stainless steel tubing, gas supply lines were 1/8" o.d., other lines were 1/16" o.d. The couplings used included conventional Swagelok, Swagelok chromatography and Valco chromatography fittings. The fabrication of the reactor was such that any dead volume, particularly after the catalyst bed, was reduced to a minimum.

Analysis of the reaction products was performed on-line using the GC-MS system detailed in section 2.1.2., fitted with the quadrupole mass spectrometer.

2.2.2. EXPERIMENTAL PROCEDURE

The catalysts were loaded into the reactor tube in powdered form. The catalyst bed length was typically 25 mm and held in place between two silica wool plugs. Mass flow controller settings for CH_4 and H_2/D_2 corresponded to 0.69 and 0.83 ml min^{-1} respectively. He diluent was not used in these studies. The GHSV was 290 h^{-1}, which corresponded to a contact time of approximately 12 s.

Catalysts were pre-treated in-situ with CH_4 and H_2 at 540°C for 2 hours prior to use. Approximately 120 s before the introduction of a D_2 pulse, the D_2 flow rate was set to 0.83 ml min^{-1} and allowed to stabilise. A 200 s pulse of D_2 was then introduced to the catalyst. 185 s after the pulse was commenced the reactor effluent was injected on to the GC columns. Once the pulsing valve returned to the original position the D_2 flow was stopped to preserve the supply. CH_4 was separated efficiently from residual O_2 and N_2, by the GC system and the CH_4 peak analysed by monitoring m/e values 15, 16, 17, 18, 19 and 20. Masses 15 and 16 were measured on a 10^{-5} torr partial pressure range, and masses 17-20 on a 10^{-7} torr range. These analyses were repeated until concordant results were obtained. The reaction temperature was then decreased and allowed to stabilise for 15 minutes, further pulses of D_2 were introduced.

2.2.3. CALCULATION METHOD FOR EXCHANGE RESULTS

The CH_4 chromatographic peak shapes were found to differ between analyses, this was probably due to H_2O accumulation on the Molesieve column affecting performance. Hence it proved unreliable to directly use m/e partial pressure ratios from peak heights. However, the software used allowed areas to be integrated for each m/e peak.

The cracking patterns for CH_4 and deuterated methanes have been well established [93-95]. In our study we have used m/e 16 to identify CH_4, and m/e 17, 18, 19 and 20 were used to identify the species CH_3D, CH_2D_2, CHD_3 and CD_4 respectively. In order to quantify the deuterated compounds, the MS response factor was calculated by calibration with CH_4 in He. The response factor obtained was applied directly to quantify the deuterated products. This approach has been based on the assumption that the relative MS sensitivities for deuterated species were identical, as has been demonstrated in studies by Hill et. al. [93].

The integrated peak area for m/e 17 was corrected for contributions from naturally abundant ^{13}C in CH_4. Under conditions where the exchange reaction produced CH_2D_2 the m/e 17 peak area was also corrected for contributions from the cracking pattern of the CH_2D_2 molecule. The 18/17 m/e ratio from the CH_2D_2 species was taken to be 0.55 [93]. In reality this contribution was always small, and proved insignificant in the final calculation. Interfering contributions to peak areas introduced via the reactor, such m/e 17 and 18 from atmospheric H_2O or m/e 16 from O_2, did not influence the results as they were removed chromatographically.

The MS was also calibrated for higher levels of CH_4, around 40-50%, the subsequent response factor was used to calculate the exact CH_4 concentration in the feed. From these figures it was possible to calculate the conversion to CH_3D, CH_2D_2, etc, and to the total deuterated product. The conversion was calculated on the detected products, in a similar manner to that outlined in equation 2.1.4.1.

2.3. PARTIAL OXIDATION OF METHANE

2.3.1. REACTOR DESIGN

The microreactor designed and used for CH_4 partial oxidation experiments is shown schematically in figure 2.3.1.1. on the following page.

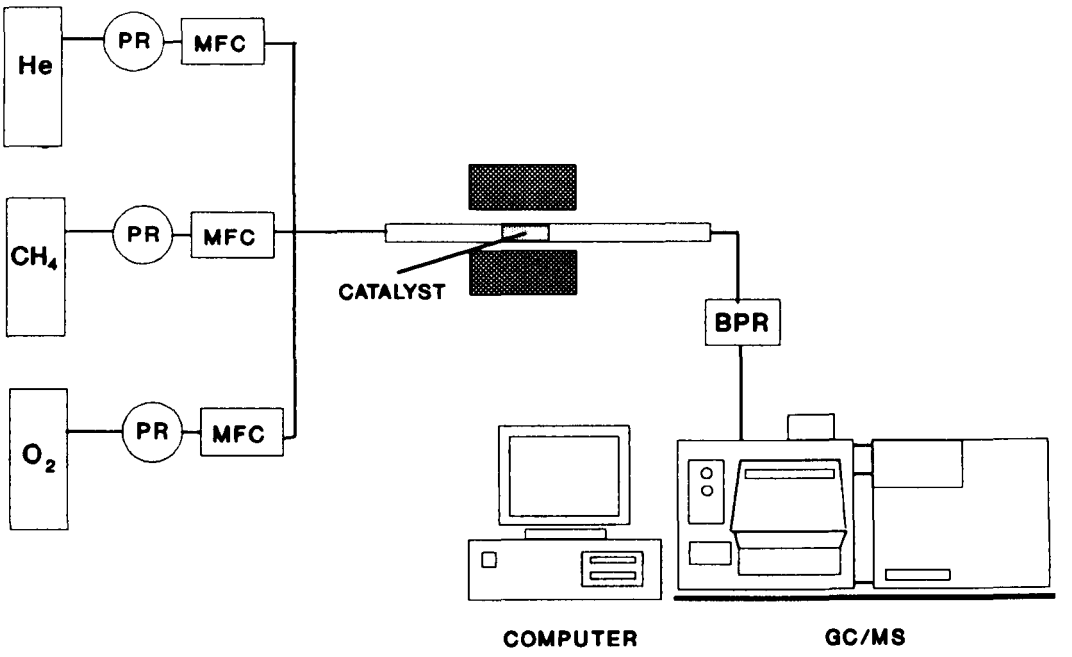

Figure 2.3.1.1. Reactor design for CH_4 partial oxidation experiments. Key: MFC=mass flow controller; BPR=back pressure regulator.

Brooks 5850TR mass flow controllers were used to regulate the flow rates of CH_4 (99.0%), O_2 (99.5%) and He (99.999%). The reactor was made from 1/2" o.d. stainless steel lined with a fused silica tube. On heating to ca. 800°C the silica tube was adequately sealed into the stainless steel jacket. The reactor pressure was controlled by a Tescom high temperature back pressure regulator. The pressure in the system was indicated by a Bourdon gauge.

The catalyst charge was held in place between two silica wool plugs, and heated by a Carbolite tube furnace. Reaction temperatures were measured by a thermocouple located centrally in the heated zone of the furnace. After the catalyst bed the microreactor lines and back pressure regulator were trace heated to 200°C. Reaction

products were analysed using the Varian GC-MS system fitted with the ion trap detector, previously described in sections 2.1.2. and 2.1.3.

2.3.2. EXPERIMENTAL PROCEDURE

Catalysts were pelleted to a 0.6-1.0 mm size by the same procedure formerly adopted (see section 2.1.4.), and loaded to a constant volume of 0.75 cm^3. The catalyst were all of similar density, and approximately 1.1 g of catalyst was used. Flow rates were set to 46, 6 and 10 ml min^{-1} respectively for CH_4, O_2 and He. Gas hourly space velocities were roughly 5,000 hr^{-1}.

Feed gas analysis was made at 250°C, similar analysis methods and equilibration times to those for CH_3OH oxidation experiments were used. Catalytic activity was investigated in the temperature range 350-550°C.

As a consequence of the high CH_4 concentration, conversion was calculated on the basis of detected products, as shown similarly in equation 2.1.4.1. O_2 conversion was calculated by difference, (equation 2.3.2.1.).

$$O_2 \text{ Conv.} = \frac{O_{2in} - O_{2out}}{O_{2in}} \times 100\% \qquad (2.3.2.1.)$$

Where,
O_{2in} = volume % O_2 in reactant feed,
O_{2out} = volume % O_2 in reactor effluent.

Product selectivities were calculated as indicated in equation 2.1.4.3.

2.3.3. CATALYST PREPARATION

The Ga_2O_3 and MoO_3 catalysts were used as supplied by Aldrich. Ga_2O_3/MoO_3 and ZnO/MoO_3 catalysts were prepared by grinding the oxides in a 1/1 Mo/M, (where M = Ga or Zn), molar ratio in a large mortar and pestle for 20 minutes. The resulting finely divided powder was calcined in static air at 650°C for 3 hours, in a fused silica boat. The calcined sample was ground for a further 20 minutes before use.

2.4. METHODS OF CATALYST CHARACTERISATION

2.4.1. POWDER X-RAY DIFFRACTION

A crystalline powder may be assumed to consist of a large number of microcrystalline particles. If this powder is packed in a totally random manner, then all crystal lattice planes will be present in every orientation. When an X-ray beam is incident on this sample, a specific set of crystal planes may be orientated such that the incident beam is diffracted in accordance with the Bragg equation (2.4.1.1).

$$n\lambda = 2\,d\,\mathrm{Sin}\Theta \qquad (2.4.1.1.)$$

Where,
λ= wavelength of incident radiation,
d = inter planar spacing,
Θ = diffracted angle.

It follows that if the sample is moved through an angular range Θ, with respect to the source, different sets of crystal planes will satisfy the criteria in the Bragg equation, producing a diffracted beam at an angle 2Θ.

The plot 2Θ against the intensity of the diffracted X-ray beam gives rise to the familiar powder diffraction pattern. The diffraction pattern may be regarded as the 'fingerprint' of the sample, from which phase identification is possible. The technique is limited by particle size dimensions, typically crystalline particles with diameters smaller than 30 Å are not detectable, due to extensive line widths.

2.4.2. DETERMINATION AND ANALYSIS OF X-RAY DIFFRACTION PATTERNS

X-ray diffraction patterns were recorded using a Hiltonbrooks modified Phillips 1050W diffractometer, designed on the Bragg-Brentano geometry. The diffractometer consisted of essentially three components, these were the X-ray source, sample mounting compartment and the X-ray detector. The X-ray source used was a Cu target with a Ni filter, producing Cu $K\alpha_1$ and Cu $K\alpha_2$ radiation with wavelengths 1.54056 Å and 1.54439 Å respectively. The $K\alpha_1/K\alpha_2$ intensity ratio of the source was 1.92. For phase identification purposes it was acceptable to use the

weighted average of these wavelengths. The source was operated at 40 KeV with a 20 mA current.

Samples were packed into a cut-out in a flat aluminium holder. It was important to produce a flat surface relative to the holder, to minimise errors in peak position associated with sample height displacement [96]. Diffracted X-rays were detected using a scintillation counter. Diffractometer control and data acquisition were controlled by computer.

Diffraction data were recorded in the scan range $5 < 2\Theta < 75$, with a step size of 0.05° and a counting time of 1 s per interval. Data were analysed using Sietronics Trace Processing software V2.2., this allowed the background contribution to be removed, and peak positions and relative intensities determined. Phase identification was performed using Fein Marquart Associates Micro Powder Diffraction Search and Match, (μ-PDSM), software. Experimental patterns were compared against entries in the Standard Powder Diffraction File [97].

2.4.3. BET SURFACE AREAS

Catalyst surface areas were measured by physical adsorption of N_2 in accordance with the method developed by Brunauer, Emmett and Teller (BET) [98]. The BET method was based on a theoretical model describing the physical adsorption of an inert gas on a solid. The BET equation which was derived from this model may be rearranged and expressed in the linear form shown in equation 2.4.3.1.

$$\frac{P}{V(P_0-P)} = \frac{(C-1)}{V_mC}\frac{P}{P_0} + \frac{1}{V_mC} \qquad (2.4.3.1.)$$

Where,
V = volume adsorbed at pressure P,
V_m = volume of gas required for monolayer coverage,
P_0 = saturated vapour pressure of adsorbate at temperature of determination,
C = constant.

Thus, if the gaseous uptake is measured in the range $0.05 < P/P_0 < 0.3$, the constant C and V_m can be readily obtained. Subsequently the surface area of the sample can be calculated from the volume of gas required for monolayer coverage, assuming an

average molecular cross sectional area for the adsorbate. The value for N_2, generally the most widely used adsorbate, is 0.162 nm^2 at 77 K [99]. The value for C in the BET equation is related exponentially to the heat of adsorption of the monolayer, and is generally similar for classes of materials, such as oxides and metals.

However, this method of surface area measurement does have certain limitations, and is only strictly valid up to P/P_0 values of 0.3. Above this value the process of liquid condensation begins in the smallest micropores of the catalyst.

2.4.4. DETERMINATION OF SURFACE AREAS

Surface area measurements were carried out using a modified Digisorb apparatus. The system was computer controlled and pressure readings were made using a barocell. The powdered sample was weighed accurately into a glass sample bulb, which was attached to the vacuum manifold by a compression fitting. The weight of sample used was chosen to provide a sample area in the range 10-100 m^2. Prior to determination of the adsorption isotherm the sample was outgassed under vacuum at approximately 300°C to remove any contaminating physisorbed species. The outgassing procedure usually lasted between 2-15 hours depending on the sample type and weight. When the pressure had reached $6x10^{-2}$ torr, no further pressure drop was observed and outgassing was stopped.

Once the sample was cooled to room temperature the dead volume of the apparatus was measured accurately by expansion of He from a known volume. The sample bulb was then immersed in liquid N_2 to a fixed level, and the dead volume at this temperature determined. The remaining He was pumped from the system and the gas supply changed to N_2.

To measure the adsorption isotherm a known volume of N_2 was admitted to the sample at 77 K and the pressure allowed to equilibrate for 5 minutes. In practice there was little change in the equilibrium pressure after 1 minute. From this pressure the volume of adsorbed gas was determined and the dosing process repeated with progressively higher dosing pressures. In total six such measurements

were made to construct the adsorption isotherm. The surface area was derived from this isotherm as described in section 2.4.3.

2.4.5. X-RAY PHOTOELECTRON SPECTROSCOPY

The process of X-ray photoelectron spectroscopy (XPS) involves the irradiation of a sample with monoenergetic soft X-rays, causing the emission of electrons which are energy analysed. A proportion of these emitted electrons are called photoelectrons. The technique requires high vacuum for effective operation. The emission of a photoelectron may be represented by figure 2.4.5.1.

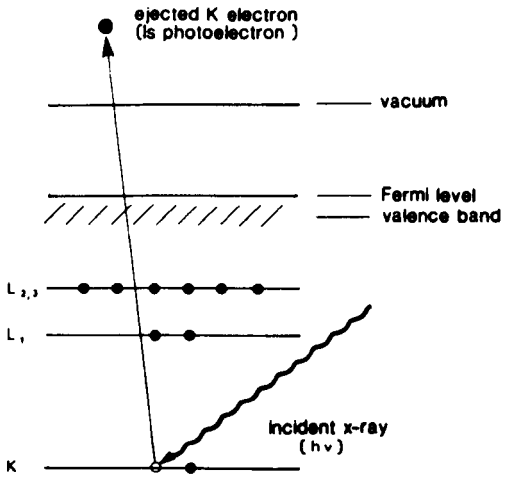

Figure 2.4.5.1. Process leading to the production of a photoelectron.

The photon energy of the source used for XPS is such that electrons are ejected from core atomic levels. The kinetic energy (K.E.) of the emitted electrons is described by equation 2.4.5.1.

$$K.E. = h\nu - (B.E. + \phi) \qquad (2.4.5.1.)$$

Where,
$h\nu$ = photon energy of the source,
B.E. = binding energy of atomic orbital from which the photoelectron is ejected,
ϕ = work function of the sample.

The emission of a photoelectron is complemented by the emission of an Auger electron, a process depicted in figure 2.4.5.2.

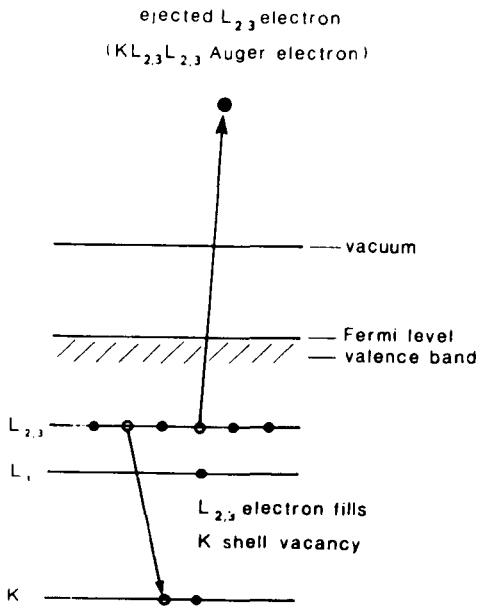

Figure 2.4.5.2. Emission process of Auger electrons.

The Auger process occurs when an electron from an outer orbital falls into a vacancy created in an inner orbital, with the ejection of a secondary electron. The kinetic energy of an Auger electron is equal to the difference in energy between the initial ion and the final doubly charged ion, and so unlike photoelectrons the energy is independent of the ionising energy.

Incident photons typically penetrate the sample to a depth of 10^{-6} m, while the mean free path length for electrons is of the order 10^{-9} m. This implies that while ionisation occurs to a depth of 10^{-6} m only photoelectrons from a depth of 10^{-9} m below the surface can leave without energy loss. This phenomena makes XPS a surface sensitive technique providing information about the few uppermost atomic layers. Ejected electrons which are submitted to energy loss processes contribute to the background.

The technique is capable of identifying chemical states from the chemical shift of line positions, quantitative data may also be obtained from peak areas.

2.4.6. DETERMINATION OF X-RAY PHOTOELECTRON SPECTRA

The instrument used to record spectra was an ESCA 3 apparatus manufactured by VG. Al and Mg X-ray sources were used, in both cases the Kα lines were filtered for use. The X-ray photon energies were 1486.6 and 1253.9 eV for Al and Mg

respectively, with representative line widths of ca. 0.7 eV. The majority of analyses were performed using the Al source, the Mg source was used to determine positions of photoelectron peaks which overlapped with Auger peaks when the Al source was employed. The X-ray source in these experiments was operated at 8 KeV and 20 mA.

Samples were mounted on a probe in powdered form using a piece of double sided adhesive tape. The probe assembly was evacuated in a preparation chamber until pressures in the range 10^{-7} torr were achieved. The X-ray beam was incident on the sample at a 45° angle normal to the sample, the analyser was also mounted at the same orientation to the sample and 90° to the source, in order to enhance surface sensitivity. The electron energy analyser was an energy dispersive type, operating with a typical pass energy of 100 eV giving maximum sensitivity. To improve the resolution of some doublet species the pass energy was reduced to 50 eV but the increase in resolution was at the expense of sensitivity. Electron signals were amplified using a channel electron multiplier which was operated with an amplification voltage of 3.3 KeV.

Data were recorded and analysed by computer using Spectra v5.0 software. Initially wide scans over a 1000 eV binding energy range were made using a 0.500 step size and a 0.08 dwell time. Once peak positions were established approximately, narrower regions covering peaks of interest were scanned, with a decreased step size of 0.100. Scans were repeated several times to improve the signal to noise ratio.

Peak positions were corrected for charging effects by referencing spectral lines relative to the C1s peak which was always present from residual carbon. The binding energy of the C1s peak was assumed to be at 284.6 eV [100].

Quantitative data were based on integrated peak areas corrected for the number of scans accumulated. The surface atomic concentrations of elements, C_x, were subsequently calculated using equation 2.4.6.1.

$$C_x = \frac{A_x/S_x}{\Sigma A_i/S_i} \qquad (2.4.6.1.)$$

Where,
A_x = corrected peak area of element x,
S_x = atomic sensitivity factor for element x.

Atomic sensitivity factors have been tabulated for many of the photoelectron lines of the elements [101].

CHAPTER 3

METHANOL OXIDATION STUDIES

3.1. INTRODUCTION

This study was undertaken with the objective to investigate the stability of CH_3OH over a wide range of single oxides. CH_3OH is a polar compound and can act as a Lewis base due to the presence of the non bonding lone pairs of electrons on the oxygen atom. These may be donated to a proton or to another Lewis acid. CH_3OH may also act as a weak Bronsted acid, due to the dissociation of the hydrogen atom of the hydroxyl group. The interaction of CH_3OH with a dehydroxylated oxide surface results in heterolytic dissociative adsorption, shown in figure 3.1.1.

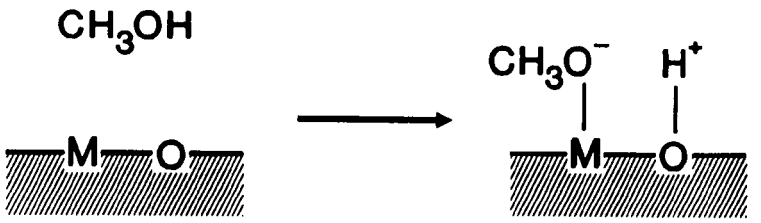

Figure 3.1.1. Dissociative adsorption of CH_3OH on an oxide surface.

The initial surface species formed is methoxide, bonded to a surface cation, and a proton associated with lattice oxygen.

CH_3OH decomposition has been investigated over several oxides, ZnO has been the most studied, arising from the incorporation of ZnO in the $Cu/ZnO/Al_2O_3$ CH_3OH synthesis catalyst [11]. Tawarah and Hansen [102] have investigated CH_3OH decomposition over ZnO in a flow system. The reaction was studied in two different temperature ranges, 180-240°C and 290-340°C. In the lower temperature range CH_3OH decomposed to HCHO and H_2, whilst in the higher range HCHO, CO, CO_2 and H_2 were the decomposition products. Interaction of CO with ZnO in the higher temperature range did not yield CO_2, indicating that CO_2 was not produced by further oxidation of CO. Isotopic studies showed that CO and CO_2 were produced by the participation of lattice oxygen. These products were considered to

have been formed either through HCHO or more probably via a surface formate species.

Ultra High Vacuum (UHV) investigations have shown that adsorbed methoxide reacts by two distinct pathways on the surface of ZnO, depending on the temperature of reaction [103]. At lower temperatures CH_3OH reacted in accordance with the scheme shown by figure 3.1.2.

$$OH^-_{(s)} + CH_3O^-_{(ad)} \text{ ----> } HCHO_{(ad)} + O^{2-}_{(s)} + H_{2(g)}$$

$$\Big|$$

$$HCHO_{(g)} \text{ or } CO_{(g)} + H_{2(g)}$$

Figure 3.1.2. Low temperature CH_3OH decomposition pathway over ZnO.

This pathway produced adsorbed HCHO and gaseous H_2 from the methoxide species, subsequently HCHO was desorbed into the gas phase. At higher temperatures a new pathway predominated, this is shown in figure 3.1.3.

Methoxide was oxidised to an adsorbed formate species which decomposed to carbon oxides, H_2 and H_2O. The latter

$$CH_3O^-_{(ad)} + ZnO \text{ ----> } HCOO^-_{(ad)} + Zn_{(ad)/(g)} + H_{2(g)}$$

$$\Big|$$

$$CO_{(g)}, CO_{2(g)}, H_{2(g)}, H_2O_{(g)}$$

Figure 3.1.3. High temperature CH_3OH decomposition pathway over ZnO.

pathway involved the reduction of ZnO, with the possibility that at elevated temperature Zn atoms were evolved into the gas phase. Indeed, experiments using a flow reactor have demonstrated that metallic Zn was condensed on cold reactor surfaces [102]. Generally, agreement between the two types of studies is good, with the possible exception of CO production by the lower temperature pathway.

Other oxides have also been investigated for CH_3OH decomposition. Cr_2O_3 has been studied by Yamashita et. al. [104], major products at 400°C were CO, CO_2 and H_2; CH_4 and $(CH_3)_2O$ were also produced in minor quantities. The sole surface

species detected by infra-red spectroscopy was the formate species. Decomposition of formate was found to be highly dependent on the presence of CH_3OH vapour, since it decomposed more easily in the presence of CH_3OH than in vacuum. The difference in activation energy between the different conditions was ca. 71 kJ mol^{-1}. It was proposed that electron donating properties of the methoxy group caused the facile decomposition of the formate species.

Kagel has studied the interaction with gamma-Al_2O_3 [105], in the temperature range 25-500°C, three different surface species were identified by infra-red spectroscopy. At ambient temperature physisorbed CH_3OH and chemisorbed methoxide were present, methoxide was continuously present up to 430°C. Between 150-430°C adsorbed carboxylate was also observed. Above 500°C only carboxylate was present. No desorbed decomposition products were reported, but this study has shown that the carboxylate is a possible alternative surface species, formed by reaction of CH_3OH on the surface.

CH_3OH decomposition on CuO and Cu_2O at 200°C initially produced CO_2, H_2 and H_2O [106]. As the extent of reaction increased methyl formate ($HCOOCH_3$) was produced, in a similar manner to a Cu wire, indicating that under these conditions the oxides were completely reduced to metallic Cu.

Somewhat different behaviour has been demonstrated over highly dehydroxylated TiO_2 [107]. Temperature Programmed Desorption (TPD) showed that at 250°C coke was readily formed on the rutile phase, and CH_4 was the major product, with minor quantities of CO, CO_2 and H_2. On the contrary, the anatase phase produced large quantities of $(CH_3)_2O$ at 335°C, with some coking and traces of C_2H_6 at higher temperature. The same trends were observed when studies were repeated in a flow system. The formation of $(CH_3)_2O$ was thought to take place by reaction of methoxide groups on adjacent sites, and was influenced by methoxide coverage.

These studies indicate the ways in which CH_3OH can react with some representative oxide surfaces. They do not however indicate the stability of CH_3OH under oxygen

rich conditions, which are closer to the catalytic conditions expected in the present study.

The majority of research which has been published concerning CH_3OH oxidation has concentrated on the selective oxidation to HCHO over vanadium and molybdenum oxide systems [108,109]. In general these studies have been performed at 200-350°C, attempting to maximise HCHO yields. The catalysts were often multi-component oxides, which makes the identification of discrete phases with low CH_3OH oxidation activity difficult.

Studies of CH_3OH oxidation have been made with respect to emission control from alcohol fuelled vehicles. These have focussed on supported group 9, 10 and 11 metals [110]. One interesting paper in the same area of research has considered CH_3OH oxidation over a gamma-Al_2O_3 supported transition metal oxides [111]. Catalysts were prepared by impregnation followed by calcination, and results of characterisation by Scanning Electron Microscopy (SEM) and XRD indicated the supported oxides were CrO_3, Mn_2O_3, Fe_2O_3, Co_3O_4, NiO and CuO. Oxide loadings were all calculated to be 0.08 oxide/support molar ratios.

Catalytic activity was investigated between 25-300°C, at 1.5 bar, using a $CH_3OH/O_2/N_2$ feed with the ratio 1/11/300, in a recirculating reactor. The Cr, Mn, Fe, Co and Ni oxide catalysts all showed similar reaction profiles, forming $(CH_3)_2O$, CO and CO_2 as the major carbon products, whilst the CuO catalyst produced only CO_2. Untreated gamma-Al_2O_3 was also tested, showing high selectivity to $(CH_3)_2O$ with lower levels of carbon oxides than the supported catalysts.

Comparison of CH_3OH conversion at set temperatures indicated little difference between catalysts, but CO_X yields at 150 and 200°C were significantly different. The ranking order at 200°C based on CO_X yield was CuO > CrO_3 > Mn_2O_3 > Co_3O_4 > NiO > Fe_2O_3.

The effect of oxide loading was studied for the CuO system. Decreasing the loading decreased CO_X selectivity, whilst $(CH_3)_2O$ increased as a consequence of increased

exposure of the gamma-Al_2O_3 support. The studies mentioned above have the opposing aim to that of the present study, i.e. the best catalyst was the most efficient for CH_3OH combustion and not preservation.

There is a shortage of comparable data concentrating on the oxidation of CH_3OH over simple oxides, under relevant reaction conditions, therefore, this study was carried out. Results from these studies will be used in the wider context of catalyst design for CH_4 partial oxidation.

3.2. RESULTS

3.2.1. CATALYST CHARACTERISATION

The metal oxides used for CH_3OH oxidation and CH_4/D_2 exchange studies have been characterised by powder X-ray diffraction and surface area measurement. The results obtained are shown in table 3.2.1.1.

Catalyst surface areas varied considerably. The highest was 278 m^2g^{-1} for SiO_2, a commercial grade Aerosil 380 supplied by Degussa. Al_2O_3, also supplied by Degussa, grade Aluminoxid C, also showed a relatively high area of 78 m^2g^{-1} compared to the other oxides of this study. These findings are consistent with the use of these materials for high area catalyst supports.

Ga_2O_3, MgO and TiO_2 all had intermediate surface areas in the range 22-51 m^2g^{-1}. Most oxides showed low surface areas, less than 7.5 m^2g^{-1}, and a considerable number were less than 2 m^2g^{-1}. The surface areas of Bi_2O_3 and Ta_2O_5 were too low to be measured by the apparatus employed, even though a considerable mass of catalyst was used. For both of these materials the surface area has been quoted as less than the lowest area measured, which was 0.5 m^2g^{-1} for La_2O_3 and MoO_3.

Powder X-ray diffraction showed that the majority of oxides were present as a single crystalline phase. The exceptions were Al_2O_3, Ga_2O_3, Nb_2O_5, Pr_6O_{11} and TiO_2. Phase identification of Al_2O_3 proved difficult due to low intensity broad diffraction peaks, the same type of diffraction pattern was also observed for Ga_2O_3, although these effects were less extreme. These observations may be attributed to

the presence of transitional defective spinel type phases [112]. This structure has both octahedrally and tetrahedrally coordinated cations, as opposed to the thermodynamically stable corundum structure, with cations only in octahedral coordination. The Al_2O_3 sample was a mixture of the gamma, delta and theta phases. The Al_2O_3 phase transitions are continuous making the isolation of any one phase difficult, the same considerations apply to the closely related Ga_2O_3 phase.

Table 3.2.2.1 BET surface area and phases identified by powder X-ray diffraction.

Oxide	BET Surface Area/m^2g^{-1}	Identified phase	Crystal system
Al_2O_3	78	transitional	N/A
Bi_2O_3	<0.5	Bismite	Monoclinic
CaO	3.1	Lime	Cubic
CdO	1.3	Monteponite	Cubic
CeO_2	11.0	Cerianite-(Ce)	Cubic
Co_3O_4	3.3	Co_3O_4 (Spinel)	Cubic
Cr_2O_3	4.2	Eskolaite	Rhombohedra
CuO	1.4	Tenorite	Monoclinic
Fe_2O_3	5.2	Hematite	Rhombohedral
Ga_2O_3	22	Alpha-Ga_2O_3	Hexagonal
		Beta-Ga_2O_3	Monoclinic
		Gamma-Ga_2O_3	Cubic
Gd_2O_3	1.3	Gd_2O_3	Cubic
La_2O_3	0.5	La_2O_3	Hexagonal
MgO	51	Periclase	Cubic
Mn_2O_3	3.8	Bixibite-C	Cubic
MoO_3	0.5	Molybdite	Orthorhombic
Nb_2O_5	2.1	T-form	Orthorhombic
		M-form	Monoclinic
Nd_2O_3	1.6	Nd_2O_3	Hexagonal
NiO	1.9	Bunsenite	Cubic
Pr_6O_{11}	2.3	$PrO_{1.83}$	Cubic
		PrO_2	Cubic
Sb_2O_3	1.8	Senarmontite	Cubic
SiO_2	278	amorphous	N/A
Sm_2O_3	4.3	Sm_2O_3	Cubic
SnO_2	4.6	Cassiterite	Tetragonal
Ta_2O_5	<0.5	Ta_2O_5	Monoclinic
Tb_4O_7	0.7	Tb_4O_7	Cubic
TiO_2	48	Rutile	Tetragonal
		Anatase	Tetragonal
V_2O_5	6.7	Shcherbinaite	Orthorhombic
WO_3	0.8	WO_3	Monoclinic
Y_2O_3	3.8	Y_2O_3	Cubic
Yb_2O_3	3.8	Yb_2O_3	Cubic
ZnO	7.4	Zincite	Hexagonal
ZrO_2	6.5	Baddelyite	Monoclinic

The structure of Nb_2O_5 is complex in nature, with many forms identified [113]. The T form, commonly denoted as the low temperature form, transforms to the M or medium temperature form around 800°C. The mode of preparation is critical, strongly influencing the phases produced, some of which do not have resolved structures.

The identified praseodynium oxide phases, $PrO_{1.83}$ and PrO_2 are consistent with the findings of Hyde et. al. [114]. Oxidation and reduction between these states is relatively facile at low temperatures. Nine stable states, with metal/oxygen ratios from 1.5 to 2.0 have been identified at 1 bar oxygen pressure up to 1050°C.

Two phases of TiO_2 were identified, these were anatase and rutile. An approximate evaluation of relative phase concentrations showed that the anatase/rutile ratio was ca. 2, consistent with findings that anatase is the more stable phase by 8-12 kJ mol^{-1} [115].

All oxides were highly crystalline with the exceptions of Al_2O_3 and Ga_2O_3, which have been noted previously, and SiO_2 which was totally amorphous. The SiO_2 used was a fumed material manufactured by the hydrolysis of a volatile silane compound in an O_2/H_2 flame. This method is used specifically to produce a finely divided, high area and high purity material, which is not expected to be crystalline. The assessment of crystallinity of Fe and Co oxides was complicated by the background contribution from fluorescence. This effect was due to the excitation of Fe and Co atoms by the Cu Kα source. On relaxation X-rays are emitted at indiscriminate angles, contributing to the background. Although this process was evident it was still possible to easily detect diffracted peaks above the enhanced background.

3.2.2. CATALYTIC ACTIVITY

The conversion of CH_3OH and the selectivity to products over the temperature range 150-500°C are shown for all oxides in figures 1-30 in Appendix B. The reaction conditions used a $CH_3OH/O_2/He$ feed ratio of 1/5/12 with a GHSV of 12,000 h^{-1}. Carbon balances were in excess of 95% for all results shown.

The results showed a wide range of activity, but in many cases CH_3OH conversion and the distribution of products followed broadly similar patterns. On this basis it was possible to categorise oxides together in groups, these are shown in table 3.2.2.1.

Table 3.2.2.1. Classification of oxides based on CH_3OH conversion and product distributions.

Group	Oxide
1	Bi_2O_3, CdO, CuO, Cr_2O_3, PbO
2	CaO, CeO_2, Gd_2O_3, La_2O_3, MgO, Mn_2O_3, Nd_2O_3, NiO, Pr_6O_{11}, Sm_2O_3, SnO_2, Tb_4O_7, Y_2O_3, Yb_2O_3, ZnO
3	Al_2O_3, Co_3O_4, Fe_2O_3, Ga_2O_3, SiO_2, TiO_2, V_2O_5, ZrO_2
4	Nb_2O_5, Ta_2O_5, WO_3
5	MoO_3
6	Sb_2O_3

The oxides of Bi, Cd, Cu, Cr, Mn, Ni and Pb all showed similar behaviour. CH_3OH conversion was observed at relatively low temperatures. This was particularly noticeable for Cr_2O_3 and CuO which showed 100% conversion at 200°C. Carbon oxides were the main products, with CO_2 predominant at all temperatures. CdO and CuO produced CO_2 alone, whilst Bi_2O_3, Cr_2O_3 and PbO also showed low selectivity to CO, with a maximum of 2-3% around 300°C.

Mn_2O_3 and NiO exhibited slightly different behaviour, showing some selectivity to $HCOOCH_3$ and HCHO respectively, at very low levels of conversion. These oxides were still included in this group due to their typically steeply rising conversion with temperature, and the production of CO_2 as the major product.

Oxides classed in group 2 also showed the general trends of relatively steeply rising CH_3OH conversion with temperature, but the major products were still carbon

oxides. Unlike oxides in group 1, these materials tended to produce high levels of CO as well as CO_2. Y_2O_3 and all the rare earth oxides were included in this group, all of which, with the exception of Yb_2O_3, produced $HCOOCH_3$ at low CH_3OH conversion. The yield of this product was low and it was only observed below 300°C. Above this temperature CO and CO_2 were the sole products. CO selectivity passed through a maximum in the range 300-400°C, in cases were CH_3OH conversion was close to 100%. For the oxides Gd_2O_3, Nd_2O_3, Sm_2O_3 and Yb_2O_3 this maximum was mirrored by a decrease in CO_2 selectivity. At 500°C CH_3OH conversion was 100% in all cases.

MgO showed 6% selectivity to HCHO at 10% conversion and 250°C, above this temperature only CO and CO_2 were produced. Selectivity to CO increased steadily with temperature at the expense of CO_2 selectivity, and at ca 500°C CO became the most selective product.

The remaining two oxides in this group, SnO_2 and ZnO, did not produce any oxygenated species at low conversion, both produced only carbon oxides.

Oxides assigned to group 3 showed appreciable selectivity to $(CH_3)_2O$ and HCHO at all levels of conversion. Fe_2O_3, Co_3O_4 and V_2O_5 all gave similar product distributions, showing high selectivity to HCHO below 325°C. V_2O_5 was the most selective, initially showing 100% selectivity at up to 20% conversion. The maximum per pass yield was obtained at 250°C, with 92% selectivity at 94% conversion. As temperatures were increased selectivity to CO and CO_2 increased until at 500°C CO_2 was almost the exclusive product. A maximum CO selectivity was observed for Co_3O_4 and Fe_2O_3 at the highest temperature at which HCHO was no longer detected. Full reaction profiles were not determined for SiO_2, but it was clear that HCHO was a major product at lower temperatures, while CO and CO_2 were exclusive products above 400°C.

The other oxides in this group, Al_2O_3, Ga_2O_3, TiO_2 and ZrO_2, all exhibited significant selectivity to $(CH_3)_2O$. Al and Ga oxides proved highly selective towards $(CH_3)_2O$, both showed 100% selectivity at the onset of activity. As the

temperature and CH_3OH conversion increased, selectivity to the ether fell steadily to 91% at 300°C for Ga_2O_3, and 89% at 350°C for Al_2O_3. Above these temperatures $(CH_3)_2O$ selectivity fell sharply, accompanied by an increase in CO_X levels. A CO maximum was observed with Ga_2O_3 at ca. 390°C, around the temperature at which $(CH_3)_2O$ was no longer detected. Ga_2O_3 also showed the lowest light-off temperature of all the materials investigated, this was around 150°C.

Full reaction profiles could not be obtained for Al_2O_3 and TiO_2 due to chromatographic problems, but general features could be distinguished. TiO_2 and ZrO_2 were similar in many respects to Al_2O_3 and Ga_2O_3, but $(CH_3)_2O$ selectivities were lower and CH_3OH conversion did not commence until 250°C.

Although the oxides in this group may be subdivided into those that produced HCHO, and others which produced $(CH_3)_2O$, there are general similarities. Above 400°C CH_3OH conversion was always 100%, and oxygenated products were not detected with carbon oxides formed exclusively.

Nb_2O_5, Ta_2O_5 and WO_3 were classed in group 4. These oxides showed high selectivity to the oxygenated products HCHO and $(CH_3)_2O$, at all temperatures. Catalysts in this group did not show complete CH_3OH conversion even at the highest temperature investigated. All three oxides showed remarkably similar behaviour, at lower temperature $(CH_3)_2O$ was the most selective product. The highest per pass yield was 86% for WO_3 at 400°C, compared to 39% for Nb_2O_5 also at 400°C. Above 400°C $(CH_3)_2O$ selectivity decreased, this was accompanied by an increase in selectivity to HCHO and carbon oxides. At ca. 500°C $(CH_3)_2O$ selectivity was considerably reduced and in the case of WO_3 it was zero, whilst HCHO was the most selective product. Carbon oxide selectivities were relatively low in comparison with the previous groups. Carbon oxides were first detected at 250°C, and as expected increased with temperature. CO_2 was produced in greater quantities than CO.

CH_3OH conversion over WO_3 increased sharply from 0 at 250°C to 88% at 350°C, and then less sharply above this temperature to 99% at 500°C. Initial conversion over Nb_2O_5 did not increase as significantly as that over WO_3, but at 500°C CH_3OH conversion was 97%, at the same temperature conversion over Ta_2O_5 was markedly lower, at 65%.

MoO_3 was the only oxide in group 5. CH_3OH conversion was not detected below 350°C, above this temperature it increased to a maximum of 92% at ca. 500°C. The selectivity to HCHO was extremely high, falling slightly from 100%, between 350°C to 450°C, to 97% at ca. 500°C. No carbon oxides were produced below 450°C, above this CO and CO_2 were detected with selectivities rising to 1% and 2% respectively at 500°C.

Group 6 contained only Sb_2O_3, over which CH_3OH exhibited significantly different behaviour from the other oxides. CH_3OH conversion was exceptionally low at all temperatures, reaching only 3% at 500°C. From 250-400°C $(CH_3)_2O$ was the only product, above 400°C selectivity fell linearly to 0% at 500°C. HCHO was also formed, increasing from 60% selectivity at 450°C to 87% at 500°C. At 500°C CO was the only other product detected with 13% selectivity. The product selectivity over Sb_2O_3 was broadly similar in manner to Nb_2O_5, Ta_2O_5 and WO_3 in group 4, but the CH_3OH conversion was significantly different.

The range of CH_3OH oxidation results are very diverse, since conversion data covered a wide temperature range, with many different products formed. These differences make comparisons of catalysts and their suitability for incorporation into CH_4 partial oxidation catalysts complex. It was not considered appropriate to derive kinetic data from the results for two reasons. Firstly the experimental conditions dictated that conversion was often substantial, creating a concentration profile across the catalyst bed, which would yield results of no significant value. Secondly even it were possible to extrapolate rates to a common temperature, the conversion for several catalysts would almost certainly exceed 100%, and no longer have any physical significance. Choosing a temperature at which the most active catalysts

showed 100% conversion was also not viable, as this temperature was low, and many catalyst were inactive.

To rationalise these data, and make a valid comparison between oxides, a ranking order has been devised based on the temperature at which 30% of the CH_3OH feed was converted to carbon oxides (CO_X). This temperature was denoted as T_{30}. The ranking order produced is shown in figure 3.2.2.1.

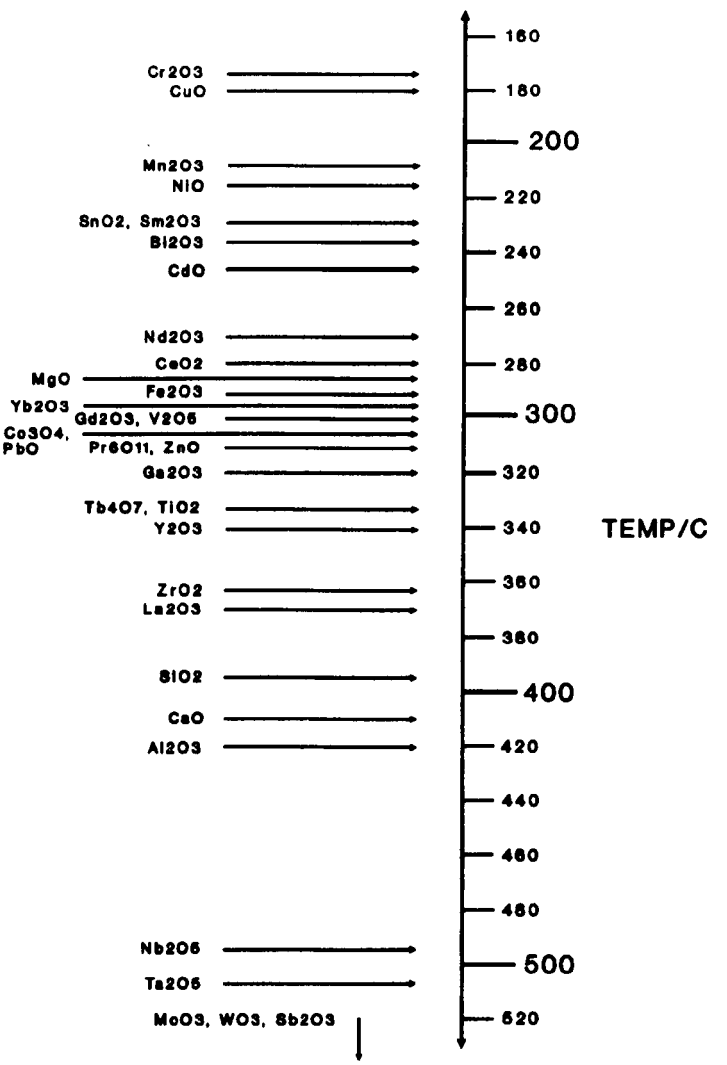

Figure 3.2.2.1. Catalyst ranking, based on the temperature at which 30% of CH_3OH was converted to carbon oxides.

Similar rankings to this one were also obtained if oxides were ranked on differing levels of CO_X production. This ranking has not been normalised for surface area effects due to difficulties in obtaining reaction rates for all the oxides. These difficulties have been outlined above. However, it is considered that oxide surface

areas were typical for these materials. That is if a catalyst for CH_4 partial oxidation were to be produced from TiO_2, for example, it would have a similar surface area to that studied here and so demonstrate similar activity for CH_3OH oxidation.

For many of the materials (particularly groups 3-5) the CH_3OH conversion at this temperature was notably higher than 30%, since products other that CO_X were also formed, namely $(CH_3)_2O$ and HCHO. However, these were not undesirable as they would be useful by-products of any CH_4 partial oxidation process.

The T_{30} catalyst ranking covered a temperature range of over 340°C. CH_3OH was most unstable over Cr_2O_3, which had a T_{30} of 175°C, closely followed by CuO at 180°C. The majority of oxides appeared in the low to mid range, between 200 and 340°C. Above this temperature oxides were more widely distributed. CH_3OH was relatively more stable over five oxides, these were Nb_2O_5, MoO_3, Sb2O3, Ta_2O_5 and WO_3.

Due to their low CH_3OH conversion to CO_X over the full range of temperature studied it was not possible to determine T_{30} for MoO_3, Sb_2O_3 and WO_3, so they cannot be ranked on figure 3.2.2.1. The per pass yields of CO_X in the temperature range 400-500°C are shown for these oxides, along with Nb_2O_5 and Ta_2O_5 for comparison, in figure 3.2.2.2.

The carbon oxide yield over Sb_2O_3 was very low, due to the low CH_3OH conversion, no CO_X were detected at or below 450°C. At 500°C the yield was less than 0.5%. The CO_X yields over MoO_3 were similar to those over Sb_2O_3, but in this case this was due to low selectivity rather than low conversion. Below 450°C CO_X were not produced, whilst at 450°C the yield was 0.5% increasing to 2.5% at 500°C. At 400 and 450°C CO_X yields over WO_3 were virtually identical to those of Nb_2O_5 and Ta_2O_5, values were in the range 5% and 10% respectively. It was only at 500°C that the yield was lower at 21%.

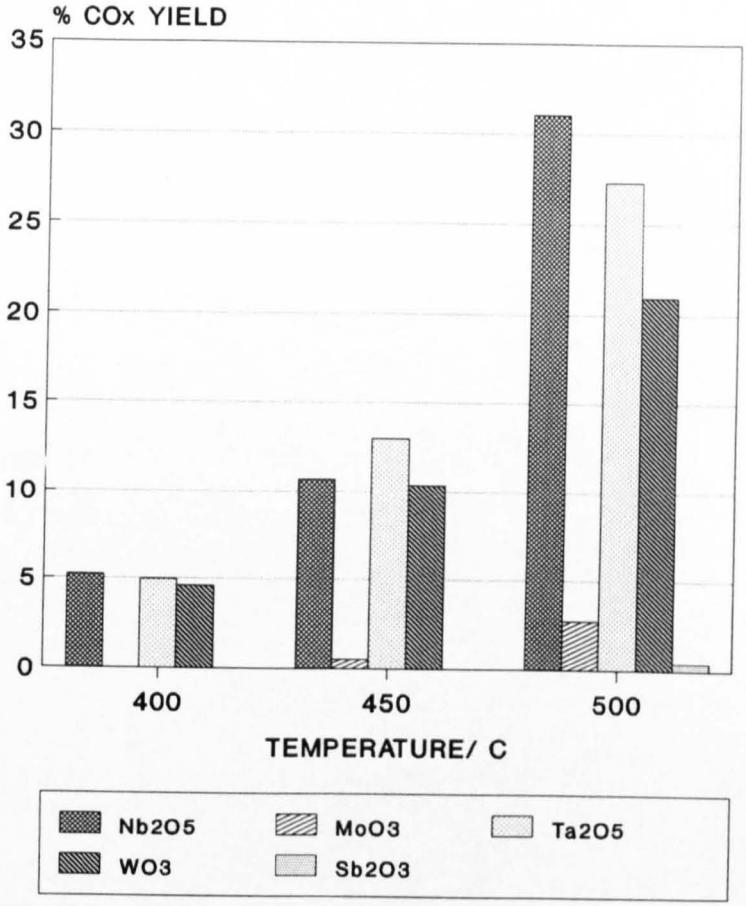

Figure 3.2.2.2. CO_X per pass yields for Nb_2O_5, MoO_3, Sb_2O_3, Ta_2O_5 and WO_3 in the temperature range 400-500°C.

3.3. DISCUSSION

The investigation of CH_3OH stability towards catalytic oxidation has shown high conversion over all oxides with the exception of Sb_2O_3, over which CH_3OH stability was outstanding even at 500°C. Although Sb_2O_3 had a low surface area of 1.8 m^2g^{-1}, the low activity cannot alone be attributed to this. Other oxides such as Bi_2O_3 and PbO had significantly lower surface areas by a factor greater that 3, yet they showed complete CH_3OH conversion at temperatures lower than 350°C. Therefore, it was clear that effects other than those of surface area were important for CH_3OH stability.

The oxidation of CH_3OH has been used as a probe reaction by Abadjieva et. al. [116], investigating $VSbO_4$ catalysts. Results were also reported for V_2O_5 and Sb_2O_4, a phase closely related to Sb_2O_3 in this study. The activity and selectivity of these oxides observed by Abadjieva et. al. bear a striking resemblance to those of

this study. Very few data were presented, but over Sb_2O_4 CO was only observed above 500°C. It was stressed by Abadjieva et. al. that the specific activity observed was two orders of magnitude lower than that of V_2O_5, throughout the temperature range of the experiment. Evidence from the present study, and that of others on a related antimony oxide phase [116] have shown that antimony oxides do not readily destroy CH_3OH, which may be stable up to 500°C. This is clearly an important observation, particularly with respect to the activity shown by other oxides. Sb_2O_3 is an acidic oxide which also has known redox properties, many other oxides in this study also have these properties but they destroy CH_3OH readily. These observations suggest that CH_3OH stability over Sb_2O_3 may be related to structural aspects of the oxide, possibly by hindering the approach of CH_3OH to sites active for oxidation.

The range of products which have been observed may in the majority of cases be related to the acidic, basic and redox nature of the oxides. The strongly basic oxides used in this study, e.g. MgO, CaO and the lanthanide oxides, all tended to be gathered in group 2 of the classification. These materials were characterised by their affinity for carbon oxide production. It is recognised that basic oxides usually show dehydrogenation activity [117]. The dehydrogenation of CH_3OH can eventually lead to CO. and then to CO_2 by a further oxidation step.

One feature that was particularly prominent for the oxides of the lanthanide group was the formation of $HCOOCH_3$. This product was detected at low temperature and conversion suggesting that it was relatively unstable, and susceptible to further oxidation. In studies by Ai [118] it has been demonstrated that under similar flow conditions to those employed in our experiments, $HCOOCH_3$ was oxidised to CO and CO_2 at relatively low temperatures of less than 200°C. The materials tested were a range of molybdate catalysts. The most active catalyst was MoO_3-SnO_2, it was concluded that $HCOOCH_3$ was formed from CH_3OH via the dimerisation of an HCHO intermediate. It was also suggested that the reaction was catalysed by basic

sites. Interestingly this mechanism is very similar to the HCHO dimerisation reaction, or Tishchenko reaction, which is used to produce $HCOOCH_3$ and is catalysed in solution by highly basic alkoxide ions [119]. If such a mechanism was operating in these studies it is unusual that HCHO was not detected simultaneously with $HCOOCH_3$, even in trace quantities. Therefore, it appears likely that $HCOOCH_3$ was formed via a different route. One such possibility is by the reaction of CH_3OH with a partially dehydrogenated CH_3OH surface species. This reaction scheme is shown schematically in figure 3.3.1.

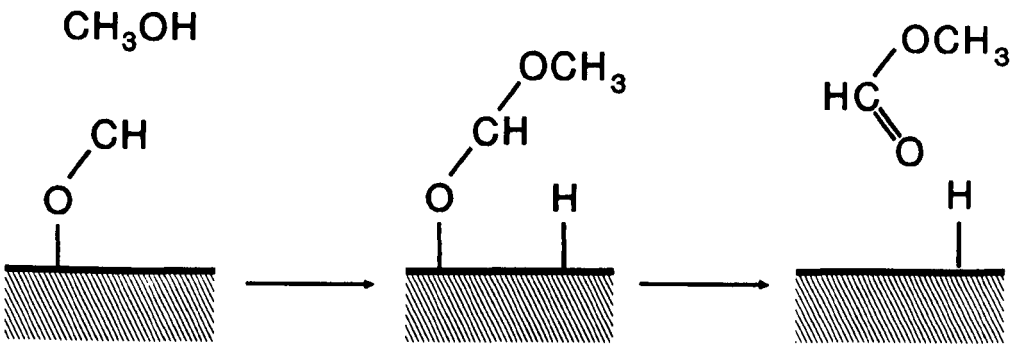

Figure 3.3.1. Schematic representation for the production route of $HCOOCH_3$.

The maximum production rates of $HCOOCH_3$ normalised for surface area effects are shown as a function of ionic radius for the lanthanide sesquioxide in figure 3.3.2.

The type of distribution was reminiscent of a 'volcano' type plot, a maximum rate was shown by Sm_2O_3. The basicity of the lanthanide sesquioxides decreases as the radius of the +3 ion decreases [120]. Therefore, La_2O_3 was the most and Yb_2O_3 the least basic oxide. In this series it appears that oxides of intermediate basicity were most effective for $HCOOCH_3$ production. This may be related to the formation of the partially dehydrogenated surface species, as the surface concentration of this species on the less basic oxides would tend to be low, whilst the more basic oxides could dehydrogenate further to CO, leading to CO_2.

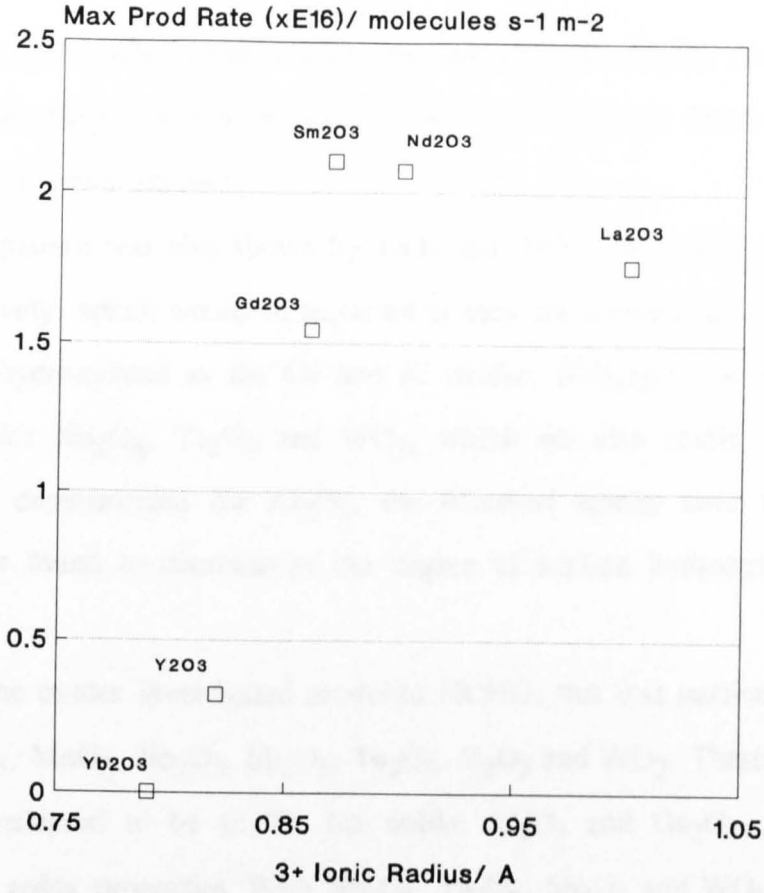

Figure 3.3.2. Maximum $HCOOCH_3$ production rates m^{-2} for lanthanide sesquioxides against ionic radius.

The exact route for $HCOOCH_3$ formation is not clear, but it certainly appears that it is the product from a base catalysed reaction.

Al_2O_3 and Ga_2O_3 produced considerable amounts of $(CH_3)_2O$, which is the alcohol dehydration product expected from a CH_3OH substrate. This conversion is known to be catalysed by acidic oxides. As the temperature increased the selectivity towards $(CH_3)_2O$ decreased. It may be considered that $(CH_3)_2O$ was produced by the interaction of CH_3OH with Bronsted acid sites on the catalyst surface. Pines and Haag [121] have shown that alcohol dehydration over gamma-Al_2O_3 was principally a function of the number of acid sites, and was catalysed by relatively weak sites. The best alumina sample for alcohol dehydration possessed the largest number of weak acid sites. Heating samples to higher temperatures decreased the number of weak acid sites due to dehydroxylation of the surface, which subsequently reduced the extent of the dehydration reaction. The same type of mechanism may be

operating over Al_2O_3 in our studies. By analogy with Al_2O_3, chemically similar hydroxylated Ga_2O_3 would be expected to show the same Bronsted acidity, and function in a similar manner.

A similar pattern was also shown by TiO_2 and ZrO_2, but $(CH_3)_2O$ was produced less selectively, which would be expected as they are considered less acidic and not as highly hydroxylated as the Ga and Al oxides. $(CH_3)_2O$ was initially a major product over Nb_2O_5, Ta_2O_5 and WO_3, which are also acidic oxides. As was previously demonstrated for Al_2O_3, the Bronsted acidity over transition metal oxides was found to decrease as the degree of surface hydroxylation decreased [122].

Many of the oxides investigated produced HCHO, this was particularly noticeable with Fe_2O_3, MoO_3, Nb_2O_5, Sb_2O_3, Ta_2O_5, V_2O_5 and WO_3. These oxides are also mainly considered to be acidic, but unlike Al_2O_3 and Ga_2O_3, they also have recognised redox properties. With Nb_2O_5, Ta_2O_5, Sb_2O_3 and WO_3 there appeared to be a shift in the major selective product, from $(CH_3)_2O$ to HCHO as the reaction temperature was raised. Oxides found to be particularly selective for the oxidation of CH_3OH to HCHO were MoO_3 and V_2O_5, both of which have been studied extensively for selective CH_3OH oxidation [108, 109]. It has already been mentioned in section 1.3, that some commercial catalysts for this reaction are based on MoO_3.

V_2O_5 produced HCHO at a lower temperature than MoO_3, but HCHO was considerably less stable over the former oxide. The HCHO yields over Nb_2O_5, Ta_2O_5 and WO_3 were lower, but still significant. One common feature between all these oxides is the existence of surface M=O bonds, which have been invoked in many selective oxidation reactions [123], and more implicitly for CH_3OH oxidation to HCHO [124]. These oxides also show the formation of shear structures [125, 126] this process, which involves the loss of oxygen from the oxide lattice, is a reversible one which can introduce redox behaviour to the catalysts.

A possible schematic mechanism for HCHO formation over these oxides is shown in figure 3.3.3.

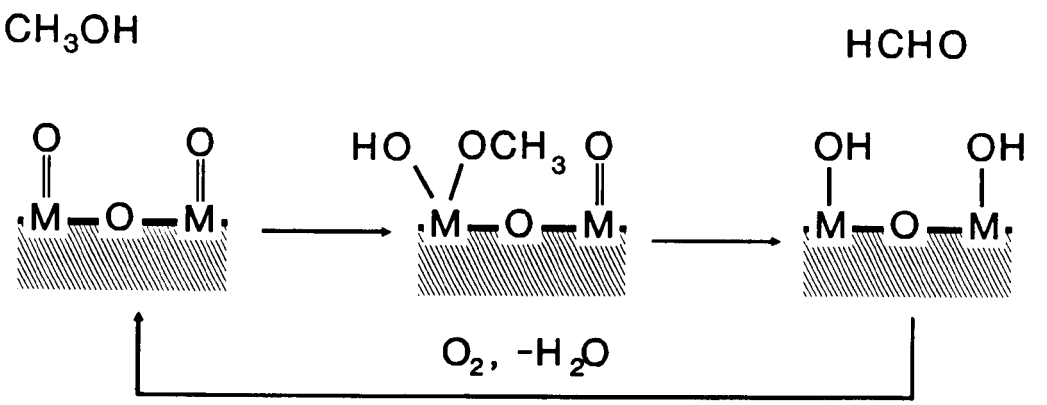

Figure 3.3.3. Schematic mechanism for HCHO formation from CH_3OH.

The formation of HCHO over MoO_3 has been previously proposed to occur on adjacent Mo=O sites [124]. This process over MoO_3 has also been investigated by theoretical ab initio quantum mechanical calculation studies [127]. These studies concluded that adjacent Mo centres were required for the production of HCHO to be energetically favourable. However, it was also concluded that tetrahedrally coordinated Mo, which has two doubly bonded oxygens to the metal ion, opposed to octahedrally coordinated Mo which only has one such oxygen group was required. Further evidence in support of the above scheme has been presented by Groff [128] who identified the surface OCH_3 group by infrared spectroscopy when CH_3OH was adsorbed on MoO_3. The loss of further hydrogen from the surface methoxy group, possibly by H^+ abstraction by Mo=O as shown above or by a O^{2-} lattice ion, would be facilitated by an electron transfer process to the reducible metal cation. The catalytic cycle is completed by the loss of H_2O from the surface and subsequent catalyst re-oxidation to regenerate the active sites. The common features of shear plane formation and surface M=O bonds for the oxides Nb_2O_5, Ta_2O_5, V_2O_5 and WO_3 with MoO_3 may indicate similarities in the mechanism of HCHO production.

It has been suggested that the conversion of CH_3OH to HCHO over MoO_3 proceeds by a Mars van Krevelan mechanism, involving the incorporation of lattice oxygen into the product molecule [129]. The mechanism proposed in figure 3.3.3. clearly does not require the incorporation of lattice oxygen. Evidence for the Mars van Krevelan mechanism was obtained by isotopic studies [129]. However, a recent study by Mauti and Mimms [63] has concluded that no information on the origin of oxygen in HCHO can be obtained due to the rapid secondary exchange between HCHO and M=O surface species (figure 1.9.1.).

Ai [130] and Jehng and Wachs [131] have both investigated the interaction of CH_3OH with oxides. There is general agreement between these studies and the results presented here. Both groups have concluded that CO and CO_2 were produced from basic oxides, HCHO from redox oxides and $(CH_3)_2O$ from acidic oxides.

The catalysts can also be compared on electrical conductivity characteristics, e.g. insulators and semi-conductors. The semi-conductor oxides are extrinsic semi conductors, produced by their deviation from specific metal oxygen stoichiometry. The materials which are extrinsic semiconductors include both n-type and p-type. These differences do not seem to influence the conversion or product distributions, as in many cases insulators, n-type and p-type oxides produce similar results. This may be illustrated by the oxides in group 2, e.g. NiO p-type semiconductor, ZnO n-type semiconductor and MgO an insulator, all showed the same behaviour.

The large number of oxides used in this study allows for the investigation of common trends between CH_3OH oxidation activity and physical and chemical properties of the oxides. The data were examined for relationships between CH_3OH conversion and the ability of an oxide to produce carbon oxides with nearest metal-oxygen distance, nearest oxygen-oxygen distance, unit cell volume and metal ionic radius. No reasonable correlation between any of these parameters were observed for the full data set. Considering the wide range of metal ion valencies, which varied from +2 to +5, and the differences in crystallographic systems, this is

possibly not surprising, as a broad range of surface structures would be exposed. However, grouping oxides together which had the same metal ion valency and belonged to the same crystal structure group still did not reveal any correlation.

The exchange of oxygen isotopes with oxides is a well established technique studied by many groups (see Appendix A). One such study of particular interest has been conducted by Winter [132, 133]. The mechanisms of exchange were represented by three types, R_1 and R_2 involving surface exchange. The R_3 mechanism took place by a combination of R_1 and R_2 mechanisms, but rapid oxygen diffusion throughout the oxide produced exchange with the whole of the bulk oxide, not merely the surface. A comparison between the temperature for 30% CH_3OH conversion to carbon oxides and the observed R_1 and R_2 oxygen exchange rates has been made for the oxides common to both studies, and is shown in figure 3.3.4.

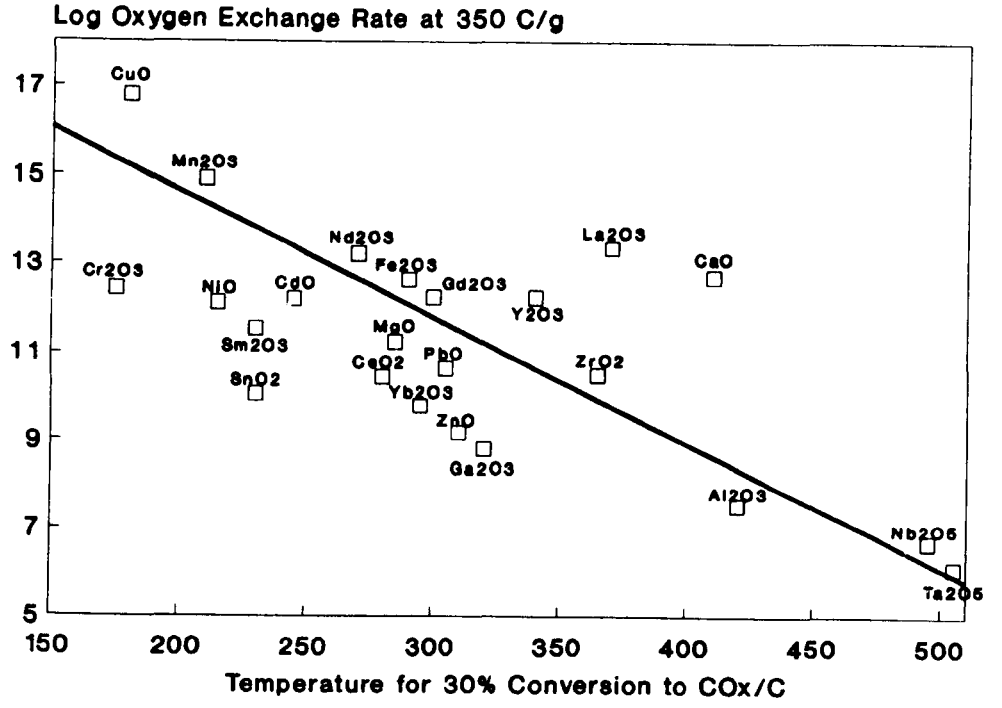

Figure 3.3.4. Relationship between temperature for 30% CH_3OH conversion to CO_X and oxygen exchange activity.

The oxygen exchange rates used in this study were those determined by Winter at 350°C and normalised by weight [132, 133]. The data showed a weak but statistically significant correlation. Linear regression analysis showed a correlation

coefficient equal to 0.472, which was significant at the 98% level for two sets of independent variables with 23 data pairs. The correlation is weak, but it interesting to note that the oxides Nb_2O_5 and Ta_2O_5, the highest in the T_{30} ranking order, both showed considerably lower than average oxygen exchange activity. Conversely CuO, which was one of the most active oxides, readily oxidised CH_3OH to CO_X, had the highest oxygen exchange rate. The oxides CaO and La_2O_3 did not fit the correlation particularly well. Both oxides are highly basic and it may be possible that under reaction conditions CO_2 was adsorbed to form surface carbonate. Such a process could modify the surface, possibly by blocking active sites and increasing CH_3OH stability.

Boreskov [134] has drawn together examples showing that the activity for H_2 oxidation, CO oxidation and CH_4 combustion were closely correlated with the rates of homomolecular or R_0 oxygen exchange. It is also apparent in the present study that oxygen exchange rates can provide some indication of the expected level of combustion products. However, it has to be recognised that the exchange rates used in the present study involved an exchange mechanism with lattice oxygen and not the R_0 mechanism used by Boreskov.

As a note to the dehydration of oxides in relation to their Bronsted acidity, it has been shown that the oxygen exchange rate over Al_2O_3 increased dramatically as the amount of dehydroxylation increased [134]. This may explain why carbon oxides yields increased over Al_2O_3 and Ga_2O_3 as selectivity to $(CH_3)_2O$ decreased.

It has proved a difficult task to establish a link between oxygen exchange and catalytic activity in more complex oxidation reactions. Klissurski [135] has attempted to establish such relationships for the selective oxidation of CH_3OH to HCHO over first row transition metal oxides, lanthanide oxides, Sb_2O_3, WO_3 and SnO_2. It was found that over transition metal oxides the activation energy of oxygen exchange correlated with HCHO selectivity and catalyst activity. This activation energy was used as a measure of oxygen bond strength, relating to the oxidation/reduction enthalpy of surface sites. Oxides which showed a large

activation energy for the process were less active but more selective, and vice versa. Boreskov [136] has noted the dependence of catalytic reactivity with oxygen bond strength of the surface oxide layer of the first row transition metal oxides. It was found that the enthalpy of oxide formation relative to that of atomic oxygen formation could be used as a measure of the surface oxygen bond strength. Data from our study have been examined in this context, but it appears that no similar patterns exist.

Interestingly, as a general observation, oxides which produced high yields of oxygenated products, operating by R_1 and R_2 oxygen exchange mechanisms, all tended to show relatively high activation energies for the oxygen exchange process [132]. The other oxides, producing mainly CO_X, which also operated by the R_1 and R_2 mechanisms showed activation energies within a wide range. This would suggest that oxygen involved with the production of HCHO was a more tightly bound species.

The study by Klissurski also showed that over lanthanide oxides, HCHO was produced most selectively by oxides with the lowest exchange rate. Oxides showing the highest rate were again more prone to producing carbon oxides. We have not detected HCHO over lanthanide oxides under experimental conditions used in the present study but these findings agree well with ours, as the trends for CO_X production correlated with oxygen exchange during CH_3OH combustion.

A more recent study by Maltha and Ponec [137] has addressed the same types of relationships and concluded that reactions which require the dissociation of oxygen on the catalyst are those which correlate well with oxygen isotope exchange rates. If such a case were true then it would follow that CH_3OH combustion could be attributed to such an oxygen species.

3.4. CONCLUSIONS

From the perspective of CH_3OH stability it was evident that a great number of oxides oxidised CH_3OH to carbon oxides below 400°C. The oxides over which

CH_3OH was stable above 400°C were CaO, Gd_2O_3, La_2O_3, MoO_3, Nb_2O_5, Sb_2O_3, Ta_2O_5, WO_3 and Y_2O_3. From these materials the oxides of Ca, Gd, La and Y all showed exclusive selectivity to carbon oxides. MoO_3, Nb_2O_5, Ta_2O_5 and WO_3 showed high conversion to $(CH_3)_2O$ and HCHO, which were not regarded as wholly undesirable products. It can be concluded that over these oxides $(CH_3)_2O$ and particularly HCHO were relatively more stable molecules. This was especially true for MoO_3, which produced HCHO with high selectivity and very little carbon oxides. CH_3OH was exceptionally stable over Sb_2O_3 even up to 500°C, as the conversion was only a few percent and virtually no carbon oxides were produced.

Common features for CH_3OH oxidation allowed oxides to be classified into 6 groups. These groups were based on CH_3OH conversion, product type and distribution with temperature. The products observed were, in a lot of cases, related to the acidic, basic or redox properties of the oxides. Basic oxides produced CO_X and $HCOOCH_3$, acidic oxides $(CH_3)_2O$ and materials which were acidic and also showed redox properties gave $(CH_3)_2O$ and HCHO depending on the reaction temperature. This distribution of products is summarised in figure 3.4.1.

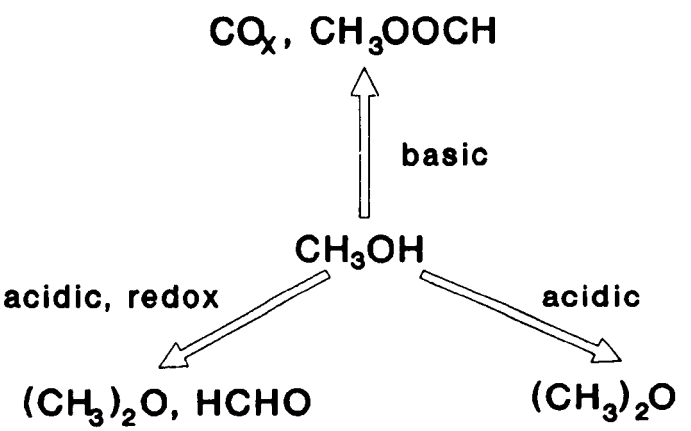

Figure 3.4.1. Summary of product types, based on acid, base and redox properties of the catalyst.

Attempts were made to correlate the results with the physical properties of the oxides, but no clear correlations were established. Comparison of the ability of an oxide to produce CO_X with the surface oxygen exchange activity demonstrated a weak but significant correlation. Endeavours to correlate selective oxidation

products with oxygen exchange data has been inconclusive. The relationship between CO_X production and oxygen exchange may well be an important observation for the design of CH_4 partial oxidation catalysts, although it should be noted that differences exist in the pre-treatment of the oxides between the two studies. The oxides investigated by Winter for oxygen exchange [132, 133] were pre-treated under rigourous conditions to remove surface hydroxylation and carbonate formation, which may be present on the oxide surface under the reaction conditions of the present study.

CHAPTER 4

METHANE/DEUTERIUM EXCHANGE STUDIES

4.1. INTRODUCTION

The exchange of CH_4 with D_2 has been extensively studied over metal catalysts, for a period of many years [138]. One of the very first publications in this area was from Taylor and co-workers in 1936, who studied the reaction using a Ni-kieselguhr catalyst at 138°C [139].

There is little doubt remaining that CH_4/D_2 exchange on metal surfaces takes place via an adsorbed methyl radical intermediate [140]. Deuterated CH_4 products from exchange reactions over these metal catalysts often include singly and multiply exchanged species, which arise from different mechanisms. Singly exchanged species originate from the reaction of a surface methyl radical with a deuterium atom. Multiply exchanged species are thought to originate from the conversion of surface methyl radicals to surface methylene radicals, and possible the inter-conversion to more highly dissociated species, which subsequently react with surface deuterium atoms.

In contrast to the exchange reaction over metals, the hydrocarbon/D_2 exchange, with particular reference to CH_4, over oxides has not received the same attention. To date, only a few studies on selected oxides have appeared in the literature.

Possibly the most studied of these oxides has been gamma-Al_2O_3. Robertson et. al. [141] have shown that CH_4 exchanged readily with D_2 in the temperature range 11-83°C, when experiments were carried out in a batch reactor. The activation energy of the process was determined to be 17 ± 4 kJ mol^{-1}, which appears to be exceptionally low. The same study included results for exchange of other hydrocarbons, the activation energies for these compounds were greater than that of CH_4. For example C_3H_8 showed an activation energy of 36 ± 4 kJ mol^{-1}. The rates for hydrocarbon exchange normalised for surface area at 25°C were of similar magnitude for all hydrocarbons. This was in sharp contrast to the observed

exchange rates over metals, where it was found that exchange rates correlated with the strength of the hydrocarbon C-H bond. The increased bond strength of CH_4 resulted in an exchange rate approximately 1000 times lower than those of other hydrocarbons. The order of hydrocarbon exchange over gamma-Al_2O_3 was explained qualitatively by considering the stability order of carbanions formed during the reaction. The most stable carbanion was formed from CH_4, which showed the highest rate of exchange for straight chain hydrocarbons.

Earlier research by Larson and Hall has studied the exchange of CH_4 and CD_4 with surface OD and OH groups, and CH_4/CD_4 exchange over Al_2O_3 catalysts [142]. The catalyst was gamma-Al_2O_3, activated at 515°C in 100 torr O_2 for 16 hours, then in vacuum for a further 16 hours before use. Experiments were performed in a recirculating flow batch reactor. The reaction was found to proceed at room temperature. It was indicated that the density of active sites were ca. $3x10^{15}$ cm^{-2}, much lower than the total number of surface OH groups. Thus, it was concluded that only certain types of OH sites were responsible for the exchange reaction. The estimation of the number of active sites was in close agreement with the amount of surface reactive hydrogen, determined by exchange with CD_4. It was also found that D on the surface from the former exchange process exchanged readily with CH_4 to produce CH_3D, in the same quantity as CD_3H produced from the initial exchange. Such an observation indicated that the reactive species was held at specific surface sites, showing no surface mobility at the temperature of reaction. These active exchange sites were selectively poisoned by the addition of CO_2, NO, H_2O, C_2H_4 and C_3H_6. Reaction rates measured for CH_4/D_2 exchange and CD_4/H_2 exchange indicated a primary isotope effect, suggesting that the rate determining step for exchange was limited by the breaking of the C-H bond.

The exchange of hydrocarbons over chromium oxide gel catalyst has been extensively studied by Burwell and co workers in a series of publications [143, 144]. Results have been reported mainly for higher alkanes, cycloalkanes, alkenes and stereochemical aspects of the exchange, but some results for CH_4 have been

included [143]. The chromium oxide gel was activated by heating in a dry inert gas, or in a vacuum above 300°C. Maximum activity was exhibited after activation treatment was carried out at, or above 470°C. Once activated the oxide was active at temperatures above 200°C. The alkanes showed two distinct mechanisms of exchange, simple exchange, which produced a random distribution of deuterium in the substrate, and multiple exchange. The simple exchange process was observed with all alkanes, and was the exclusive process with CH_4. At 235°C CH_4 showed a relatively low rate of exchange compared to other hydrocarbons, only C_2H_6 demonstrated a lower exchange rate. In a flow system the exchange of D for H was shown to proceed in a stepwise manner, exchanging one H atom for each adsorption step. Similar conclusions to those reached by Larson and Hall on gamma-Al_2O_3 were reached, with regard to the number of active sites, which were low in comparison with the possible number on the surface.

An interesting and closely related study to the present work has been reported by Utiyama et. al. [145] on CH_4/D_2 exchange over single oxides. The exchange reaction was investigated over 13 metal oxides, the most active of which were MgO, CaO, SrO, BaO and La_2O_3. These studies were carried out in a closed recirculating reactor at 50 torr pressure, with a CH_4/D_2 ratio of 1/9. The level of activity was highly dependent on the pre-treatment evacuation temperature. Maximum activity was observed when catalysts were evacuated at 650°C for La_2O_3, 700°C for MgO and CaO prepared from $Ca(OH)_2$, 800°C for BaO and CaO prepared from $CaCO_3$, and greater than 1000°C for SrO. Comparison of the maximum activities of the group 2 oxides normalised for unit area produced the order;

MgO < CaO (ex $Ca(OH)_2$) < CaO (ex $CaCO_3$) < BaO < SrO.

The only other catalyst in this study which showed comparable activity to these oxides was La_2O_3.

La_2O_3 has also been studied for alkane/D_2 exchange activity by Kemball et. al. [146]. Reactions were carried out in a 210 cm^3 volume static reaction vessel,

containing 9.1 x 10^{19} molecules of hydrocarbon, with D_2 added to produce a 5/1 D_2/hydrocarbon ratio. Exchange activity was investigated at 350°C, results indicated that CH_4 was the least active substrate compared to the others used in the study, which included propane, n-butane, 2-methylpropane, 2,2-dimethylpropane and cyclopropane. Agreement between the CH_4/D_2 surface area normalised exchange rates observed by Kemball et. al. and those of the previous study by Utiyama et. al. [145] were good. A slightly higher rate of exchange was reported in the latter study.

MgO has been studied for exchange activity of alkanes, alkenes and cyclo-hydrocarbons by Robertson et. al. [147]. General observations concluded that activity was related to the nature of reaction intermediates. High rates were shown by molecules giving π-allyl intermediates, moderate rates for vinyl species and considerably lower rates for saturated hydrocarbons, exchanging through an alkyl intermediate. Naturally CH_4 was of the latter type, and only showed low exchange activity over the MgO catalyst.

Hydrocarbon/D_2 exchange has been investigated on a TiO_2 catalyst by Haliday et. al. [148]. Experiments were carried out in a static system using a silica reactor vessel. TiO_2 was present as the single rutile phase. Studies at 440°C using a range of C_1-C_4 straight and branched chain alkanes, showed the initial rates of exchange increased in the order $CH_4 < C_2H_6 < C_3H_8 <$ i-$C_4H_{10} <$ n-C_4H_{10}. The exchange reaction was accompanied by dehydrogenation of the propane and butane substrates. Studies at 477°C showed the same order of reactivity, all the alkanes, with the exception of CH_4, exchanged at approximately equal rates. The exchange rate of CH_4 was slower by a factor of approximately 5 to 9. The activity pattern shown by the alkanes was not the same as the corresponding activity pattern shown by alkane exchange via heterolytic fission. This included the pattern based on hydrocarbon acidity which involved the intermediate alkyl species of carbanionic character, such as that demonstrated over gamma-Al_2O_3 [141], and the pattern based on the ease of carbocation formation, illustrated by silica-alumina catalysts

[149]. The activity pattern was very similar to those observed over metal catalysts, which involved homolytic fission, and was related to the strength of the C-H bond. Thus the lower rates for CH_4 exchange were observed.

This brief survey indicates the limited number of oxides which have been investigated for the CH_4/D_2 exchange reaction. These experiments have been performed in a wide variety of reactor types, under different experimental conditions and pre-treatment regimes. Comparisons between such experiments are difficult, and in many cases may be invalid, as the catalytic activity was influenced by many variables. This study was undertaken to provide an indication of the relative suitability of single oxides as catalysts for CH_4/D_2 exchange, providing information on their efficacy for CH_4 activation.

4.2. RESULTS

4.2.1. X-RAY DIFFRACTION CHARACTERISATION

The oxides used for CH_4/D_2 exchange experiments were the same as those used for CH_3OH oxidation studies. Details of the oxides as supplied were given in section 3.2.1. of the previous chapter. The CH_4, D_2 and H_2 reactants, and the high temperatures used in these studies produced a highly reducing atmosphere. The oxides which were known to reduce entirely to the metallic state, or to a toxic/volatile compound under these conditions, were not tested. These materials included Bi_2O_3, CdO, CuO, NiO, PbO and Sb_2O_3. Oxides reduced in-situ to the metallic state invariable blocked the reactor tube and deposited metallic films in the reactor lines.

The remaining 27 oxides were tested for activity in the CH_4/D_2 exchange reaction. The phases identified by X-ray diffraction before and after use for these oxides are shown in table 4.2.1.1.

Table 4.2.1.1. Phases identified by X-ray diffraction before and after use in CH_4/D_2 exchange studies.

Before use		After use	
Oxide	Phase	Identified Phase	
Al_2O_3	transitional	Al_2O_3	transitional
CaO	Lime	CaO	Lime
		$Ca(OH)_2$	Portlandite
CeO_2	Cerianite-(Ce)	CeO_2	Cerianite-(Ce)
Co_3O_4	Co_3O_4 (spinel)	Co	FCC unit cell
Cr_2O_3	Eskolaite	Cr_2O_3	Eskolaite
Fe_2O_3	Hematite	Fe_3O_4	Magnetite
		Fe	BCC unit cell
Ga_2O_3	alpha-Ga_2O_3	Ga_2O_3	alpha-Ga_2O_3
	beta-Ga_2O_3		beta-Ga_2O_3
	gamma-Ga_2O_3		
	GaO(OH)		
Gd_2O_3	Gd_2O_3 (Cubic)	Gd_2O_3	Gd_2O_3 (Cubic)
La_2O_3	La_2O_3 (Hex)	La_2O_3	La_2O_3 (Hex)
		$La(OH)_3$	$La(OH)_3$ (Hex)
MgO	Periclase	MgO	Periclase
Mn_2O_3	Bixybite-C	MnO	Manganosite
MoO_3	Molybdite	MoO_3	Molybdite
		MoO_x	reduced phases
Nb_2O_5	T-form	Nb_2O_5	T-form
	M-form		M-form
Nd_2O_3	Nd_2O_3 (Hex)	Nd_2O_3	Nd_2O_3 (Hex)
		$Nd(OH)_3$	$Nd(OH)_3$ (Hex)
Pr_6O_{11}	$PrO_{1.83}$	$PrO_{1.83}$	$PrO_{1.83}$ (Cubic)
	PrO_2		
SiO_2	amorphous	SiO_2	amorphous
Sm_2O_3	Sm_2O_3 (Cubic)	Sm_2O_3	Sm_2O_3 (Cubic)
SnO_2	Cassiterite	SnO_2	Cassiterite
		Sn	beta form (Tet)
Ta_2O_5	Ta_2O_5 (Mono)	Ta_2O_5	Ta_2O_5 (Mono)
Tb_4O_7	Tb_4O_7 (cubic)	Tb_2O_3	Tb_2O_3 (Cubic)
TiO_2	Anatase	TiO_2	Anatase
	Rutile		Rutile
V_2O_5	Shcherbinaite	V_2O_3	Karellenite
WO_3	WO_3 (Mono)	WO_3	WO_3 (Mono)
		$W_{25}O_{73}$	shear structure
Y_2O_3	Y_2O_3 (Cubic)	Y_2O_3	Y_2O_3 (Cubic)
Yb_2O_3	Yb_2O_3 (Cubic)	Yb_2O_3	Yb_2O_3 (Cubic)
ZnO	Zincite	ZnO	Zincite
ZrO_2	Baddelyite	ZrO_2	Baddelyite

Approximately half of the oxides, including Al_2O_3, CaO, CeO_2, Cr_2O_3, Ga_2O_3, Gd_2O_3, La_2O_3, MgO, Nd_2O_3, Pr_6O_{11}, SiO_2, Sm_2O_3, TiO_2, Y_2O_3, Yb_2O_3, ZnO and ZrO_2 showed essentially the same phases after use, which were present initially.

The highly basic oxides CaO, La_2O_3 and Gd_2O_3 showed the formation of hydroxide phases as minor constituents. The hydroxide phases would almost certainly be present to some extent on these oxides, and the other basic oxides, before use due to the adsorption of atmospheric water vapour. On cooling at the end of the experiment it would be likely that the hydroxide phase re-formed on all these oxides. However, it appears that hydroxide formation on the most basic oxides was more pronounced, and detectable by XRD.

The opposite effect was observed with Ga_2O_3, before use a distinct set of diffraction peaks attributed to a GaO(OH) phase were present. After use no trace of the hydroxide phase was detected, while the residual Ga_2O_3 phases were unchanged. About 3 months after use, XRD analysis showed that the sample was again hydroxylated, and the GaO(OH) phase detected.

After use the oxides Co_3O_4, Fe_2O_3 and SnO_2 showed the presence of metallic phases. Co_3O_4 was reduced completely to metallic Co, which crystallised in a face centred cubic unit cell structure. The oxides Fe_2O_3 and SnO_2 were not completely reduced. The major phase from Fe_2O_3 after use was the spinel structure Fe_3O_4. A metallic Fe phase was also present in a minor quantity, identified in the body centred cubic unit cell structure. The SnO_2 catalyst showed that after use a considerable proportion of the oxide was unchanged, but Sn was also present in the beta form, crystallised in a tetragonal structure.

The oxides Mn_2O_3, Tb_4O_7 and V_2O_5 were reduced to the single phase oxides MnO, Tb_2O_3 and V_2O_3 respectively. After use MoO_3 and WO_3 proved difficult to characterise by X-ray diffraction, both oxides are well known for their tendency to form shear structures [126]. Both oxides showed evidence of partially retaining their original structure, but many new diffraction lines were detected many of which were broad. One phase which was unequivocally identified was $W_{25}O_{73}$, due to the loss of oxygen and the formation of shear planes. It is likely that many of the unassigned diffraction peaks were due to these types of phases, which are expected for these oxides under the reaction conditions.

It was not possible to measure the surface areas of the used catalysts, as typically 5-25 g was required for the measurement, while catalyst charges were usually 0.1-0.6 g. The reduction of catalysts was most likely accomplished during the pre-treatment of the oxides at 540°C.

4.2.2. CATALYTIC ACTIVITY

The results showing the extent of exchange against temperature are shown in Appendix C. All results were obtained at steady state operation, under these conditions it may be assumed that catalyst reduction was not taking place.

Blank reactions were carried out at temperatures up to 540°C. No activity was detected either with an empty reactor or a reactor tube packed with silica wool.

The initial oxides Nb_2O_5, MoO_3, SiO_2, SnO_2, Tb_4O_7, WO_3 and Y_2O_3 were all inactive, and showed no exchange above the lowest detectable limit, even after 5 hours at 540°C. The remaining oxides all exhibited appreciable activity.

Initially activity increased with time on line until after approximately 1.5 to 2 hours steady state operation was attained. The majority of catalysts, (including the oxides of Al, Ca, Gd, La, Mg, Nd, Pr, Sm, V, Yb and Zr) , showed initial activity around 420°C, which was measured over a temperature range of approximately 100°C, of these oxides the total conversion over transitional Al_2O_3 was the greatest, showing ca. 21% at 520°C. Generally the other oxides showed conversions of 8-14% at this temperature. At levels of conversion to CH_3D above 6% CH_2D_2 was also produced, but at substantially lower levels. The conversion to CH_2D_2 was in the region of 5-15% of the conversion to the singly deuterated CH_3D. Over MgO conversion to CH_2D_2 was higher, accounting for approximately 27% of conversion to CH_3D. It was clear that for all the oxides mentioned above CH_2D_2 formation was related to that of CH_3D, as both increased in a similar manner with temperature.

The activities of Fe_3O_4, MnO and TiO_2 were also determined in the same temperature limits as the afore-mentioned materials. Conversion over these oxides

were significantly lower, showing around 2.4% and 4.2% at 540°C for TiO_2 and Fe_3O_4, with 4.6% at 520°C for MnO. None of these oxides showed conversion to the doubly exchanged CH_2D_2 species.

The conversions over Cr_2O_3, Ga_2O_3 and ZnO were large in the temperature range 420-540°C, and consequently the MS dynamic range for monitoring ions m/e 17 and 18 was exceeded. Changing the mass spectrometer range gave an indication of the extent of exchange, but these ranges were not accurately calibrated and absolute values were not determined. Therefore, the activity of these oxides were investigated at lower temperatures, corresponding to 370-450°C for Cr_2O_3, 290-330°C for Ga_2O_3 and 350-400°C for ZnO. Exchange at these temperatures formed predominantly CH_3D, with some CH_2D_2, produced in relative quantities to CH_3D similarly to that formerly described.

Somewhat different exchange results were shown by the Co and Ta_2O_5 catalysts. The magnitude of exchange over these materials was extremely small, so much so that peak areas could not be accurately integrated. Although quantitative data could not be acquired qualitative aspects can be described. Between 490-540°C for Ta and 470-540°C for Co, the deuterated species CH_3D, CH_2D_2, CHD_3 and CD_4 were all formed. The order of magnitude was;

$$CH_3D > CH_2D_2 > CHD_3 > CD_4.$$

The low levels of conversion increased with temperature, but the maximum conversion observed was $<0.2\%$, even at these low conversions all deuterated species were produced simultaneously.

Reaction rates have been derived from CH_4 conversion data. The rates calculated were total conversion rates to deuterated products at varying temperatures. The data have been treated in accordance with the Arrhenius equation. The Arrhenius plots for the oxides are shown figure 4.2.2.1.

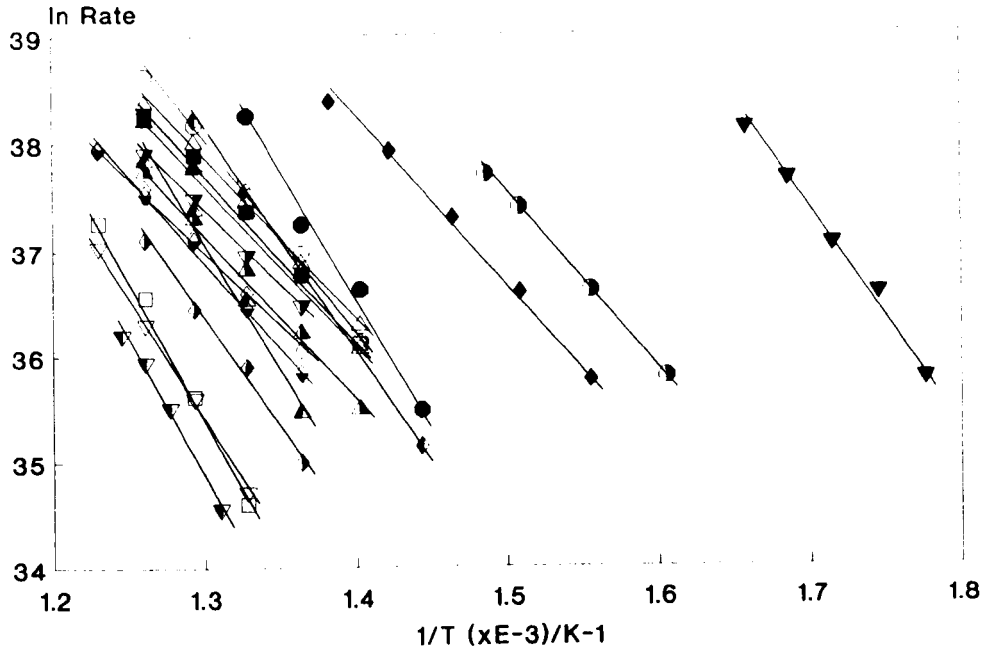

Figure 4.2.2.1. Arrhenius behaviour of oxides for the CH_4/D_2 exchange reaction. Key: ○ Al_2O_3; ◇ CaO; □ CeO_2; ◆ Cr_2O_3; ▽ Fe_3O_4; ▼ Ga_2O_3; △ Gd_2O_3; ▲ La_2O_3; ● MgO; ◑ MnO; ■ Nd_2O_3; ◐ Pr_6O_{11}; ◥ Sm_2O_3; ◤ TiO_2; ◭ V_2O_3; ◮ Yb_2O_3; ◑ ZnO; ◆ ZrO_2.

Linear regression was performed to fit a straight line function to the data sets, correlation between data sets were excellent, exceeding a correlation coefficient of 0.985 in all cases. Activation energies were calculated from the gradient which was equal to $-E_a/R$, while the intercept indicated the pre-exponential factor, ln A. Table 4.2.2.1. shows the resulting activation energies and pre-exponential factors derived from results in figure 4.2.2.1.

Activation energies for the exchange process varied over a range of 111 kJ mol^{-1}. The lowest was shown by CaO at 116 kJ mol^{-1}, closely followed by Sm_2O_3 at 117 kJ mol^{-1}, both were considered equivalent within experimental error. The highest activation energy was shown by CeO_2 with a value of 227 kJ mol^{-1}. High activation energies were also shown by Fe_2O_3, MgO and TiO_2, which were in the region of 195-199 kJ mol^{-1}. Experimental errors on these higher values were considerably greater in comparison to the lower values of activation energy. Pre-exponential factors were also found to vary over a suitably wide range, CeO_2 was the highest at ln 71.0, and CaO the lowest at ln 55.2.

Table 4.2.2.1. Activation energies and pre-exponential factors for CH_4/D_2 exchange rates.

Oxide	E_a/ kJ mol^{-1}	±Error/ kJ mol^{-1}	ln A	±Error
Al_2O_3	145	8	60.7	1.3
CaO	116	2	55.2	0.3
CeO_2	227	7	71.0	2.2
Cr_2O_3	127	5	59.6	0.9
Fe_3O_4	195	5	65.9	0.8
Ga_2O_3	163	8	70.7	1.7
Gd_2O_3	124	4	57.3	0.6
La_2O_3	124	6	57.1	1.0
MgO	193	14	69.0	2.1
MnO	167	10	62.4	1.6
Nd_2O_3	128	5	57.7	0.8
Pr_6O_{11}	168	5	64.4	0.8
Sm_2O_3	117	3	55.6	0.4
TiO_2	199	15	66.0	2.3
V_2O_3	133	7	58.0	1.0
Yb_2O_3	188	12	66.4	1.9
ZnO	134	7	61.8	1.4
ZrO_2	133	7	57.7	1.2

Activation energies and pre-exponential factors from table 4.2.2.1. were used to calculate exchange rates at 500°C, the results are shown in table 4.2.2.2.

Table 4.2.2.2. Comparison of absolute CH_4/D_2 exchange rates at 500°C.

Oxide	Rate/ molecules s^{-1}	ln Rate	Total S.A. /m^2g^{-1}
Al_2O_3	$3.70x10^{16}$	38.1	2.8
CaO	$1.25x10^{16}$	37.1	0.7
CeO_2	$2.86x10^{15}$	35.6	5.9
Cr_2O_3	$1.99x10^{17}$	39.8	2.1
Fe_3O_4	$2.74x10^{15}$	35.6	2.2
Ga_2O_3	$4.79x10^{19}$	45.3	4.4
Gd_2O_3	$3.05x10^{16}$	38.0	0.8
La_2O_3	$2.58x10^{16}$	37.8	0.3
MgO	$8.72x10^{16}$	39.0	8.0
MnO	$6.97x10^{15}$	36.5	2.1
Nd_2O_3	$2.72x10^{16}$	37.8	0.4
Pr_6O_{11}	$4.05x10^{16}$	38.2	1.1
Sm_2O_3	$1.84x10^{16}$	37.5	1.7
TiO_2	$1.66x10^{15}$	35.0	4.1
V_2O_3	$1.62x10^{16}$	37.3	2.5
Yb_2O_3	$1.43x10^{16}$	37.2	3.1
ZnO	$5.57x10^{17}$	40.9	2.1
ZrO_2	$1.20x10^{16}$	37.0	4.6

The calculated exchange rates were in close agreement with the measured values, and were well within the limits of experimental errors. Calculated rates at 500°C were used for consistency between all catalysts.

The exchange rate catalysed by Ga_2O_3 was considerably higher than the other oxides, by nearly two orders of magnitude. The exchange rates over Cr_2O_3 and ZnO were also significantly higher than over the majority of oxides. The bulk of catalysts showed exchange rates between 7.11×10^{15} molecules s^{-1} and 8.66×10^{16} molecules s^{-1}. TiO_2, Fe_2O_3 and CeO_2 showed the lowest rates, approximately four orders of magnitude lower than Ga_2O_3. The rates shown in table 4.2.2.2. are absolute rates of exchange over a fixed volume of oxide. These rates have been normalised for the effect of surface area, based on the surface areas of the starting material, shown in table 3.2.1.1. The order of activity for exchange rates at 500°C normalised for surface areas are shown in figure 4.2.2.2.

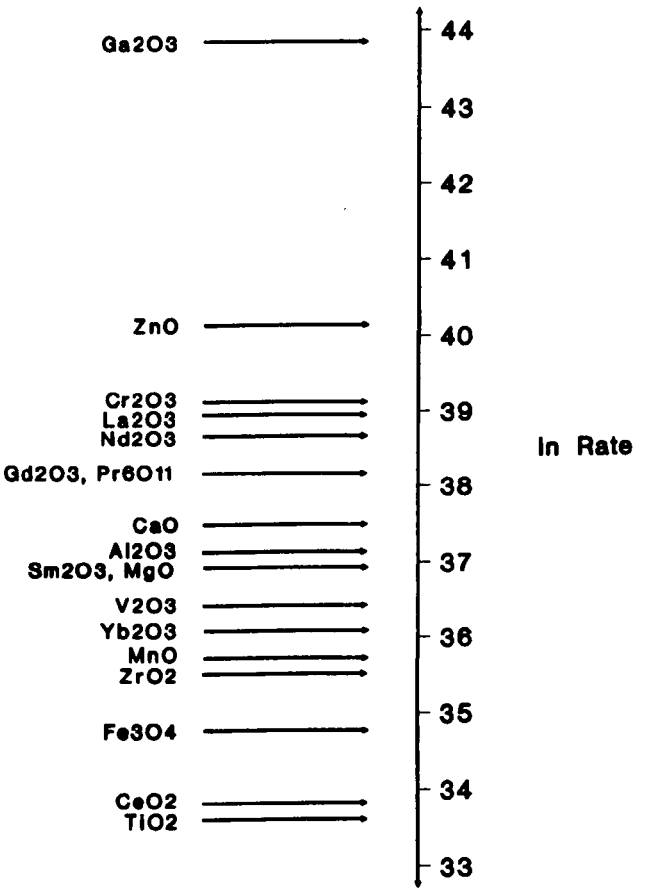

Figure 4.2.2.2. CH_4/D_2 exchange rates at 500°C normalised for the influence of surface area.

The surface area of oxides which underwent major phase transitions during reaction may well have been altered. Therefore, the normalised activity of these oxides, which include Fe_3O_4, V_2O_3 and MnO may not be accurate. However, it has been assumed that in these cases the change in surface area exerted little influence as the initial surface areas were low and further changes would be relatively insignificant.

No major changes in the order of activity were observed, Ga_2O_3 was still the most active, followed by ZnO then Cr_2O_3. La_2O_3 increased in the activity order due to the very low surface area, conversely MgO decreased as a consequence of the relatively high surface area. Al_2O_3 had the highest surface area of all the active oxides, but the oxide had a very low density and the total area of the catalyst bed was not significantly different from the other oxides. For this reason the Al_2O_3 catalyst remained in the intermediate range of activity. TiO_2 was still the least active catalyst on the normalised scale, followed closely by CeO_2.

4.3. DISCUSSION

Reactions carried out in the blank reactor tube showed no activity, indicating the homogeneous gas phase reactions were not responsible for activating CH_4 under these reaction conditions. If it were the case that radical gas phase reactions took place, the extent of exchange would almost certainly be high, due the self propagating nature of this type of reaction mechanism. The initial increase in the rate of exchange with time, and the attainment of steady state exchange rates, may be attributed to the activation of the oxide surface, due to dehydroxylation. Once the oxide was fully dehydroxylated or had reached an equilibrium coverage at the reaction temperature, the rate of exchange remained constant for the duration of the experiment, for each temperature investigated.

The similarities in trends for CH_3D and CH_2D_2 production were previously noted. From the data presented in Appendix C it is evident that conversion to the CH_2D_2 species, based on the concentration of CH_3D showed a similar value to that of the conversion to CH_3D, based on initial CH_4 concentration. This observation indicated

that the exchange reaction took place via a sequential process, and CH_3D was a primary product while CH_2D_2 was a secondary product. This reaction scheme is illustrated below (4.3.1.).

$$CH_4 \xrightarrow{D_2} CH_3D \xrightarrow{D_2} CH_2D_2 \qquad (4.3.1.)$$

CH_2D_2 was below detectable limits until the singly exchanged species was present in significant concentration. Analogously CHD_3 and CD_4 were not observed in the investigated temperature ranges due to the limiting level of CH_2D_2. At very high levels of exchange, for example those demonstrated by Ga_2O_3 at 540°C, all four consecutively deuterated products were formed in the order CH_3D > CH_2D_2 > CHD_3 > CD_4. The proportions of these products further demonstrated the operation of a sequential exchange mechanism. This step wise exchange of CH_4/D_2 on oxides has been readily observed in previous studies, for example over Cr_2O_3 catalysts [144].

Conversion figures to CH_3D from CH_4 and to CH_2D_2 from CH_3D were similar, but they were not identical. On average the latter conversion was ca. 85% of the former, although extreme values ranged from 45% to 129%. Nevertheless, the average figure was less than 100%, this may be justified by considering the relative concentration of reactants. Initially CH_4 may only react with D_2 to give CH_3D, but at higher conversion, where CH_2D_2 was formed, hydrogen would also be present, possibly on the catalysts surface or in the gas phase, as H_2 or HD. Therefore, the successive exchange reaction of CH_3D had an increased probability of exchange with hydrogen, relative to the initial exchange of CH_4. Such hydrogen-hydrogen exchange was not detected and may in some cases lead to the formation of the initial CH_4 reactant. The major source of hydrogen for such a process was from CH_4, impurities in the D_2 supply were of minor importance.

The patterns of exchange over Co and Ta_2O_5 was very similar to those which have been demonstrated over metal catalysts [140]. That is, all deuterated species were produced simultaneously, and it appeared that the stepwise exchange of the CH_3D

primary product did not take place. It is not likely that metallic Ta was formed on the oxide surface, but if this was the case it would probably be undetectable by XRD, due to its low levels or high dispersion. Metallic Co and Ta_2O_5 would both be expected to have low surface areas, which may provide an explanation for the low activity. Indeed the initial surface area of Ta_2O_5 was one of the lowest in this study. Although these catalysts have shown interesting and different mechanisms of exchange when compared to the bulk of the oxides, the primary objective of this study was to identify catalysts effective for CH_4 activation. From this perspective Co and Ta_2O_5 were poor, exhibiting low levels of conversion. The mechanism of CH_4/D_2 exchange on metals takes place via an adsorbed methyl radical, this process has been described in section 4.1., it is proposed that the same mechanism is operating on the Co and Ta_2O_5 catalysts in this study.

Activity patterns may be established for the basic non reducible oxides in this study, these include the rare earth sesquioxides, as well as MgO and CaO. It has been mentioned previously in section 3.3.2., that the basicity of the rare earth oxides decreased in a gradual manner as the +3 metal ionic radius decreased [120]. There is also an increase in the basicity of the group 2 oxides, as the atomic number was increased. The exchange rate of the rare earth sesquioxides at 500°C normalised for surface area as a function of ionic radius is shown in figure 4.3.1.

Generally good agreement was observed between the decrease in the +3 metal ionic radii of the lanthanide sesquioxides and the normalised rates of CH_4/D_2 exchange. The same trend was also observed over MgO and CaO. The normalised rate at 500°C over CaO was greater than the equivalent rate over MgO by a factor of approximately 1.8. It should also be noted that these basic catalysts were some of the most active, with the exceptions of Ga_2O_3, ZnO and Cr_2O_3.

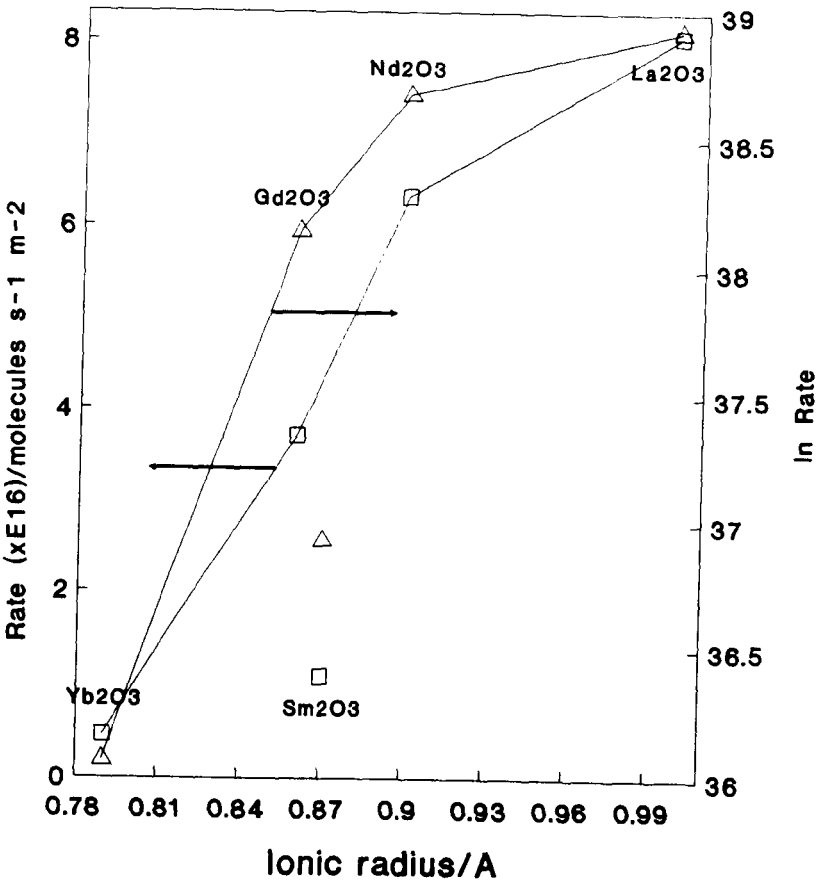

Figure 4.3.1. Normalised CH_4/D_2 exchange rate at 500°C over rare earth sesquioxides as a function of ionic radius.

The relationship shown in figure 4.3.1. was not a linear one, and may not be expected to be so, due to the different oxide structures, which may expose different densities of surface sites. Sm_2O_3 showed lower activity than would be expected. A possible explanation for this anomaly may be derived from evidence shown by the XRD pattern of the used sample. After use line widths in the XRD pattern were decreased considerably, also the signal to background ratio increased by over 80%. The most probable explanation for these observations would be an increase in the Sm_2O_3 crystallite size, induced by the high temperatures at which the experiment was conducted. Such an increase in crystallite size for a non porous oxide such as Sm_2O_3, will reduce the surface area. If this process has taken place then the normalised rate of exchange would be higher than the value indicated. It should also be noted that the initial surface area of Sm_2O_3 was twice the typical area of the other rare earth sesquioxides (table 3.2.1.1.). Unfortunately the surface area of the

used sample could not be determined due to the small catalyst bed volumes employed, this was highlighted previously in section 4.2.1.

The correlation shown in figure 4.3.1. indicates that the activation of CH_4 was related to the strength of basic sites on the oxide surface. The dehydroxylation of an oxide surface leads to the generation of surface ions, which have lower coordination than those of the bulk or the hydroxylated surface. These surface ions are coordinatively unsaturated. The surface metal cation, M^{n+}, behaves as a Lewis acid site, while the surface oxygen anion, O^{2-}, is more basic than those of the bulk. These two surface ions, which have been called an ion pair or an acid-base pair [150], act as important sites for the heterolytic dissociative adsorption of molecules. The relationship between basicity and CH_4/D_2 exchange rate implies that CH_4 was activated by the initial abstraction of H^+ on basic sites of the oxide. The abstraction of a proton from CH_4 would lead to the formation of a methyl anion. This carbanion species contains a central carbon atom with a pair of non bonding electrons, and has a negative charge associated with it. CH_4 is a weak acid and consequently the conjugate base carbanion is a very strong base. The process of CH_4 activation by heterolytic dissociation to form the methyl carbanion is shown in figure 4.3.2.

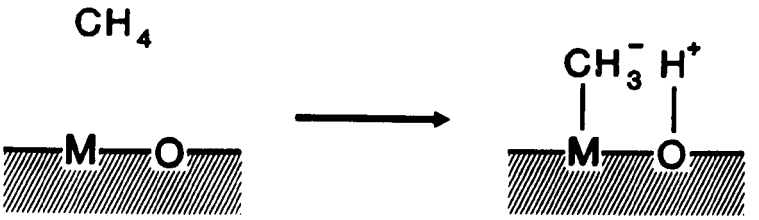

Figure 4.3.2. Heterolytic dissociation of CH_4 on an oxide surface to a methyl carbanion species.

The process of heterolytic dissociative adsorption may also take place by the abstraction of a hydride ion, H^-, initiated by a Lewis acid site. Activation by this mode would lead to the formation of a methyl carbocation, CH_3^+, associated with the surface oxygen species. The oxides TiO_2 and ZrO_2 are considered to be catalysts of higher Lewis acidity than those shown by the correlation in figure

4.3.1., MgO and CaO. The oxides of Ti and Zr showed relatively low CH_4 activation rates compared to these oxides, indicating that the acidity function of the catalyst was not as important as that of basicity.

The determination of acid sites on a catalyst may be elucidated by the measurement of the isoelectric point (IEP) of the oxide. The IEP depends on the net surface charge of the oxide in an aqueous solution. This charge arises from the difference in the adsorption of H^+, OH^- and ionised surface OH groups. The magnitude of the surface charge depends on the pH of the solution, the pH at which the charge is zero is the IEP. Thus the IEP provides an indication of the oxide acidity, although limitations on the acidity at different levels of hydroxylation are imposed by the measurement taking place in an aqueous solution. The IEP of a large number of oxides have been determined by Park [150, 151], who has proposed a generalised order of acidity, based on the oxide stoichiometry, this order is illustrated in Table 4.3.1.

Table 4.3.1. Generalised Isoelectric points based on oxide stoichiometry.

Oxide	Isoelectric point (IEP)
MO	$8.5 < IEP < 11.5$
M_2O_3	$6.5 < IEP < 10.4$
MO_2	$0 < IEP < 7.5$
M_2O_5, MO_3	$IEP < 0.5$

The oxides indicated to be highly acidic by the measurement of IEP were MoO_3, WO_3, Nb_2O_5 and Ta_2O_5. These dehydroxylated oxides may also be considered to show high Lewis acidity, as a consequence of the high oxidation state of the metal ion. The oxides MoO_3, WO_3 and Nb_2O_5 were all inactive for CH_4 activation, whilst Ta_2O_5 showed very low activity. Although MoO_3 and WO_3 were partially reduced, the resultant phases were also considerably acidic. The acidic catalysts SiO_2 and SnO_2 were also inactive for CH_4 activation, even though metallic Sn was detected on the used SnO_2 catalyst. The IEP of Fe_3O_4 was 6.5, in the same region as the MO_2 stoichiometric oxides, which may explain the relatively low CH_4

activation rate. However, the phase transition from the initial Fe_2O_3 catalyst also makes the surface area used for normalisation doubtful. The relative inactivity of the more acidic oxides of this study signified that activation via the CH_3^+ intermediate did not take place to a significant extent. The oxides with the lowest activity in this study, such as TiO_2, CeO_2 and ZrO_2, are predominantly acidic, but simultaneously they also show weak basicity, and are considered to be amphoteric [153]. On the contrary, over oxides such as MoO_3 and WO_3, which are purely acidic [153], CH_4 activation did not take place.

Ab initio Molecular Orbital calculations on a MgO (100) surface have indicated that CH_4 adsorbs by a heterolytic dissociative process, initiated by the abstraction of H^+ [154]. This is the same process which has been shown in figure 4.3.2., and proposed for CH_4 activation in this study. The homolytic adsorption of CH_4 on Mg^{2+} and O^{2-} surface sites, and the heterolytic adsorption to CH_3^+ and H^- have all been shown to be energetically unfavourable. Experimental studies of CH_4 adsorption on MgO have also provided evidence for CH_4 activation by heterolytic dissociation via the carbanion, which has been positively identified by infrared spectroscopy [155]. This adsorption process took place at ambient temperature, on an outgassed MgO sample. The active sites for this process were considered to be an acid-base pair of low coordination. The involvement of the carbanion intermediate has also been strongly invoked as the surface intermediate for CH_4/D_2 and hydrocarbon/D_2 exchange over the single oxides La_2O_3 [146], MgO [147], gamma-Al_2O_3 [141] and a range of basic oxides, including the lanthanide oxides, MgO, CaO, BaO and SrO [145]. The study by Utiyama et. al. has investigated C_2H_6/D_2 exchange rates over the same oxides, and showed that the activity was lower than for CH_4/D_2 exchange. This may be explained by the fact that C_2H_6 was less acidic than CH_4, since the ethyl carbanion is less stable than the methyl carbanion, due to the inductive effect of the additional methyl group. Both these factors provide further evidence for the involvement of carbanionic intermediates in the exchange process.

The activation of CH_4 is an important step in the oxidative coupling of CH_4 to C_2H_6 and C_2H_4. The heterolytic dissociation to H^+ and CH_3^- has been postulated as the initial reaction step on an MgO catalyst [156]. The rate of CH_4 coupling was observed to increased linearly with the concentration of surface basic sites, determined by the adsorption of benzoic acid. The methyl anion was formed on the Mg cation, as indicated by evidence from infrared spectroscopy. The rates of CH_4/CD_4 exchange over the same catalyst was much greater than the production rates of coupled products, and this was interpreted as indicating that dissociative adsorption was not the rate determining step. The rate determining step was proposed to be the breaking of the $M\text{-}CH_3^-$ bond to produce gas phase CH_3 radicals. The heterolytic process of CH_4 activation in the CH_4 coupling process has by no means been widely accepted. A process involving CH_4 homolytic adsorption has also been proposed for the initial activation step. Active sites responsible for this type of activation include the radical surface site, O^-, which has been suggested on catalysts such as Li/MgO [157], and the peroxide ion, O_2^{2-}, on the basic and lanthanide oxides [158].

There are distinct differences in the experimental conditions between studies of CH_4/D_2 exchange and the CH_4 oxidative coupling reaction. The major differences in these studies arise from the use of O_2 as reactant, and the higher temperatures, usually $> 650°C$, used for the coupling reaction. Although the activation of CH_4 for the process of CH_4 coupling has been widely disputed, the activation of other hydrocarbons by the abstraction of H^+ on the oxide basic sites has been more widely accepted. This is particularly evident for the activation process in the selective oxidation and ammoxidation of propene, where the allylic intermediate has been invoked by experimental [159] and theoretical [160] studies.

ZnO and the oxides of the first row transition metals are well represented in the present study. Cr_2O_3 and ZnO have both demonstrated high activity for the exchange process, surface area normalised rates have shown that ZnO was slightly more active. In comparison to many metals, oxide catalysts are considered relatively

inert for hydrogenation reactions. However, the oxides which have shown moderate activity for hydrogenation were Co_3O_4, Cr_2O_3 and ZnO [161]. The normalised exchange activities at 500°C are shown in figure 4.3.3. for the first row transition metal oxides and ZnO. The relative rates for ethylene hydrogenation are also shown in the same figure, for the equivalent oxides.

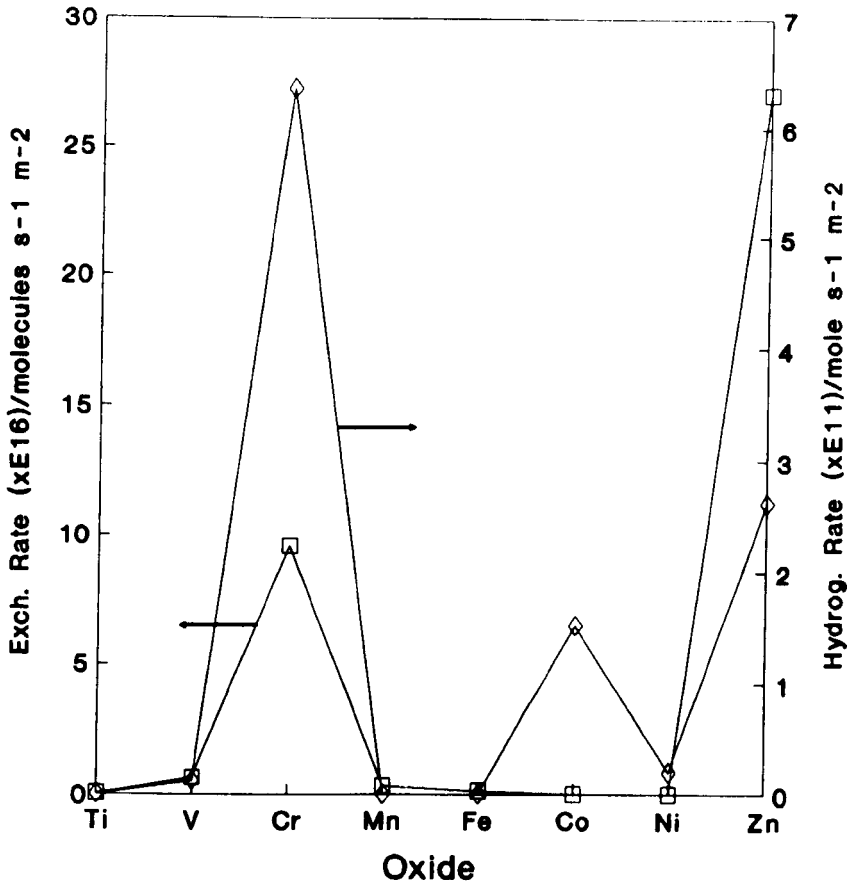

Figure 4.3.3. CH_4/D_2 normalised exchange rates at 500°C and ethylene hydrogenation activity for the first row transition metal oxides and ZnO.

The activity patterns for the both reactions were very similar. Reaction rate maxima for ethylene hydrogenation were observed over Cr_2O_3, Co_3O_4 and ZnO. Similar maxima were also observed for the exchange reaction over Cr_2O_3 and ZnO, although the order of activity was reversed, with ZnO showing the highest activity for exchange. The high activity of ZnO may to some extent be a consequence of oxide reduction. XRD analysis has showed that after use the bulk phases detected was ZnO, unchanged from the original catalyst. However, ZnO is known to reduce to a certain degree, by losing O_2 when heated in a vacuum. This process leads to

the production of interstitial Zn^+ ions or Zn atoms [162], which may well be more active centres for CH_4/D_2 exchange than those on fully oxidied ZnO. ZnO is also a relatively basic oxide and would certainly dissociate CH_4 heterolytically, in the manner described previously for the other basic oxides (figure 4.3.2.). The detection of such Zn/Zn^+ species would prove difficult by the technique of XRD, unless the formation of interstitial species caused significant distortion of the ZnO lattice, which has not been indicated in this case. Under the reaction conditions employed in these studies Co_3O_4 was reduced completely to the metallic state, and showed low exchange activity.

NiO was not tested as it was known to reduce to metallic Ni under reaction conditions [163]. The oxides TiO_2, V_2O_3, MnO and the mixed Fe catalyst all showed the same activity pattern. The ethylene hydrogenation activity was reported over both the anatase and rutile phases of TiO_2, both showed very low activity. Although Fe_2O_3 (hematite), the catalyst used for ethylene hydrogenation, was clearly different from the Fe/Fe_3O_4 mixed catalyst used for exchange studies it was still included in the comparison. Characterisation of Fe_2O_3 after use for C_2H_4 hydrogenation indicated that Fe_3O_4 was present, also the presence of Fe could not be totally discounted [161], therefore the Fe based catalysts of these two studies may not be too dissimilar. The Cr_2O_3 catalyst was also very active for CH_4 activation, this oxide is not particularly basic and the activity may be due to some type of preferential activation site on the surface. These sites may be related to an acid base pair which are spaced at an optimum distance apart for the dissociation of the C-H bonds. It may be possible that CH_4 was not activated by a process of heterolytic dissociation, but via a different mechanism. If this was the case it does however, seem unusual that the same trends as the majority of the other oxides were observed. These similarities included an increase in activity as the extent dehydroxylation increased, and a stepwise mechanism of exchange.

The same activity patterns demonstrated for ethylene hydrogenation over the transition metal oxides have also been shown for H_2/D_2 exchange [164]. The oxides

showed much higher activity for H_2/D_2 exchange compared to CH_4/D_2 exchange, as catalytic studies were carried out below 20°C. The same activity pattern has also been observed for hydrocarbon dehydrogenation [165], more specifically for cyclohexene dehydrogenation to benzene in the temperature range 150-450°C. Thus it appears that this pattern of activity shown by the first row transition metal oxides and ZnO is relatively widespread. It has been shown to relate to processes of C-H bond breaking, demonstrated by CH_4/D_2 exchange in this study and the dehydrogenation activity [165], as well as H-H bond breaking, in H_2/D_2 exchange [164], and in the hydrogenation behaviour [161]. The similar pattern shown by these oxides for these processes may suggest that the same type of active site was responsible for the catalytic activity. It is believed that H_2 and D_2 adsorb by heterolytic dissociation on an acid base pair of ZnO [166]. Following this process it would be expected that the same type of absorption would also occur on other oxides.

Considering the dehydrogenation, hydrogenation and H_2/D_2 exchange activity of ZnO and the results obtained in this study it is surprising that previous studies have not found ZnO to be active for CH_4/D_2 exchange [145]. It is clearly evident that in many studies the pre-treatment, or dehydroxylation, of the oxides was an important factor for promoting activity. It does seem unusual however, that pre-treatment at 500°C did not produce an active ZnO catalyst in this previous studies [145]. TiO_2 and ZrO_2, activated at 500°C and 600°C respectively, were also found to be inactive by Utiyama et. al. [145]. It was concluded that neither oxide possessed sufficiently basic sites to activate CH_4, which is in conflict with results presented here and by Haliday et. al. [148], as both these oxides were found to be active.

Ga_2O_3 was the most active catalyst in the present study by a significant margin. The structural and chemical similarities between Ga_2O_3 and Al_2O_3 have been noted previously (section 3.2.1.), and demonstrated by CH_3OH oxidation (section 3.2.2.). Indeed, in this study Al_2O_3 also shows appreciable CH_4/D_2 exchange activity. After conditioning at 540°C the Al_2O_3 surface would have been considerably

dehydroxylated. Previous studies would suggest that after treatment at this temperature the extent of surface hydroxylation would be in the region of 20% [167]. The fully hydroxylated surface of Al_2O_3 was found to strongly retain about 13 molecules of H_2O per 100 $Å^2$ [167]. This corresponds to approximately $1.3x10^{19}$ H_2O molecules m^{-2}. Assuming 80% dehydroxylation, the number of exposed Al^{3+} and O^{2-} ions would be equal, and in the region of $1.0x10^{19}$ m^{-2}. Thus, the number of ion pairs were approximately three orders of magnitude greater than the exchange rate, and unless the turnover frequency of these sites was unfeasibly slow, it can be assumed that only certain sites were active. A similar conclusion was reached by Larson and Hall [142] for CH_4 (CD_4) exchange with hydroxyl groups on gamma-Al_2O_3. It was proposed that only sites produced at domain boundaries were sufficiently active for CH_4 exchange, as it was only these strong sites that were able to dissociate CH_4. Although a detailed model, such as that proposed by Peri for gamma-Al_2O_3, has not been undertaken for Ga_2O_3, it can be assumed that results would be similar, due to the structural and chemical similarities of the two oxides. It can also be assumed that only certain ion pair sites on the Ga_2O_3 surface would be operative for CH_4 activation. XRD showed that the Al_2O_3 catalyst contained a lot more amorphous material than the Ga_2O_3 catalyst (section 3.2.1.). This may indicate that phase boundaries of Ga_2O_3 between the alpha, beta and gamma phases were more pronounced. If the active sites responsible for CH_4 activation were associated with the phase boundaries, as has been suggested by Larson and Hall [142], then it follows that Ga_2O_3 would be a more active catalyst for CH_4 activation than Al_2O_3.

Studies of alkane exchange with D_2 over Al_2O_3 have shown a correlation between hydrocarbon acidity and activity [141], and this has been used as evidence for the involvement of carbanion chemistry. From the findings of Robertson et. al. and evidence from this study, it can be concluded that CH_4 activation over Al_2O_3 and Ga_2O_3 was also initiated via H^+ abstraction to form the methyl carbanion. There does however, appear to be an important structural contribution to the process,

particularly with Ga_2O_3, as the activity was not directly related to the basic strength of the oxide. Such a structural effect may be similar to that which has been proposed earlier for Cr_2O_3, that is the oxide structure exposed a surface acid base pair with optimal separation for C-H bond activation.

This discussion would not be complete without brief consideration of the participation of D_2 in the exchange reaction. The C-H bond energy in CH_4 is very similar to that of H-H in H_2, at 435 kJ mol^{-1} [17]. The bond energy of D-D in the D_2 molecule is slightly greater, by approximately 9 kJ mol^{-1}. Thus, under certain circumstances, namely where homolytic fission predominates, it may be expected that D-D bond fission would limit the rate of reaction. Adsorption of H_2 on ZnO takes place by a heterolytic dissociative process [166], as does D_2 on the same dehydroxylated oxide [168]. H_2/D_2 exchange reactions have been reported on several oxides, it was evident that exchange rates were very much higher than CH_4/D_2 exchange rates on the same materials [164]. Therefore, it would be a valid assumption that the rate determining step in these studies would be C-H bond activation and not that of D-D. Isotope studies using CH_4/D_2 and CD_4/H_2 exchange over gamma-Al_2O_3 have indicated that the rate determining step was breaking of a C-H or C-D bond and not the dissociation of H_2 or D_2 species [142]. The same conclusion has been drawn over a range of basic oxides [145], where a similar rate constant was observed for CH_4/CD_4 exchange to that of CH_4/D_2, the equilibration of H_2/D_2 over the equivalent catalysts were extremely rapid.

Closer examination of the kinetic data showed that a relationship existed between the activation energy of CH_4/D_2 exchange, E_a, and the pre-exponential factor, ln A. The relationship is shown in figure 4.3.4.

This effect, where the influence of change of one Arrhenius parameter is offset by the change of the other, has been commonly observed for many reactions. This phenomena is referred to as the compensation effect [169]. The exact nature of the compensation effect has not been fully resolved. Suggestions for the behaviour have included energetically heterogeneous catalyst surfaces, more than one active

surface, enthalpy-entropy relationships, temperature dependent concentration of active sites and surface mobility effects [170].

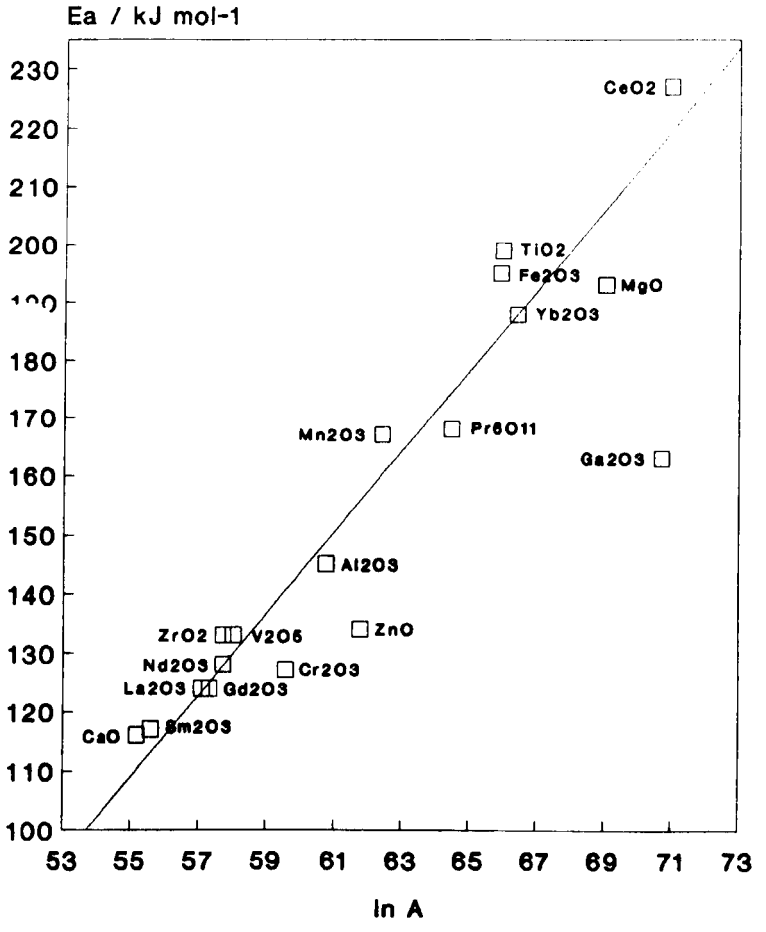

Figure 4.3.4. Relationship between E_a and ln A for the kinetics of CH_4/D_2 exchange.

The exchange reaction of CH_4 with D_2 has been shown to exhibit a compensation effect over the metals Pd, Ru, Ni, Au and Pt, although no relationship was found for the exchange between higher C_2-C_6 hydrocarbons over the same metals. A compensation effect was also observed by McKee for the CH_4/D_2 exchange reaction over Pd-Ru and Pd-Au alloys [171, 172], but no explanation as to the origin of these effects could be offered.

4.4. CONCLUSIONS

Under reaction conditions a number of the oxides used in this study were reduced, forming different oxide phases, mixed oxide phases and in some cases the metallic

states. Many catalysts were active for the CH_4/D_2 exchange reaction, at 500°C the pattern of activity, normalised for surface areas was;

$Ga_2O_3 >> ZnO > Cr_2O_3 > La_2O_3 > Nd_2O_3 > Gd_2O_3 \approx Pr_6O_{11} > CaO > Al_2O_3 > Sm_2O_3 \approx MgO > V_2O_3 > Yb_2O_3 > MnO > ZrO_2 > Fe_2O_3 > CeO_2 > TiO_2$.

Ga_2O_3 was the most active catalyst by a considerable margin, ZnO, Cr_2O_3 and La_2O_3 were also highly effective catalysts for CH_4 activation. The exchange reaction catalysed by all the oxides mentioned above took place in a step wise manner. CH_3D was the major product, with CH_2D_2 a minor product in many cases Exchange catalysed by reduced Co_3O_4 and Ta_2O_5 showed very low activity, but all possible deuterated products, CH_3D, CH_2D_2, CHD_3 and CD_4 were formed. The oxides which were inactive during these studies were MoO_3, Nb_2O_5, SiO_2, SnO_2, Ta_2O_5, Tb_4O_7, WO_3 and Y_2O_3.

Over the oxides which were known to be basic, the CH_4/D_2 exchange activity correlated with the relative basicity of the catalysts. Correlations have also been established between CH_4/D_2 exchange activity of the transition metal oxides and the activity observed for ethylene hydrogenation, hydrocarbon dehydrogenation and H_2/D_2 exchange. These were all processes which require the breaking and formation of C-H and H-H bonds, which may well occur on common catalytic sites. Over the catalysts used in this study, with the exceptions of Co_3O_4 and Ta_2O_5, the process of CH_4 activation took place by a process of heterolytic dissociative adsorption on an acid-base pair of the oxide surface. This process was initiated by the abstraction of H^+ from CH_4 by the basic O^{2-} surface species. Such a conclusion is in good agreement with other studies on hydrocarbon/D_2 exchange. Important structural factors contributed to the high activation rates of Ga_2O_3 and Al_2O_3, and probably also influenced the activity of Cr_2O_3. The information gained form this study will be combined with results from CH_3OH oxidation over the same oxides, to provide guide-lines for new catalyst formulations for CH_4 partial oxidation.

Finally, the relationship between activation energy for CH_4/D_2 exchange and the pre-exponential factor has been shown to follow that expected for a compensation effect.

CHAPTER 5

METHANE PARTIAL OXIDATION

5.1. INTRODUCTION

The detailed approach which has been adopted for the design of new catalysts was outlined in section 1.8. This design approach has been based on studies of O_2, CH_4 and CH_3OH activation, using a wide range of single oxides. Information from these studies have been used to suggest two new mixed oxide catalysts, which have been tested, along with two single oxides. Preliminary studies have been carried out to assess the efficacy of these catalysts for CH_4 partial oxidation to CH_3OH.

The single oxides which were selected for inclusion in these initial catalyst preparations were Ga_2O_3, MoO_3 and ZnO. The main criteria for selecting these constituent oxides were, the high activity for CH_4 activation of Ga_2O_3 and ZnO indicated by CH_4/D_2 exchange (Chapter 4). These two oxides were also in the intermediate range for oxygen isotope exchange activity (Appendix A), and the ranking order for CH_3OH stability, based on the temperature at which 30% was converted to carbon oxides (Chapter 3).

MoO_3 was the preferred oxide as the support component, and was combined with Ga_2O_3 and ZnO to prepare the catalyst for subsequent evaluation. In this context MoO_3 was selected in terms of performance for CH_3OH stability, as it produced very low levels of carbon oxides. It was also evident that the exchange of oxygen isotopes over MoO_3 took place by a different mechanism from the majority of other oxides, which produced higher levels of CO_X. MoO_3 did not prove active for CH_4 activation by the exchange reaction with D_2. Many previous studies have used molybdenum containing catalysts for CH_4 partial oxidation. The majority of these studies have concentrated on the highly dispersed form, supported on a high area silica. These catalysts have proved to be some of the most successful and widely studied to date. The use of MoO_3, in the bulk oxide form, has been less extensively studied, but catalysts of this type have been used and reports appeared in the

literature. Details of many of these studies have been briefly reviewed in section 1.9.

Catalysts were manufactured by physically grinding the component oxides. This method of catalyst preparation was adopted in these preliminary experiments for two main reasons. Firstly it was envisaged that a greater degree of control could be retained over the final structure of the catalyst. In contrast, catalysts prepared by solution impregnation, would tend to produce a more highly dispersed oxide phase, which may even block the active sites of the support phase, MoO_3 in this case. Also preparation by coprecipitation could readily produce a new mixed phase, with metal ions in different coordination environments. These considerations were important, as results from CH_3OH, CH_4 and O_2 activation studies were limited to a number of specific oxide phases.

The second reason for the preference of this catalyst preparation method was historical, based on preceding catalytic studies. The preparation of MoO_3/SiO_2 and V_2O_5/SiO_2 catalysts by a process of physical mixing in a ball mill [173], were found to produce HCHO from CH_4 more selectively, at 1 bar pressure, than catalysts prepared to the same loadings by impregnation of the SiO_2 support. The conversion over the mechanically mixed catalysts were lower than the impregnated catalysts. The selectivity to oxygenated products from CH_4 oxidation is often dependent on the level of CH_4 conversion, and insufficient data were included to assess the full potential benefits of the mechanical mixture. However, it is interesting to note that very low levels of CO and CO_2 were produced over the physically mixed oxides. The most promising of these catalysts was 10% V_2O_5 mixed with SiO_2 in a ball mill for 3 hours prior to use. This catalyst showed a 99.0% selectivity to HCHO at 2.5% CH_4 conversion, at 600°C using a 1/3/1 mix of $CH_4/N_2O/Ar$ as the reactant feed.

The reaction conditions used for CH_4 partial oxidation studies were selected to favour the production of CH_3OH. For reasons of experimental practicality the working pressure of the reactor was 15 bar. The use of elevated pressure has been

shown to enhance the selectivity to CH_3OH [5]. A marked advantage between experiments a 1 bar and 30 bar is clearly evident. However, there is an optimum pressure range for CH_3OH formation, as increasing the pressure had a detrimental effect on CH_3OH selectivity. This was demonstrated by Boomer and Thomas [27], who reported a fall-off in CH_3OH selectivity above 177 bar, and Morton et. al. [174], who reported the same effect above 98 bar. The main influence of pressure on the homogeneous reaction beside increasing CH_3OH selectivity, appears to lower the temperature at which CH_3OH was first produced. For example, at 5 bar CH_3OH was first detected at 450°C, decreasing to 375°C at 50 bar.

The CH_4/O_2 ratio of the reactant feed also has an effect on the product distribution. Increasing the concentration of O_2 in the reaction feed had a detrimental effect on CH_3OH selectivity [175]. The studies by Casey et. al. [176], on the gas phase oxidation of CH_4 at 30-60 bar, in the temperature range 350-550°C, have illustrated this effect adeptly. Maximum CH_3OH selectivities were 15.5%, 22%, 32% and 44%, when the O_2 mol % of the feed was 12, 6, 3 and 1.5 respectively. The decrease in the selectivity of CH_3OH, as the O_2 concentration was increased, was offset by an increase in CO_2 selectivity, while CO selectivity remained approximately constant.

5.2. RESULTS

5.2.1. POWDER X-RAY DIFFRACTION CATALYST CHARACTERISATION

Catalysts used for CH_4 partial oxidation were characterised before and after use by powder X-ray diffraction. Analysis of the ZnO/MoO_3 physical mixture prior to calcination indicated the presence of two distinct oxide phases. These were ZnO, Zincite, and MoO_3, Molybdite, the same phases which were previously observed for the single oxides used for the preparation. No significant changes in peak positions, and consequently lattice d-spacings, were observed for either of the identified phases, when compared to the single oxides. The XRD patterns for the ZnO/MoO_3 calcined catalyst, before and after use are shown in figure 5.2.1.1.

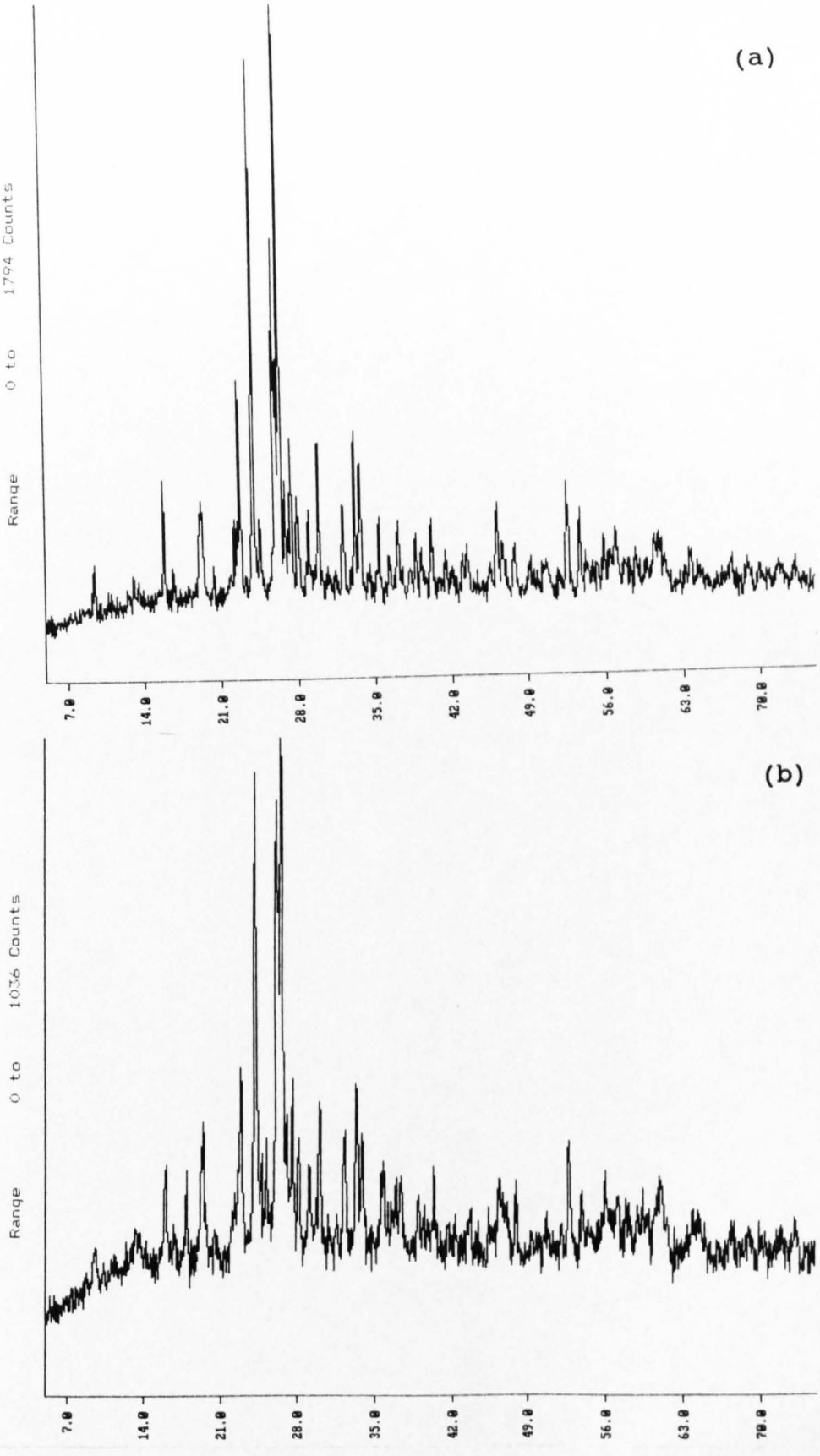

Figure 5.2.1.1. Powder X-ray diffraction patterns for the ZnO/MoO_3 catalyst after calcination, (a) before use; (b) after use.

On calcination, $ZnMoO_4$ was formed as the major bulk phase from the powdered mixture, a minor phase matching $Zn(OH)_2$ was also identified, with the Wuelfingnite structure. After use $ZnMoO_4$ remained as the major phase, $Zn(OH)_2$ was not present, but a reduced phase $Zn_2Mo_3O_8$ was detected. The XRD pattern after use showed a considerably higher background contribution, and peak widths were also increased.

The uncalcined physical mixture of Ga_2O_3 and MoO_3 showed an XRD pattern very similar to that obtained from pure Molybdite, MoO_3, except that the background intensity was marginally increased. The pattern contained only one broad peak of low intensity, at a diffraction angle of ca. 30.1°, which possibly corresponded to the most intense peak in the pattern of the Ga_2O_3 starting material. Comparison between the XRD patterns of the Ga and Mo oxides from which the catalyst was prepared showed that the maximum intensity for MoO_3 was approximately 14 times greater than that of Ga_2O_3. It may therefore be expected that peaks from a Ga_2O_3 phase would be small compared to those from MoO_3. Inter-plannar spacings of MoO_3 in the Ga_2O_3/MoO_3 mixture were not significantly different from those of pure MoO_3. The diffraction patterns of the calcined Ga_2O_3/MoO_3 catalyst before and after use for CH_4 oxidation are shown in figure 5.2.1.2.

After calcination the XRD pattern did not alter significantly. MoO_3, Molybdite, remained the only positively identified phase, as no significant diffraction peaks attributed to a Ga phase were distinguished. Relative to the uncalcined sample the background was increased and slight peak broadening was observed.

After use, the diffraction pattern of the Ga_2O_3/MoO_3 catalysts was notably different. MoO_2 with the Tugarmovite structure was the major identified phase, MoO_3 was also present, but diffraction peaks from this phase were of low intensity. Peak widths from the MoO_3 phase were much broader than peaks from the MoO_2 phase. The pattern still did not show any evidence for a phase containing Ga. The background of the used sample was higher than that of the calcined sample prior to use.

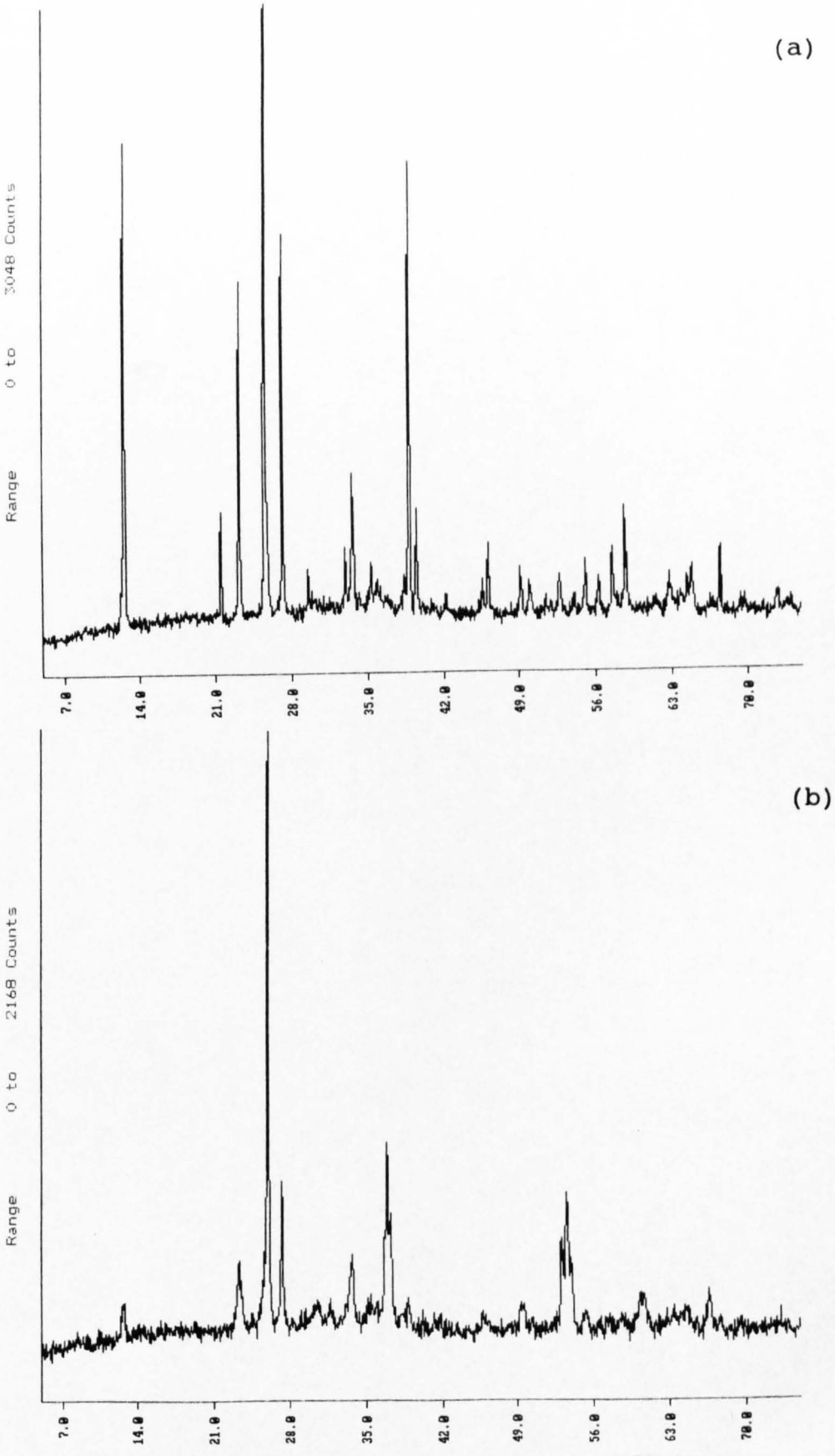

Figure 5.2.1.2. Powder X-ray diffraction patterns of the Ga_2O_3/MoO_3 catalyst after calcination, (a) before use; (b) after use.

It was mentioned previously that the XRD pattern for the uncalcined Ga_2O_3/MoO_3 catalyst was very similar to that of MoO_3. These similarities continued through to the used MoO_3 catalyst, which showed the Tugarmovite MoO_2 phase, with a minor MoO_3 phase. The same characteristic broader MoO_3 peaks, and a higher background level were also noted.

Ga_2O_3 before use was a mixture of phases consisting of Ga_2O_3 with the alpha, beta and gamma structures, further details of these phases were highlighted in section 3.2.1. After use, the diffraction pattern of Ga_2O_3 was unchanged, but an increase in the background level was observed.

5.2.2. X-RAY PHOTOELECTRON SPECTROSCOPY CATALYST CHARACTERISATION

The catalysts MoO_3, Ga_2O_3/MoO_3 and ZnO/MoO_3 were also characterised by X-ray photoelectron spectroscopy. The binding energies of relevant photoelectron lines for the elements Mo, Ga, Zn and O are presented in table 5.2.2.1.

Table 5.2.2.1. Binding energies for selected X-ray photoelectron lines of the used and unused catalysts.

Catalyst	Binding Energy/eV			
	$Mo3d_{5/2}$	O1s	$Ga2p_{1/2}$	$Zn2p_{3/2}$
MoO_3	233.0	530.0	-	-
used MoO_3	232.2	530.3	-	-
Ga_2O_3/MoO_3	231.8	530.6	1116.7	-
used Ga_2O_3/MoO_3	233.6	530.7	1116.6	-
ZnO/MoO_3	232.2	527.8	-	1021.4
used ZnO/MoO_3	232.4	528.7	-	1021.3

The binding energies in table 5.2.2.1. were referenced using the C1s peak at 284.6 eV as a standard. The $Mo3d_{5/2}$ binding energy of the used MoO_3 catalyst was decreased, relative to MoO_3 before use, by 0.8 eV. The same shift was also observed for the $Mo3d_{3/2}$ line, details of which have not been included in the above table. The shift in the O1s peak before and after use was negligible.

X-ray photoelectron lines originating from Ga 2p, 3s, 3p and 3d levels were major features of the spectra for the Ga_2O_3/MoO_3 catalyst, before and after use. The binding energy of the most intense $Ga2p_{1/2}$ line was not shifted significantly after use, whilst the $Mo3d_{5/2}$ line was. No shift in the O1s line was detected between the used and unused catalyst.

The binding energy of the $Mo3d_{5/2}$ line in the ZnO/MoO_3 catalyst was unchanged after use. The average binding energy for these two lines was 232.2 eV, some 0.7 eV less than that observed for the unused MoO_3. The binding energies for the $Zn2p_{1/2}$ line was also unchanged after use. The situation was somewhat different for the O1s peak which was shifted to a higher binding energy by 1.1 eV for the used catalyst.

X-ray photoemission peaks for Ga, Mo, Zn and O showed no evidence for peak broadening, either for the initial catalysts, or after they had been used. The assessment of line widths for the $Mo3d_{5/2}$ peak was complicated as it constituted a doublet with the $Mo3d_{3/2}$ peak, which was not fully resolved. However, examination of the $Mo3p_{3/2}$ peak at a higher binding energy did not show any signs of peak broadening. Considerable broadening of the C1s peaks were observed for the used Ga_2O_3/MoO_3 and ZnO/MoO_3 catalysts. After use the full width half maximum of the C1s peak increased from 3.4 eV to 4.3 eV for Ga_2O_3/MoO_3, and from 3.5 eV to 5.4 eV for ZnO/MoO_3.

The surface elemental concentrations were determined before and after use, based on the peak areas of specific photoemission lines. The peaks used to draw quantitative conclusions were $Mo3p_{3/2}$, $Ga2p_{1/2}$, $Zn2p_{3/2}$, O1s and C1s. These results are shown below in table 5.2.2.2.

After use the Ga_2O_3/MoO_3 catalyst showed an increased concentration of surface carbon, whilst that of oxygen remained constant, and Mo and Ga concentrations decreased. The Mo/Ga surface ratio of the as prepared catalyst was ca. 2.0, after use the ratio had increased to 5.9.

Table 5.2.2.2. Surface elemental concentrations of the catalysts, before and after use.

Catalyst	Element	% Surface Concentration	
		Before use	After use
MoO_3	Mo	19.7	17.8
	C	35.9	30.7
	O	44.4	51.6
Ga_2O_3/MoO_3	Mo	28.9	19.7
	Ga	14.6	3.3
	C	12.0	31.7
	O	44.5	45.4
ZnO/MoO_3	Mo	18.1	6.4
	Zn	7.8	3.3
	C	22.4	63.8
	O	51.7	26.5

The used ZnO/MoO_3 catalyst showed a considerable increase in the concentration of surface carbon, over the unused catalyst, by a factor of approximately 2.8. As a major consequence of this increase surface levels of Mo, Zn and O were depleted. The Mo/Zn ratio of the initial catalyst was 2.3, after use this had decreased slightly to 1.9.

The variations in elemental surface concentrations on MoO_3 after use were minor. The most prominent difference noted was the slight increase in the concentration of surface oxygen.

Under the normal spectrometer scan conditions, at which the instrument was most sensitive, no peaks were detected which could not be assigned to X-ray photoelectron or Auger emissions from the surface elements shown in table 5.2.2.2.

5.2.3. CATALYTIC ACTIVITY FOR CH_4 PARTIAL OXIDATION

Catalysts were tested at 15 bar pressure, using the experimental conditions described in section 2.3.2. Results for the partial oxidation of CH_4 over MoO_3 are shown in figure 5.2.3.1.

This catalyst was inactive at 400°C, activity was first exhibited at 425°C with a CH_4 conversion of 0.32%. CO was the most selective product, with CO_2 also

formed. At 425°C CH_3OH was also detected, with a selectivity of 13%. Above 450°C CH_4 conversion increased gradually with temperature, simultaneously CO_2 selectivitv steadily increased, while overall CO selectivity declined. At 503°C and above C_2H_6 was formed.

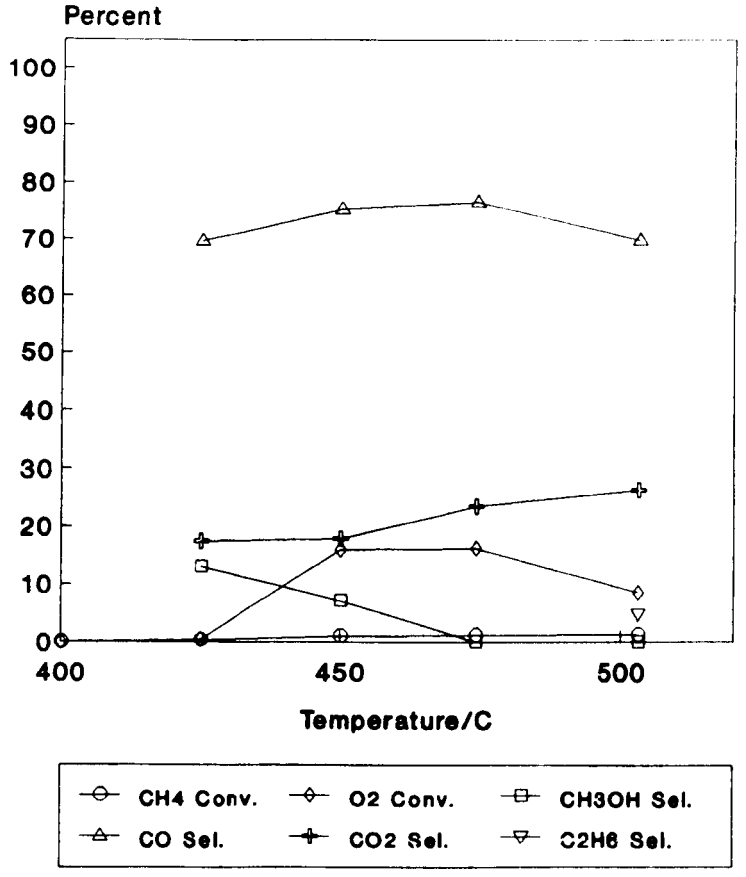

Figure 5.2.3.1. CH_4 partial oxidation over the MoO_3 catalyst (GHSV = 4,960 hr^{-1}, $CH_4/O_2/He$ = 46/6/10).

The other single oxide tested for CH_4 oxidation was Ga_2O_3, the results of which are shown in figure 5.2.3.2.

CH_4 conversion increased from 400°C to 500°C, and tended to level off at this temperature, the same trend was observed for O_2 conversion. CO_2 selectivity was high throughout the entire range of CH_4 conversion. Generally it was observed that CO_2 selectivity declined as the temperature was increased, this was accompanied by a decrease in CO selectivity. CH_3OH was observed at low selectivity, 3%, at 450°C, but was no longer detected at 500°C, where a slight maximum in CO_2

selectivity was observed. At 450°C and above C_2H_6 was produced, selectivity to this product increased as the temperature was elevated.

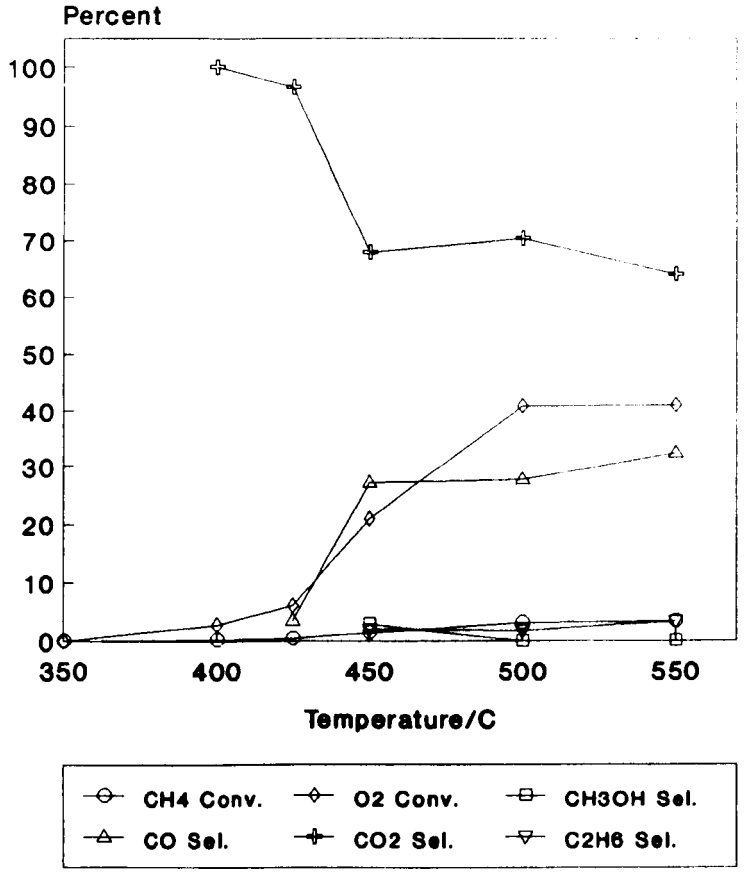

Figure 5.2.3.2. CH_4 partial oxidation over the Ga_2O_3 catalyst (GHSV = 4,960 hr^{-1}, $CH_4/O_2/He$ = 46/6/10).

The results obtained for CH_4 partial oxidation over ZnO/MoO_3 are shown below in figure 5.2.3.3.

Activity was first observed at 400°C, with a trace CH_4 conversion. Under these conditions CO_2 was the sole product. CH_4 and O_2 conversion increased with temperature reaching a maximum of 4.5% and 64.1% respectively at 550°C. After the high initial selectivity towards CO_2 levels decreased as the temperature was increased to 500°C, accompanied by an increase in CO selectivity. Above 500°C, CO selectivity decreased and CO_2 increased. Up to 500°C carbon oxides were the only reaction products, while C_2H_6 was produced at 500°C and 550°C. CH_3OH was not formed at any reaction temperature.

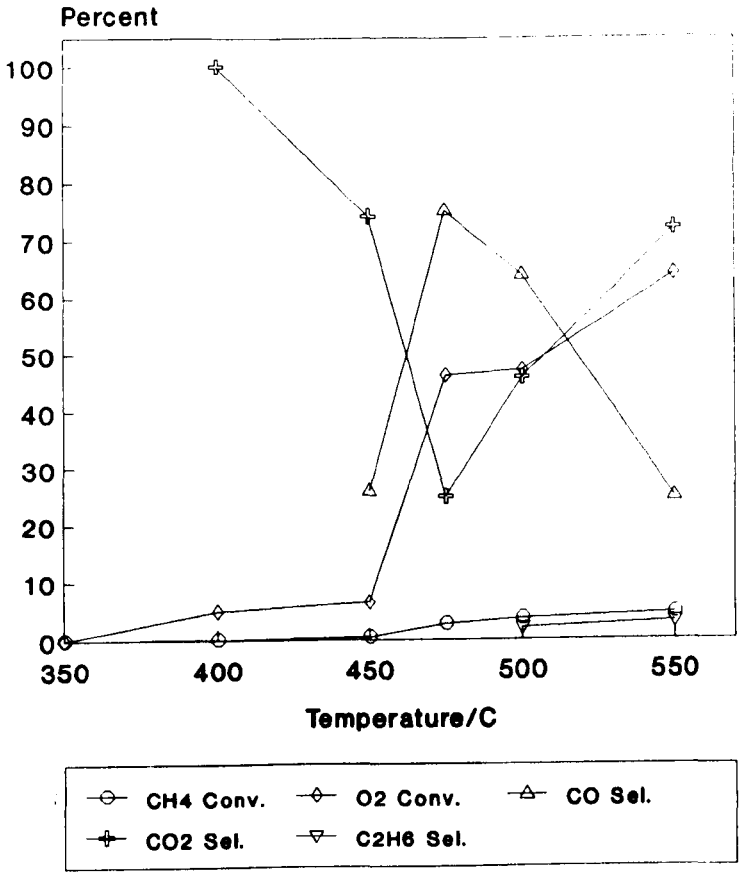

Figure 5.2.3.3. CH_4 partial oxidation over the ZnO/MoO_3 catalyst (GHSV = 4,960 hr^{-1}, $CH_4/O_2/He$ = 46/6/10).

The conversion of CH_4 and the product distribution over the Ga_2O_3/MoO_3 catalyst are shown in figure 5.2.3.4.

Initial activity was detected at 350°C, with 100% selectivity to CO_2. CO_2 selectivity declined as the temperature was raised from 350°C to 460°C, above this temperature CO_2 selectivity again increased. CO selectivity showed the reverse effect passing through a maximum selectivity of 62% at 502°C. This pattern shown by the CO_X products was very similar to that shown by ZnO/MoO_3 under the same conditions. CH_4 conversion rose sharply from 400°C to 460°C over Ga_2O_3/MoO_3, and reached a plateau above 460°C, remaining ca. 3.0%. The same trend was repeated for O_2 conversion. At 460°C CH_3OH was produced with a selectivity of 22%, as was C_2H_6 at 1% selectivity. CH_3OH was no longer detected as the temperature was raised, while C_2H_6 levels continued to increase.

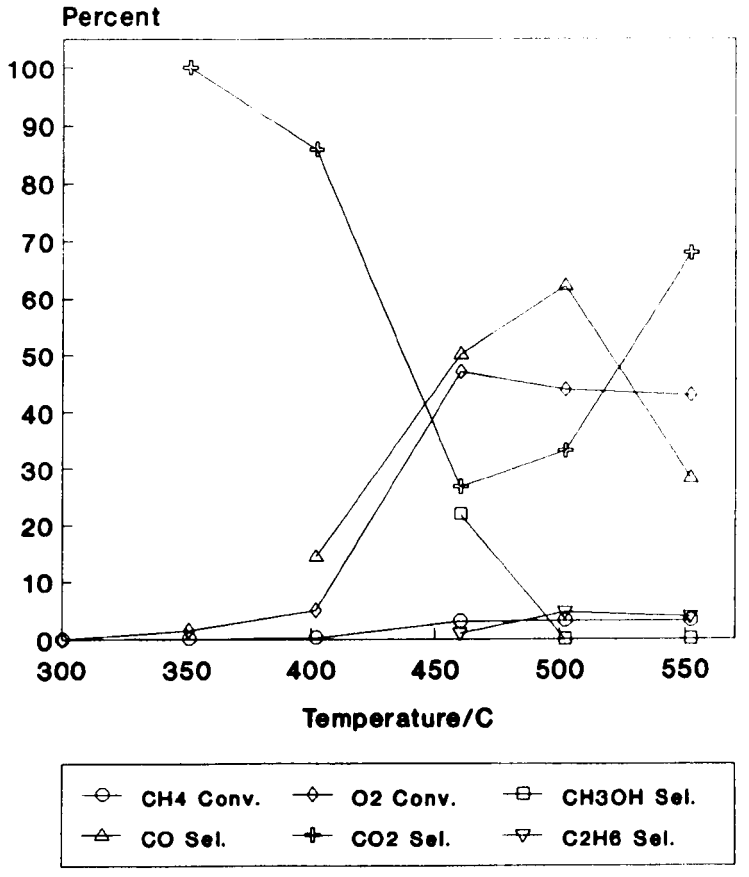

Figure 5.2.3.4. CH_4 partial oxidation over the Ga_2O_3/MoO_3 catalyst (GHSV = 4,960 hr^{-1}, $CH_4/O_2/He$ = 46/6/10).

Experiments were also performed using the same conditions to investigate the behaviour of CH_4 partial oxidation in a blank reactor tube. Two experiments were carried out, the first investigated activity of the empty fused silica reactor. The second investigated the activity of a reactor filled with quartz chips. The quartz chips were chosen as an inert material. The quartz chips were sieved to a uniform 0.6-1.0 mm uniform particle size range, and the bed packed to the same volume as in the previous catalytic experiments.

The results obtained for CH_4 partial oxidation in the empty reactor tube are shown in figure 5.2.3.5.

No conversion was observed at 400°C, whilst at 450°C almost complete O_2 conversion, 99.6%, was observed. CO was the most selective product, with lower levels of CO_2 also detected. At 450°C CH_3OH selectivity was 29%, this declined steadily as the reaction temperature increased, the major compensation for the loss

of this product was offset by the increase in selectivity towards C_2H_6 and CO. Above 450°C O_2 conversion was 100%, while CH_4 conversion remained approximately constant. The selectivity to CO_2 was not enhanced as the temperature was raised. CH_3OH fell from a maximum at 450°C, but the product was still detected at 550°C with 17% selectivity.

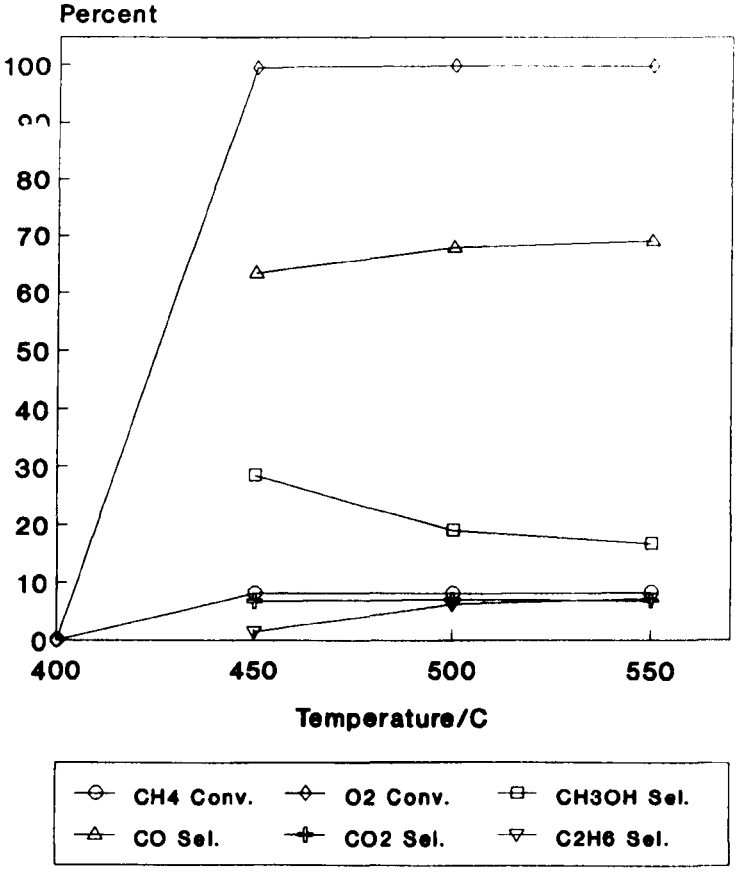

Figure 5.2.3.5. CH_4 partial oxidation in the empty fused silica reactor tube (GHSV=4,960 hr^{-1}, $CH_4/O_2/He$=46/6/10).

The corresponding results obtained over the quartz chips bed are shown in figure 5.2.3.6.

Trace CH_4 conversion was initially shown at 400°C, producing CO_2 with 100% selectivity, this pattern was repeated at 450°C, where CH_4 conversion was still low. CH_4 conversion was considerably higher at 475°C, where it was 3.5%, rising steadily to 4.0% at 550°C. At 550°C O_2 conversion was approaching 100%. CO_2 selectivity decreased from the initial 100% to a minimum value at 475°C. Above 475°C CO_2 selectivity increased steadily as the temperature was increased, but levels were always lower than CO. This variation of CO_2 selectivity with

temperature was very similar to that observed during CH_4 oxidation over Ga_2O_3/MoO_3 and ZnO/MoO_3, although with these oxide catalysts CO_2 was the predominant product at higher temperatures. CH_3OH selectivity over the quartz chips was 15% at 475°C, decreasing to 8% at 550°C. As was previously observed for the empty tube data, the decline in CH_3OH selectivity was accompanied by a simultaneous increase in C_2H_6 selectivity as the temperature was increased.

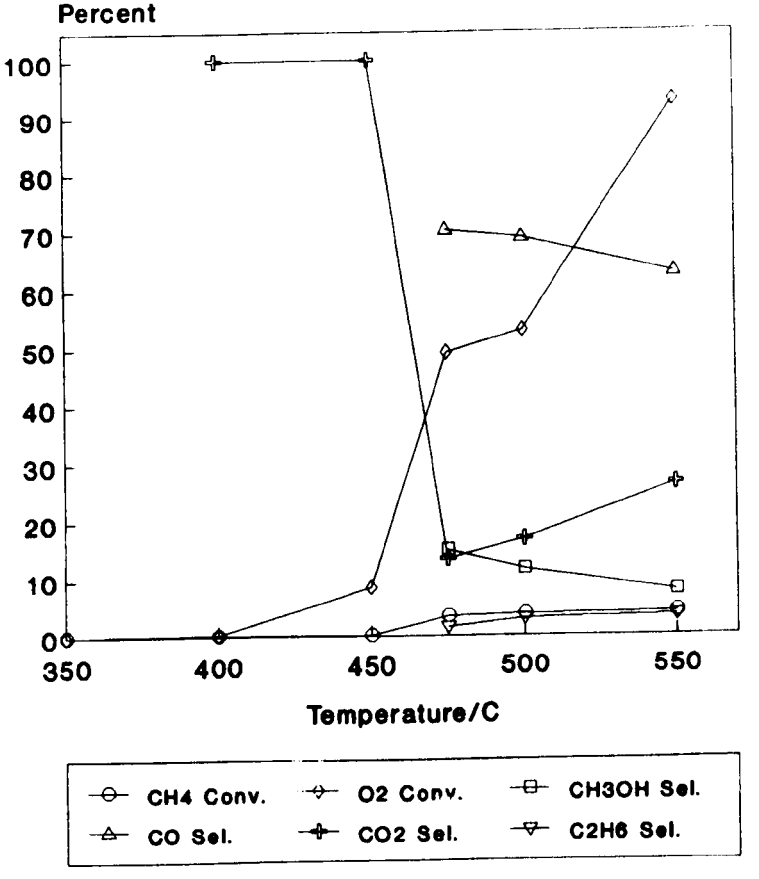

Figure 5.2.3.6. CH_4 partial oxidation over the quartz chips bed (GHSV = 4,960 hr^{-1}, $CH_4/O_2/He$ = 46/6/10).

In all cases the measured carbon balances were close to 100%, generally values were in the range 98-102%. The oxygen balances were not in such good agreement, for the majority of reported results values were in the range 87-104%. Tables of data for CH_4 partial oxidation results are presented in Appendix D.

5.3. DISCUSSION

5.3.1. CHARACTERISATION BY POWDER X-RAY DIFFRACTION

The ZnO/MoO_3 physical mixture before calcination showed no formation of new phases. The inter-plannar spacings and consequently unit cell dimensions were unchanged, for both the MoO_3 and ZnO phases, indicating that no bulk chemical interaction had occurred. However, during calcination at 650°C a $ZnMoO_4$ phase was produced. It is often the case that solid-solid interactions are governed by elemental mobilities, which in turn are related to the melting points of the solids involved. As a general rule bulk diffusion requires a temperature of $>0.5\ T_m$, where T_m is the melting point of the solid in K, this temperature is called the Tamman temperature. The Tamman temperatures (in °C) for MoO_3 and ZnO are 320°C and 850°C respectively. Above the Tamman temperature it is expected that solid-solid interactions proceed at an appreciable rate. Even though the Tamman temperature of ZnO was not exceeded under conditions used for calcination, the solid surface is still able to diffuse and the reaction may still take place. The temperature at which the surface is recognised to be mobile is in the region of 0.3 T_m, which is the Huttig temperature, and has been exceeded by ZnO during calcination. A common example demonstrating these principles of solid state reactivity is the reaction between $MgCO_3$ and CaO to form MgO and $CaCO_3$. This reaction takes place at 525°C in the solid state even though the melting point of CaO is 2850°C and the Tamman temperature 1150°C [177].

The absence of diffraction lines from a Ga phase in the XRD patterns of Ga_2O_3/MoO_3 catalysts indicates that average crystallite size for the Ga phase or phases was less than 30 Å. Particles in diameter less that 30 Å cause X-ray line broadening to such an extent that diffraction lines are not determinable above the background [178]. One low intensity diffraction peak was identified which was probably due to Ga_2O_3, this suggests, not unsurprisingly, that the grinding process adopted in catalyst manufacture was responsible for the decrease in Ga_2O_3

crystallite size. However, the only evidence relating to this conclusion was based on one peak of the XRD pattern.

No new phases were observed, nor was the unit cell of MoO_3 distorted in any manner by the addition of Ga_2O_3, either before or after calcination. This implies that Ga was not incorporated into the MoO_3 lattice, which would provide an alternative explanation why no sole Ga oxide phase was identified.

After use the catalysts $ZnMoO_4$, Ga_2O_3/MoO_3 and MoO_3 all showed similar characteristics, with evidence for bulk phase reduction to MoO_2 for Ga_2O_3/MoO_3 and MoO_3, and to $Zn_2Mo_3O_8$ from the $ZnMoO_4$ phase. The formation of shear structures, similar to those observed after use in CH_4/D_2 studies, were not evident for the Mo containing catalysts. All catalysts showed increased background in the XRD pattern after use, indicating that the degree of amorphous material was increased during use, also peak broadening, which was especially prevalent for residual MoO_3 phases, may also suggest an accompanying decrease in the crystallite size.

5.3.2. CHARACTERISATION BY X-RAY PHOTOELECTRON SPECTROSCOPY

The results from XPS showed that the surfaces of the catalysts were free from residual contaminating elements, introduced during preparation and use. The exception was residual carbon, detected on all samples, but this is a common feature observed for virtually all solids [179].

The determination of surface oxidation states, especially for Mo proved difficult from the XPS data. Patterson et. al. [180] have assigned $Mo3d_{5/2}$ binding energies of 232.5 eV, 229.4 eV and 231.8 eV for the compounds MoO_3, MoO_2 and $CoMoO_4$ respectively. These lines were referenced to the $Au4f_{7/2}$ line at 83.0 eV, and were in exact agreement with the earlier results of Grim and Matienzo [181], who also used $Au4f_{7/2}$ line as the reference. Studies investigating MoO_3, which have used the C1s peak as a standard, have demonstrated a range of binding energies for the $Mo3d_{5/2}$ line. These differing binding energies include 233.2 eV

[182], 232.5 eV [183] and 233.1 eV [184]. Thus it appears that the use of the C1s line as the reference peak, which has been the case in this study, may be inadequate as the internal calibration standard. Further evidence for the problems associated with referencing to the C1s peak have been demonstrated by the variations in C1s binding energies by 1.5 eV, relative to $Au4f_{7/2}$, on oxides containing Mo in different oxidation states and coordination [180]. Considering these complications involved with accurately determining the $Mo3d_{5/2}$ binding energy relative to C1s, only general observations can be made. The binding energies for the used and unused MoO_3 and Ga_2O_3/MoO_3 catalysts were closer to Mo^{6+} in MoO_3, as opposed to Mo^{4+} in MoO_2. The literature binding energies for these two Mo states were considered to be 232.5 eV and 229.4 eV for the $Mo3d_{5/2}$ line [180]. This suggests that although bulk MoO_3 was reduced to MoO_2 after use, indicated by XRD results, the surface remained more highly oxidised, with Mo in the +6 state. This is consistent with the lower O_2 conversion over these catalysts, which did not approach 100%, and may well be responsible for maintaining an oxidised surface. These observations are also consistent with the re-oxidation of the Mo^{4+} surface after reaction. The intense $Ga2p_{1/2}$ peak confirms the presence of Ga on the catalyst surface before and after use, a conclusion which could not be made on the evidence provided by XRD alone. The binding energies for the $Ga2p_{1/2}$ peaks before and after use were in good agreement with those obtained by Battistoni et. al. [185] for Ga in Ga_2O_3 at 1116.9eV.

The comparison between unused ZnO/MoO_3, identified as $ZnMoO_4$ by XRD, and the unused MoO_3 catalyst, showed trends which were common to the comparison between $CoMoO_4$ and MoO_3 [180]. The binding energy of the $Mo3d_{5/2}$ peak decreased, as did that of the O1s peak, relative to the values for MoO_3, the same pattern was also shown by the used catalysts in this study. These XPS results are consistent with the XRD results, for the formation of a mixed oxide phase. No line broadening was observed for the $Mo3p_{3/2}$, $Ga2p_{1/2}$ or $Zn2p_{3/2}$ lines, indicating that

mixed oxidation states were not present on the initial catalyst surfaces, or introduced during reaction.

The used Ga_2O_3/MoO_3 and $ZnMoO_4$ catalysts both showed an increase in the surface carbon species, which was accompanied by peak broadening. The peak broadening indicated that more than one type of carbon species was present on the surface. The new carbon species was probably formed during the process of CH_4 oxidation, although formation could also take place on cooling in the atmosphere, however, this seems less likely. The production of an additional carbon species further increased the uncertainty of referencing peak positions, especially for the used samples. This may offer an explanation for the unusually high binding energy of the $Mo3d_{5/2}$ line in the Ga_2O_3/MoO_3 catalyst after use.

The Mo/Ga ratio for the Ga_2O_3/MoO_3 catalyst increased on use, showing a possible surface enrichment of Mo, although the overall concentrations of these elements were decreased as the concentration of surface carbon increased. It would be expected that Mo of MoO_3 would be more mobile than Ga of Ga_2O_3 at these reaction temperatures, which related to the Huttig temperatures of the oxides.

The surface ratios between Zn, Mo and O for the $ZnMoO_4$ catalyst before and after use did not change significantly, although the absolute concentrations of these elements were reduced. This suggests that no surface enrichment of any element took place, while a surface layer of carbon was uniformly deposited, reducing signal intensity from these elements.

5.3.3. CATALYTIC ACTIVITY

Microreactor studies showed that the empty reactor tube was the most selective for CH_3OH production. CH_4 and O_2 conversions were also higher than in any of the other systems investigated. As a consequence of the large excess of CH_4 over O_2, CH_4 conversion was limited by the extent of the O_2 supply. Maximum CH_3OH selectivity was 29% at 450°C, this was lower than many other studies which have concentrated on the homogeneous gas phase oxidation of CH_4 to CH_3OH [3]. The principal aims of this study were directed towards investigation of the heterogeneous

reaction, and no attempt has been made to modify reaction conditions in order to maximise CH_3OH selectivity.

A theoretical maximum CH_3OH selectivity of 67% has been proposed for the homogeneous gas phase reaction [3, 7] on the basis of the hydrogen balance. Hydroxyl radicals produced in the gas phase are highly efficient for the abstraction of hydrogen atoms to form H_2O. CH_4 is often in a large excess and provides the major source for hydrogen atom abstraction. Since CH_4 and CH_3OH both contain four hydrogen atoms, the loss of hydrogen from CH_4 to produce H_2O implies that not all the available carbon from CH_4 can react to form CH_3OH. The limiting selectivity was subsequently derived from the appropriate stoichiometric reactions.

The addition of quartz chips into the heated zone of the reactor depressed both the CH_4 and O_2 conversion, over the entire reaction temperature range, relative to the empty tube results. These observations may be influenced by the effect on residence time in the reactor heated zone, by the addition of an inert bed [79]. The definition of residence time, t_r, in the heated zone may be described by equation 5.3.3.1.

$$t_r = \frac{1}{S_v} \times \frac{273}{T} \times P \qquad (5.3.3.1.)$$

Where,

S_v = $\frac{\text{feed volumetric flow rate at 273 K, 1 bar}}{\text{void volume of reactor heated zone}}$

T = reaction temperature/K

P = reaction pressure/bar

The net volume occupied by the packed bed was 0.75 cm^3 and the GHSV was 4960 h^{-1}. In experiments with the empty reactor tube the S_v was therefore 1.37 s^{-1}, which at 500°C was equivalent to a residence time of 3.6 s in the net volume of the packed bed. It is difficult to accurately determine the void volume of the quartz chips bed, but an approximate calculation can be made based on several assumptions. It was assumed that quartz chips particles were spherical and of uniform dimension, adopting a close packed structure with a packing efficiency of 74% [186]. Using these assumptions the void volume in the 0.75 cm^3 quartz chips bed was 0.195 cm^3 and S_v was increased to 5.82 s^{-1}. Consequently the residence

time in the presence of a catalyst was 0.9 s, reduced by a factor of 4 from the empty tube. It is this reduction which may be an important factor for the reduction of the CH_4 and O_2 conversions.

The presence of the quartz chips may also effect the conversion of CH_4, as it has been suggested that they influence radical reactions, by promoting quenching reactions [187]. The homogeneous oxidation reaction of CH_4 is known to occur via initial hydrogen abstraction to form the radicals $CH_3\cdot$ and $OH_2\cdot$, after this initiation the reaction is self propagating. Baldwin et. al. [187] have concluded that the use of SiC or a ground quartz glass (SiO_2) inert packing, considerably decreased the rate of CH_4 oxidation up to 5 bar, by radical quenching at the surface. Interpretation of these results in this manner may be somewhat simplistic, as no consideration of residence time in the reactor heated zone has been undertaken. A more comprehensive study on the effect of an inert packing material has been made by Chun and Anthony [79], who investigated the contribution from radical quenching whilst maintaining a constant residence time. Results have shown that a reactor packing of inert Pyrex beads did exert an effect by inhibiting free radical reactions, but only under extreme circumstances. Experiments at 50 atm and 433°C showed that the inhibiting effect was insignificant when the inert Pyrex packing used had a surface area to volume ratio, S/V, of 32 cm^{-1} or lower. The inhibiting effect of the inert material only became significant when the S/V was increased to 300 cm^{-1}. The quartz chips in this study had a S/V in the region of 20 cm^{-1}, and would therefore not be expected to affect significantly the CH_4 conversion by radical quenching.

The product distributions from the empty tube and over the quartz chips were not dissimilar. This would suggest that homogeneous gas phase reactions in the void space of the quartz chips bed were the predominant influence on product selectivities. Considering the reduced residence time in the case of the quartz bed, it may be expected that CH_3OH selectivity would be higher than in the empty tube, as further oxidation of CH_3OH to the thermodynamically favoured carbon oxides would be suppressed. In fact the opposite trend has been observed, and CH_3OH

selectivity was lower over the quartz chips. The increase in CO_2 and the decrease of CH_3OH selectivity over the quartz chips, compared to the empty tube, indicated that CH_3OH may well have been oxidised to CO_2. The decline in CH_3OH selectivity with temperature, in the empty tube was offset by an increase in CO and C_2H_6, not CO_2 which remained constant.

CH_3OH oxidation results presented earlier suggest that CH_3OH was stable in the presence of O_2 in a blank tube at atmospheric pressure up to 500°C. A similar conclusion has also been reached after CH_3OH oxidation studies in the pressure range 1-50 bar at 475°C in an empty Pyrex reactor [188]. However, in the presence of CH_4 and O_2, CH_3OH was less stable, under the same conditions a significant proportion of CH_3OH was oxidised to CO_X. A possible explanation for the decrease of CH_3OH selectivity and the increase of CO_2 over the quartz chips, compared to the empty tube, may be related to the surface area within the heated zone. This area was very much larger with the quartz chips in place, compared to the empty tube. The increased heated surface may well facilitate further CH_3OH oxidation, which appears to be more facile in the presence of CH_4 and O_2, opposed to O_2 alone. This effect of further oxidation with a larger heated surface area may be due to the more efficient heat transfer characteristics of the quartz chips, relative to the empty tube.

The addition of the quartz chips bed have also created a more turbulent reactant flow, increasing mixing in the reactor. Considering the importance of reactor geometry on the selectivity of CH_3OH (section 1.9.), the disturbances of flow pattern, created by the quartz chips, may also influence the reaction products.

The discussion above highlights factors such as residence time, radical quenching ability, increased heated surface area and disruption of flow which may all influence the nature of gas phase reaction occurring in the empty tube and the quartz chips bed. Homogeneous gas phase reactions clearly play an important role in CH_4 partial oxidation. Therefore, the activity of any catalyst must be considered in context with the reactivity of a blank reactor. The most valid comparison in this study for the catalyst performance was with the results obtained over the quartz chips. The

comparison with the empty tube has less physical significance, as a result of the reduced residence time and the decreased surface area in the reactor heated zone. Both of these effects have been discussed earlier in this section.

The $ZnMoO_4$ catalyst produced almost exclusively carbon oxides. At 550°C the CH_4 conversion was considerably higher than over the quartz chips. This implies that reactions leading to these products were not entirely homogeneous. It is possible that CH_3OH was a primary product, which subsequently underwent further oxidation to CO and CO_2. However, this cannot be established from these results, or from CH_3OH oxidation studies, as the $ZnMoO_4$ phase was not investigated for CH_3OH stability. Low levels of HCHO and CH_3OH have been produced over a $ZnMoO_4$ catalyst [189]. However, this study has concentrated on CH_4 oxidative coupling using conditions $>600°C$ and ambient pressure.

The Ga_2O_3/MoO_3 catalyst showed significantly higher selectivity to CH_3OH compared to the quartz chips. The reaction temperature at which these selectivities were determined differed slightly, they were 450°C for the quartz chips and 460°C for Ga_2O_3/MoO_3. The CH_4 conversion over the quartz chips was higher, at 3.5% compared to 3.0% over the Ga_2O_3/MoO_3 catalyst. A selectivity comparison at constant conversion cannot be made, but studies by Casey et. al. [176] have suggested that below a critical temperature, which was lower than 500°C, the product distribution was not effected by the extent of CH_4 conversion. Therefore, a possible heterogeneous or heterogeneous/homogeneous mechanism is responsible for the increased selectivity to CH_3OH.

CH_3OH was formed over MoO_3 at 425°C and 450°C. The product distribution throughout the active temperature range was very similar to that obtained over the quartz chips. Although product distributions observed for the quartz chips and MoO_3 were similar, major differences were apparent in the magnitude of CH_4 and O_2 conversion. Both CH_4 and O_2 conversion over the quartz chips were considerably higher compared to those over MoO_3. This implies that homogeneous gas phase reactions in the void volume of the MoO_3 catalyst bed are the

predominant processes taking place. CH_3OH selectivity was depressed relative to the quartz chips, with a slight increase in CO_2 selectivity. This effect may well be expected, as it has previously been demonstrated that virtually all oxide surfaces, with the possible exception of Sb_2O_3, were more active for CH_3OH oxidation, compared to an inert packing (see Chapter 3). As the temperature was increased CH_3OH selectivity over MoO_3 decreased to zero, and CO_2 selectivity increased in parallel. From these observations it appears likely that CH_3OH was oxidised to CO_2 under reaction conditions.

In many aspects the activity shown by the Ga_2O_3 catalyst was similar to that of $ZnMoO_4$. The major products were those of combustion, although low selectivity to CH_3OH was shown at 450°C. The CH_4 conversion was higher than over the MoO_3 catalyst, but still lower than the quartz chips. The major differences in product distribution from the quartz chips again indicate that heterogeneous reactions exerted a considerable influence over the gas phase chemistry. The gas phase chemistry has been demonstrated in some cases, to dominate the product distribution.

The maximum per pass CH_3OH yields based on CH_4 conversion for the four oxide catalysts and the quartz chips bed are shown in figure 5.3.3.1.

The Ga_2O_3/MoO_3 catalyst produced the highest yield of CH_3OH, approximately 20% greater than the quartz chips. The maximum CH_3OH per pass yields over MoO_3 and Ga_2O_3 were of similar magnitude. MoO_3 was the more selective, whilst CH_4 conversion over Ga_2O_3 was greater. The per pass yield of CH_3OH over $ZnMoO_4$ was zero.

The comparison of these yields suggests that the use of a Ga_2O_3/MoO_3 catalyst had an advantageous effect over the quartz chips, whereas no advantage was gained by using a $ZnMoO_4$, MoO_3 or Ga_2O_3 catalyst. On the contrary use of these latter catalysts severely impaired the production of CH_3OH, relative to the inert packing. However, comparison of CH_3OH per pass yield over Ga_2O_3/MoO_3 with that of the empty reactor presented a different conclusion. The maximum CH_3OH per pass

yield of the empty tube was 2.30% at 450°C, this represents an increase over Ga_2O_3/MoO_3 by a factor of approximately 3.5. CH_3OH selectivity from the empty tube was 29%, 7% greater than over the Ga_2O_3/MoO_3 catalyst. However, the main reason for the higher CH_3OH yield from the empty tube was CH_4 conversion, which was ca. 2.7 times greater than over Ga_2O_3/MoO_3. In this respect the addition of the Ga_2O_3/MoO_3 catalyst to the reactor heated zone had a detrimental effect on the desired product.

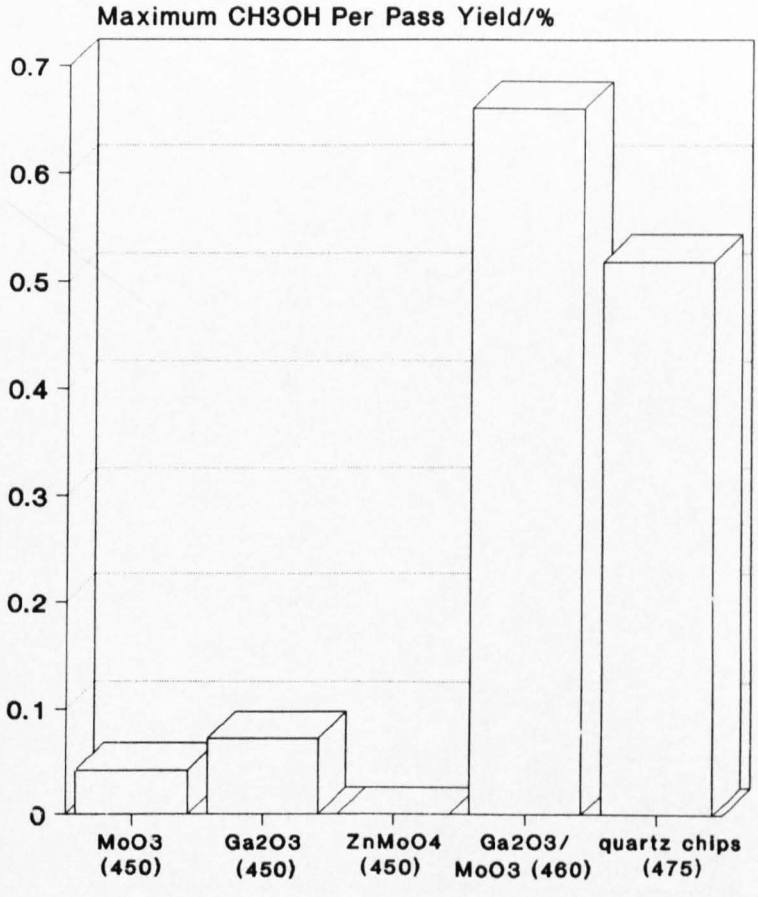

Figure 5.3.3.1. Maximum CH_3OH per pass yields over MoO_3, Ga_2O_3, $ZnMoO_4$, Ga_2O_3/MoO_3 and the quartz chips, figures in parenthesis denote the temperature of the maximum.

The catalysts $ZnMoO_4$, MoO_3 and Ga_2O_3 all showed initial activity between 400°C and 425°C, this was equivalent to the quartz chips. The Ga_2O_3/MoO_3 catalyst showed initial activity at the lower temperature of 350°C. It would be expected, from the surface areas of the single oxides, that the surface area of Ga_2O_3/MoO_3

would be greater than MoO_3 and $ZnMoO_4$, but lower than Ga_2O_3. Therefore, these observations may not be solely dependent on the effect of heated surface area.

The Ga_2O_3 phase has been shown to be extremely active for the CH_4/D_2 exchange reaction. This reaction probably involves an intermediate of surface carbanionic character. It is uncertain which would be the most advantageous intermediate, leading to the production of CH_3OH, but the initial activation of the CH_4 molecule is clearly one of the most critical steps for the overall reaction. The oxygen exchange activity of Ga_2O_3 was in the middle range of the oxides studied, and took place via a surface R_1 mechanism with no diffusion throughout the bulk oxide [132]. Such surface exchange has been implied to relate to the non-selective oxidation of CH_3OH to CO_X (section 3.3.). Accordingly Ga_2O_3 may be expected to be relatively active for CH_4 oxidation, whilst the products would most likely be those of combustion. On the other hand, CH_4/D_2 exchange over MoO_3 was not detected under the reaction conditions used in our experiments. Some similarities in the final structure were apparent between the final reduced states of MoO_3 after use for CH_4/D_2 exchange and CH_4 partial oxidation. The oxygen exchange activity of MoO_3 was very different from that shown by Ga_2O_3. The exchange over MoO_3 is considered to occur via an R_3 mechanism [132]. This mechanism of exchange involved exchange with the whole of the lattice oxygen, not merely the surface layer, as the mobility of oxygen throughout the solid lattice was a facile process. The lability of lattice oxygen is an important concept in selective oxidation reactions, particularly with regards to the Mars van Krevelan mechanism, in which lattice oxygen is the active oxygen insertion species. Other oxides which have shown the R_3 oxygen exchange mechanism were WO_3 and V_2O_5, which have found many important applications as catalysts for selective oxidations [190]. Our studies of the oxidation of CH_3OH over MoO_3 showed that although the majority of CH_3OH was destroyed the main product was HCHO, with very low levels of CO_X. Hence by comparison to the Ga_2O_3 catalyst, MoO_3 would be expected to show

lower activity for CH_4 conversion, but the selectivity towards partially oxygenated products would be increased.

The physical mixture of Ga_2O_3 and MoO_3 combined the beneficial aspects of CH_4 partial oxidation over both single oxides. These were the higher catalytic CH_4 conversion over Ga_2O_3, with the selective oxidation function of MoO_3. This combination increased the selectivity towards CH_3OH over that of the gas phase partial oxidation, under equivalent experimental conditions. This increase in CH_3OH selectivity suggests that there was the development of a cooperative or synergistic effect between the two phases. One possible explanation for this effect can be provided by considering the bifunctional nature of the dual component catalyst. The functionality of the single oxides for CH_4 partial oxidation has previously been discussed in relation to their CH_3OH, CH_4 and O_2 activation efficacy. The presence of Ga_2O_3 could provide the CH_4 activation function to produce a surface methyl activated species. Such a species would be surface mobile and able to migrate to surface sites on the MoO_3 phase responsible for oxygen insertion, eventually producing CH_3OH. The Ga_2O_3 clearly has an important role for CH_4 activation, as MoO_3 alone was not an active catalyst for CH_4/D_2 exchange, reflected in the low CH_4 conversion for partial oxidation.

M=O species on the MoO_3 surface have been proposed as active sites for CH_4 partial oxidation to HCHO at atmospheric pressure [45]. The same type of M=O sites have also been proposed as important for other selective oxidation reactions [123]. The migration of the surface methyl group to this site on MoO_3 could lead to the insertion of oxygen, and the formation of a surface OCH_3 species. The desorption of the OCH_3 species to the gas phase may be a relatively facile process, as the diffusion of oxygen through the bulk MoO_3 to regenerate surface M=O sites, would be rapid [132]. The regeneration of these M=O surface sites by oxygen diffusion through the bulk MoO_3 has been suggested by Smith and Ozkan [40] during the partial oxidation of CH_4, based on evidence from in situ Raman spectroscopy studies. XRD and XPS results for the Ga_2O_3/MoO_3 catalyst in this

study suggest that although during use bulk MoO_3 phase was reduced to MoO_2, the surface may have remained in a more highly oxidised state and no catalyst deactivation was observed. The intimate mix of the Ga_2O_3 and MoO_3 component oxides provided many phase boundaries, at which the migration process could lead to CH_3OH formation. A schematic representation of the above process for CH_3OH formation catalysed by the dual component oxide is shown in figure 5.3.3.2.

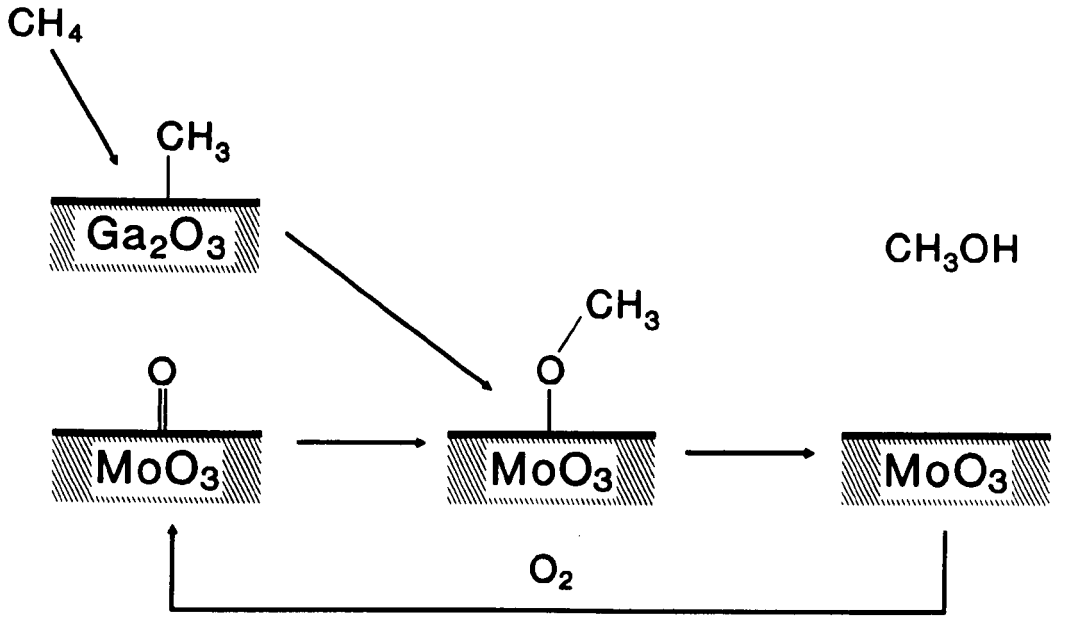

Figure 5.3.3.2. Possible reaction scheme for the production of CH_3OH over the dual component Ga_2O_3/MoO_3 catalyst.

The scheme shown in figure 5.3.2. is not intended to be a detailed reaction mechanism, as clearly specific details of many of the steps are unsubstantiated. It does however offer a possible insight into the general mode of catalyst operation. The generation of surface OCH_3 has also been invoked as an important species leading to the production of CH_3OH in mechanisms suggested by other groups [49, 52]. The surface OCH_3 species could lead to the formation of CH_3OH by two possible routes. The first could be via the generation of OCH_3 radicals on desorption, these radicals are thought to be the precursors to CH_3OH during the homogeneous gas phase reaction. CH_3OH is consequently produced by the abstraction of an H atom from an appropriate source which is usually CH_4 [4], this process is shown in equation 5.3.3.2.

$CH_3O\cdot + CH_4 \longrightarrow CH_3OH + CH_3\cdot$ (5.3.3.2.)

The alternative route could be via a surface reaction with a supply of hydrogen, possibly from OH groups, followed by desorption of the CH_3OH product.

The reaction scheme depicted in figure 5.3.3.2. requires the migration of surface species, since distinct sites are responsible for O_2 and CH_4 activation. These requirements are very similar to those of the virtual mechanism developed by Dowden et. al. [29] for the design of CH_4 partial oxidation catalysts, as described in section 1.7. Important features of the virtual mechanism were the activation of reactants, and their surface mobility, in order to react and produce HCHO. The major differences between the virtual mechanism and the process depicted in Figure 5.3.3.2. is the production of HCHO in the work of Dowden et. al., which did not require the addition of hydrogen to the surface OCH_3 species to yield HCHO.

The cooperative effect observed for the Ga_2O_3/MoO_3 catalyst could also function in the reverse mode to that previously discussed, i.e. the mobile surface oxygen species could migrate and react with an activated CH_3 species at specific sites of Ga_2O_3. This process of oxygen spillover has been suggested to be important for allylic selective oxidation reactions such as isobutene to methacrolein (C_4H_6O) over a physically mixed MoO_3/α-Sb_2O_4 (1/1) catalyst [192]. Although this process is believed to be important for some selective oxidation reactions, it is not considered the case over the Ga_2O_3/MoO_3 catalyst here, as the surface mobility of the reacting species in the two systems are clearly different. The initial radical produced during allylic oxidation is relatively large compared to the surface CH_3 species formed during CH_4 partial oxidation. Therefore the allylic surface radical is expected to be far less mobile than a surface CH_3 species, which would require an increased importance of oxygen spillover in the former process. The generation of a relatively weakly bound surface oxygen species migrating to the Ga_2O_3 phase could also promote the further oxidation reaction to combustion products [192]. Consequently it appears more likely that CH_3OH formation was associated with the surface of

MoO_3 by the migration of a CH_3 species from Ga_2O_3, and not the migration of an oxygen species.

The cooperative effects observed in catalysis have often been attributed to the formation of a new phase which is more active or selective than the initial individual phases. This has been demonstrated by the reaction of Bi_2O_3 and MoO_3 to form the Bi-Mo-O phases for selective oxidation of C_3 compounds [193]. Characterisation by XRD showed that no bulk mixed phases were produced from the Ga_2O_3/MoO_3 mix either before or after use, indicating that the higher CH_3OH yield was not due to the formation of a more active mixed phase.

The catalytic activity and the products which were formed over the Ga_2O_3/MoO_3, Ga_2O_3 and MoO_3 catalysts at lower temperatures were the same as those which have been expected by the catalyst design approach. As the temperature was increased the influence of gas phase reactions became more predominant over surface reactions, and the expected catalytic performance based on O_2, CH_4 and CH_3OH activation were no longer valid.

Further evidence to support this three tier approach to catalyst design was provided by the studies using the $ZnMoO_4$ catalyst. ZnO was chosen as a constituent oxide to replace Ga_2O_3 due to the high efficacy for CH_4 activation, the physically mixed catalyst would be expected to show similar activity to the Ga_2O_3/MoO_3 catalyst. However, during preparation the phase $ZnMoO_4$ was produced, and the single constituent oxide phases were no longer detected. No information on O_2, CH_4 and CH_3OH activation were available on this new phase, and the predictive theory for catalyst behaviour no longer applied.

A decrease in the CH_4 conversion at a specific temperature was observed over the catalysts, relative to the quartz chips bed. Residence times for these comparisons were constant, and therefore the previous arguments of residence time used for the empty bed and the quartz chips cannot be applied. The decreased CH_4 conversion may therefore be related to the ability of the oxides to quench gas phase radical reactions relative to the quartz chips. CH_4 conversion over MoO_3 was the lowest,

and consequently may be considered the most efficient catalyst for the termination of homogeneous gas phase radical reactions.

The reaction of a $CH_3\cdot$ radicals with an oxide surface may be an important contribution for the increased CO_X yield. This reaction has been shown to proceed in accordance with the scheme shown in equation 5.3.3.3. [194].

$$M^{(n+1)+}O^{2-} + CH_{3\cdot(g)} \text{ ----> } M^{n+} (OCH_3)^- \qquad (5.3.3.3.)$$

The formation of surface methoxide and formate species were confirmed by infra-red spectroscopy. The reactivity of $CH_3\cdot$ with the surface was related to the reducibility of the oxide, the radical reaction rate was greatest with the oxides most easily reduced. The surface methoxide and formate species were implied to be intermediates for the production of carbon oxides, examples of this behaviour have been shown by CH_3OH decomposition in section 3.1. This route to CO_X would be more important at the higher reaction temperatures, where contributions from radical reactions would be more pronounced. Generally the catalysts produced higher levels of CO_2 compared to the blank reactions, suggesting that if a methoxide or formate species was the intermediate, it was more likely to form CO_2 rather than CO. The origin of CO_X at lower temperatures would more likely show a greater contribution from further oxidation of CH_3OH, than via the $CH_3\cdot$ surface interaction.

The catalysts which showed increased CO_2 yields compared to the empty tube were Ga_2O_3, Ga_2O_3/MoO_3 and $ZnMoO_4$. Following reaction the latter two catalysts showed the formation of a new surface carbon species. These carbon species were different from residual carbon present in the initial catalyst. These observations are consistent with the proposed route for the formation of CO_X, particularly CO_2, by the interaction of $CH_3\cdot$ with the oxide to form the surface methoxide species. XPS was not performed on the Ga_2O_3, and it seems unlikely that Ga^{3+} would be reduced to Ga^{2+} to form the methoxide, and therefore this route to CO_X may not operate over Ga_2O_3. If surface methoxide or formate species were responsible for the increased CO_X yields in the presence of a catalyst then these species are

probably formed on different surface sites from the OCH_3 precursor species for CH_3OH production. The bond strength of these species to the surface would influence the product type, as more strongly bound species are expected to produce CO_X and not CH_3OH.

One universal feature which has been observed in the blank tube reactions was the increase in selectivity towards C_2H_6 as the temperature was increased. This was also observed in the presence of a catalyst, which in many cases was parallelled by a decrease in CH_3OH selectivity. This behaviour was particularly noticeable during CH_4 oxidation in the empty tube and over the quartz chips when the reaction was purely homogeneous. This gradual switch in product selectivity from CH_3OH to C_2H_6 may be explained by considering the reaction of $CH_3\cdot$ with O_2, shown in equation 5.3.3.4.

$$CH_3\cdot + O_2 \rightleftharpoons CH_3O_2\cdot \qquad (5.3.3.4.)$$

Below 500°C the equilibrium lies to the right hand side of the equation, in favour of the methyl peroxy radical, increasing the probability of gas phase CH_3OH production, possibly by the reactions, (5.3.3.5-7).

$$CH_3O_2\cdot + CH_4 \rightleftharpoons CH_3OOH + CH_3\cdot \qquad (5.3.3.5.)$$

$$CH_3OOH \rightleftharpoons CH_3O\cdot + HO\cdot \qquad (5.3.3.6.)$$

$$CH_3O\cdot + CH_4 \rightleftharpoons CH_3OH + CH_3\cdot \qquad (5.3.3.7.)$$

It is also evident from equation 5.3.3.4. that increased pressure would also enhances the equilibrium formation of $CH_3O_2\cdot$. This may also explain why CH_3OH is often the oxygenated product formed at elevated pressures, opposed to HCHO which is more often produced at ambient pressure [3]. Indeed, during our studies some HCHO might have been expected over the MoO_3 based catalysts, especially considering their efficiency for CH_3OH oxidation to HCHO.

Above 500°C the equilibrium shown in equation 5.3.3.4. lies to the left hand side, favouring the production of $CH_3\cdot$. The oxidative coupling of CH_4 to form C_2H_6 has been generally accepted to proceed via the dimerisation of CH_3 radicals in the gas

phase [195]. Therefore, as the temperature was increased the relative concentration of $CH_3\cdot$ also increased, and consequently so did the magnitude of coupling products.

5.4. CONCLUSIONS

Characterisation by XRD and XPS of the two component mixed oxide catalysts, prepared by physical mixing and calcination, showed that the Ga/Mo catalyst consists of two distinct Ga_2O_3 and MoO_3 phases, whilst a $ZnMoO_4$ phase was identified for the Zn/Mo mixture.

Comparison of the catalytic activity with the blank reactions showed that both CH_4 and O_2 conversion were decreased, probably due to the ability of the oxide surface to quench gas phase radical reactions. The comparison between the Ga_2O_3/MoO_3 catalyst and the blank quartz chips bed showed that CH_3OH selectivity over Ga_2O_3/MoO_3 is significantly higher. The per pass yield of CH_3OH over the Ga_2O_3/MoO_3 catalyst is also greater than over the quartz chips. The CH_3OH per pass yields over MoO_3 and Ga_2O_3 are lower than the quartz chips, mainly as a consequence of the lower CH_4 conversion and CH_3OH selectivity respectively. The $ZnMoO_4$ catalyst did not produce any detectable quantities of CH_3OH under the reaction conditions used.

The increased CH_3OH yield over the Ga_2O_3/MoO_3 catalyst is attributed to the development of a cooperative effect between the two phases, possibly by the migration of a surface CH_3 species, activated on the Ga_2O_3 phase, to the active sites on MoO_3 responsible for oxygen insertion.

CH_4 partial oxidation in the empty reactor tube produced a considerably greater CH_3OH per pass yield, than any of the catalyst, as both CH_4 conversion and CH_3OH selectivity are greater.

The mechanism of CH_4 partial oxidation in the presence of the oxide catalysts is a combination of surface and gas phase homogeneous reactions. At the lower temperatures of investigation, ca. $<475°C$, the influence of surface reactions is greatest. As the temperature was increased the formation of C_2 products are

observed, at the expense of CH_3OH, this can be explained by known gas phase radical chemistry.

The greater selectivity towards CO_2 at higher temperature over the catalysts compared to the blank reactions, may be due to the formation of a surface methoxide species by the interaction of CH_3 radicals with the oxide surface. Evidence for this route is provided by the formation of a new surface carbon species during reaction.

Powder X-ray diffraction showed that a major proportion of the bulk MoO_3 constituent of the catalysts is reduced to MoO_2 after use. The $ZnMoO_4$ phase is also partially reduced to $Zn_2Mo_3O_8$ during this study. The analysis of surface oxidation states proved difficult for the used catalysts. However, indications showed that the surfaces were still probably in a more oxidised state than the bulk.

CHAPTER 6

CONCLUSIONS

The approach which has been adopted for catalyst design has identified single oxides over which CH_3OH and HCHO were stable under reaction conditions, and oxides which were efficient for CH_4 activation. These results were considered in conjunction with the oxygen exchange activity of the oxides to formulate bi-component catalysts for the partial oxidation of CH_4 to CH_3OH.

This study has highlighted inherent problems associated with CH_4 partial oxidation to CH_3OH, particularly with reference to the activation of the reactants and the desired products. The majority of the oxides which were effective for activating CH_4 were strongly basic, the exceptions being Ga_2O_3, ZnO and Cr_2O_3. Indeed, a strong relationship was established between the basicity of La_2O_3, Nd_2O_3, Gd_2O_3, Yb_2O_3, MgO and CaO, and the rate of CH_4 activation. Investigation of the same basic oxides for CH_3OH oxidation activity showed that these oxides readily produced CO and CO_2 as the major reaction products, totally destroying CH_3OH below 400°C. CH_3OH stability over Ga_2O_3, ZnO and Cr_2O_3 was also relatively poor, Cr_2O_3 was one of the most active oxides for CH_3OH combustion, showing complete CH_3OH conversion to CO_X below 200°C. These observations indicate that the type of catalyst functionality required for CH_4 activation may co-exist with that responsible for the combustion of CH_3OH. Further evidence supporting this view is shown by the oxides MoO_3, Nb_2O_5, Ta_2O_5 and WO_3, which all exhibited low activity for CH_3OH combustion, whilst the oxides MoO_3, Nb_2O_5 and WO_3 were inactive for CH_4 activation and Ta_2O_5 only showed low activity, which could not be accurately quantified. These findings suggest that none of the single oxides in this study possessed both the CH_4 and CH_3OH activation characteristics required for a successful CH_4 partial oxidation catalyst. These observations also imply that limits may be imposed on catalytic CH_3OH yields, because although catalysts may

be formulated which are more active, they may consequently destroy more of the CH_3OH product by further oxidation.

The activation of oxygen by the single oxides, indicated by the exchange of oxygen isotopes, was also important in determining the catalytic activity. A correlation between the rate of oxygen exchange and the ease of CH_3OH combustion was established, indicating that higher rates of surface oxygen exchange promoted CH_3OH combustion. It was not only the rate of oxygen exchange which was important for catalytic activity, but also the mechanism of exchange. Oxides which showed exchange with the entire lattice oxygen, may be considered to possess more labile oxygen species. In this study oxides of this type were MoO_3, V_2O_5 and WO_3, which are all important components in selective oxidation catalysts. This type of selective oxidation function is required for CH_4 partial oxidation to CH_3OH, but it has been previously noted these oxides were not particularly effective for CH_4 activation under our experimental conditions. From the perspective of CH_4 and O_2 activation it again appears that no single oxide has both required functions, hence a bi-component catalyst system must be employed.

The main catalyst which has derived from this approach was Ga_2O_3/MoO_3, prepared by physically mixing the oxide components. This catalyst has shown an increased yield of CH_3OH over the blank reactor tube packed with inert quartz chips. The greater CH_3OH yield over this catalyst compared to the quartz chips showed that the addition of Ga_2O_3/MoO_3 had a beneficial effect over the homogeneous gas phase reactions. The increased CH_3OH yield over this catalyst has been attributed to the evolution of a cooperative effect between the CH_4 activation capability of Ga_2O_3 and the low CH_3OH combustion tendency and mechanism of oxygen exchange over MoO_3. This cooperative effect was the same as that expected from the activity shown by the single oxides in the separate activation studies. In this respect it is concluded that the approach which has been adopted for catalysts design was relatively successful, and the principles on which it

was based were valid. The approach has provided important guide-lines which can be implemented to produce further new bi-component catalysts.

Comparison of catalytic data with the empty reactor tube showed that the CH_3OH yield was higher in the empty tube than in the presence of any catalyst. It is important to stress that this comparison to assess catalytic activity is not strictly valid, as the residence time and heat transfer characteristics between the two systems were different. Although the comparison with the empty tube was not a valid one to assess catalyst performance, it does however present a comparison of economic significance, as the yield of CH_3OH in the empty tube was greater.

The catalytic results presented in this study are preliminary and it is envisaged that further catalysts will be manufactured, using the same design criteria. These proposed catalysts are to be based on the CH_3OH stability and oxygen exchange activity of Nb_2O_5, Sb_2O_3, Ta_2O_5 and WO_3, and the high CH_4 activation efficacy of Ga_2O_3. Further development work must also be performed on the efficiency of Ga_2O_3 for CH_4 activation, which is also important for the wider subject of hydrocarbon activation. The promising results which have been shown by the Ga_2O_3/MoO_3 catalyst also require further investigation, as no attempt has been made to maximise the CH_3OH yield, possible by considering the role of the Ga/Mo ratio, metal ion coordination or bulk crystalline structures.

APPENDIX A

OXYGEN EXCHANGE ACTIVITY

The exchange of oxygen isotopes with oxides has been widely studied, and the pioneering work reviewed in two publications [196, 136]. Throughout the 1950's and 60's a series of studies was published by Winter [132, 133], simultaneous studies were also published by Russian researchers led by Boreskov [134]. Such exchange reactions provide an indication of the activation of gaseous oxygen and the reactivity of oxide lattice oxygen. Generally the agreement between the two research groups was good. For the purpose of this study we have tended to concentrate on the reaction rates and mechanisms determined by Winter [132, 133].

The exchange reactions of gaseous oxygen, consisting of a $^{16}O_2/^{18}O_2$ mixture, over an oxide may take place by one, or a combination, of reaction mechanisms. The first, denoted as R_0 or homomolecular exchange, is described by equation A.1.

$$^{16}O_{2(g)} + {}^{18}O_{2(g)} \text{ ----> } 2{}^{16}O{}^{18}O_{(g)} \qquad \text{(A.1.)}$$

Homomolecular exchange is exchange catalysed by the oxide surface, but does not involve exchange with oxygen of the oxide lattice. This exchange mechanism was only observed when the isotopic species in the gas phase were not in equilibrium (A.2.).

$$K_e = \frac{[^{16}O^{18}O]^2}{[^{16}O_2][^{18}O_2]} \neq 4 \qquad \text{(A.2.)}$$

Winter observed that oxides pretreatment in oxygen reduced the extent of homomolecular exchange, whilst it was increased by pretreatment at high temperature in vacuum.

The second type of exchange mechanism was called R_1, and does involve exchange with lattice oxygen. The R_1 mechanism was proposed to occur by the reactions A.3. and A.4.

$$^{18}O_{2(g)} + {}^{16}O_{(s)} \text{ ----> } {}^{16}O{}^{18}O_{(g)} + {}^{18}O_{2(s)} \qquad \text{(A.3.)}$$

$$^{16}O{}^{18}O_{(g)} + {}^{16}O_{(s)} \text{ ----> } {}^{16}O_{2(g)} + {}^{18}O_{(s)} \qquad \text{(A.4.)}$$

The R_1 mechanism of exchange may take place as written above or it may involve the dissociative adsorption of O_2 into oxygen atoms. This process involves the incorporation of one oxygen atom into the solid whilst the other is mobile on the surface and capable of recombining and desorbing to the gas phase. This process is shown by equations A.5. and A.6.

$$^{18}O_{2(g)} + (e_2^-|\square^-)_{(s)} \text{----} > (^{18}O^{2-}|\square^-)_{(s)} + {}^{18}O_{(s)} \qquad \text{(A.5.)}$$

$$^{18}O_{(s)} + {}^{16}O_{(s)} \text{----} > {}^{18}O^{16}O_{(g)} \qquad \text{(A.6.)}$$

The recombination of two ^{18}O species may also take place resulting in no net exchange.

The final mechanism of exchange, denoted as R_2, also involves exchange with the oxide surface. This mechanism can be described by the reactions (A.7.-A.9.)

$$^{18}O_{2(g)} + 2{}^{16}O_{(s)} \text{----} > {}^{16}O_{2(g)} + 2{}^{18}O_{(s)} \qquad \text{(A.7.)}$$

$$^{16}O^{18}O_{(g)} + 2{}^{16}O_{(s)} \text{----} > {}^{16}O_{2(g)} + {}^{18}O_{(s)} + {}^{16}O_{(s)} \qquad \text{(A.8.)}$$

$$^{16}O^{18}O_{(g)} + 2{}^{18}O_{(s)} \text{----} > {}^{18}O_{2(g)} + {}^{18}O_{(s)} + {}^{16}O_{(s)} \qquad \text{(A.9.)}$$

The R_1 and R_2 mechanisms are numbered with respect to the number of lattice oxygens participating in the exchange reaction. It has also been suggested that The R_1 and R_2 mechanisms take place via the formation and decomposition of three and four centre transient complexes.

The oxides MoO_3, V_2O_5 and WO_3 showed exchange of the whole of the lattice oxygen with the gas phase. The diffusion of oxygen throughout the lattice of these solids was faster than the surface exchange, which was therefore the rate determining process. The exchange mechanism for these oxides operated by a combination of R_1 and R_2 processes. For use in this study the process of oxygen exchange over these oxides was called R_3.

The surface area normalised exchange rates at 350°C are shown in figure A.1. for various oxides exchanging by R_1 and R_2 mechanisms.

The rates shown in figure A.1. are for oxides pretreated in several portions of 1.5 torr $^{16}O_2$ for 100 hours. The results presented in this Appendix have been used as a guide for the design of CH_4 partial oxidation catalysts.

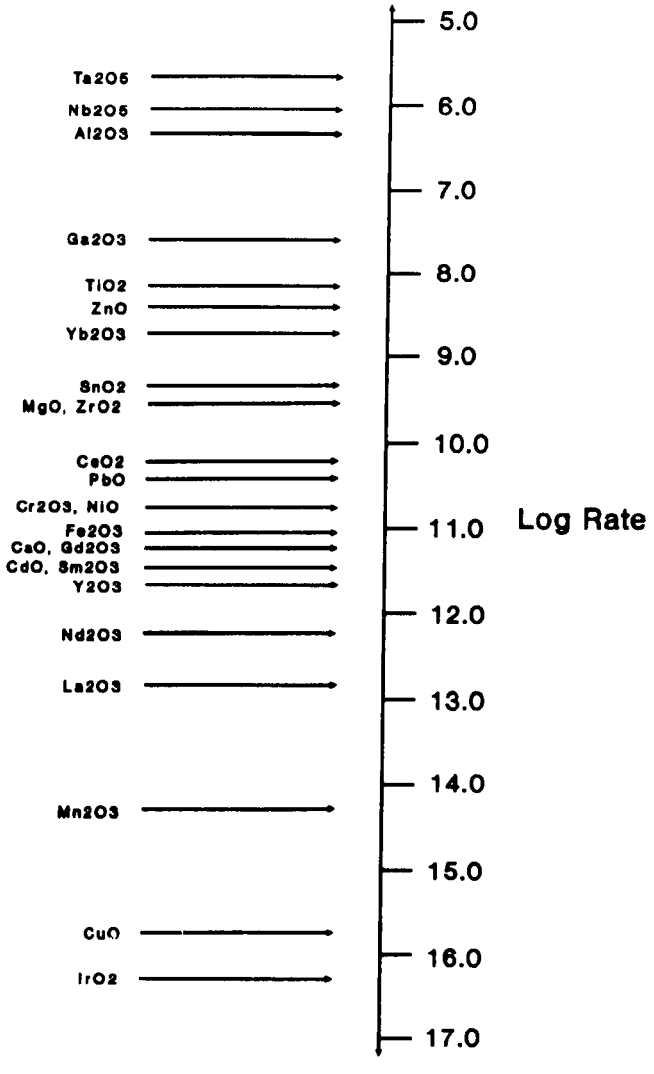

Figure A.1. Surface area normalised oxygen exchange rates for R_1 and R_2 mechanisms at 350°C.

APPENDIX B

FIGURES FOR THE OXIDATION OF METHANOL

Methanol oxidation over Bi_2O_3

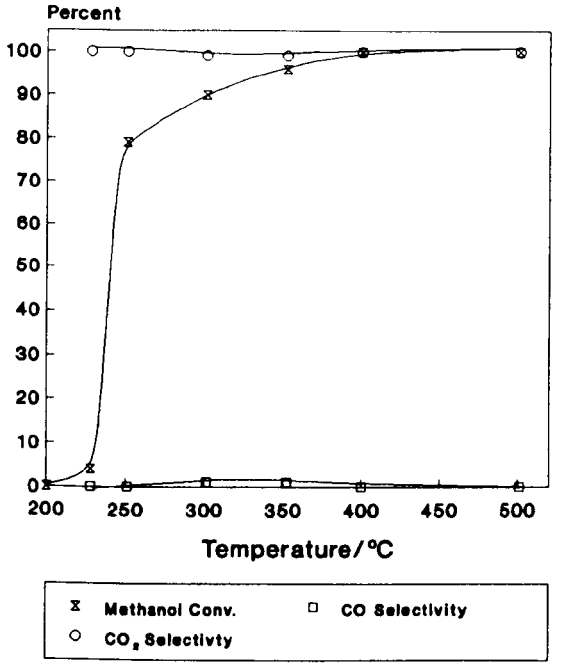

Methanol oxidation over CaO

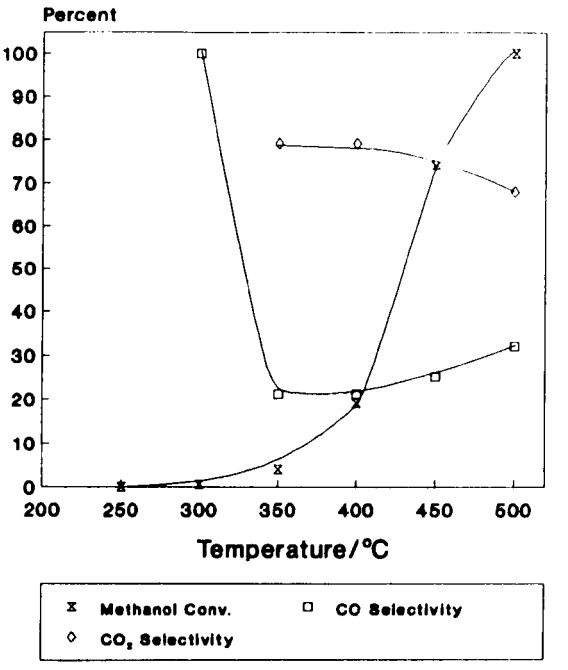

Methanol oxidation over CdO

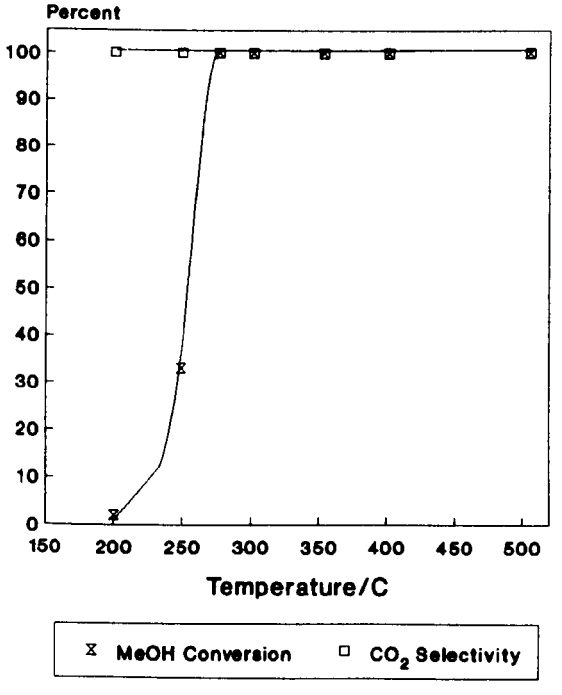

Methanol oxidation over CeO_2

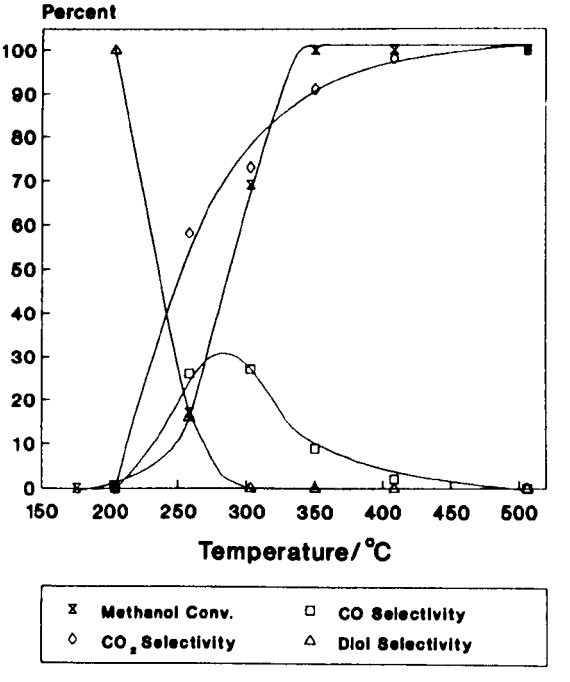

Methanol oxidation over Co_3O_4

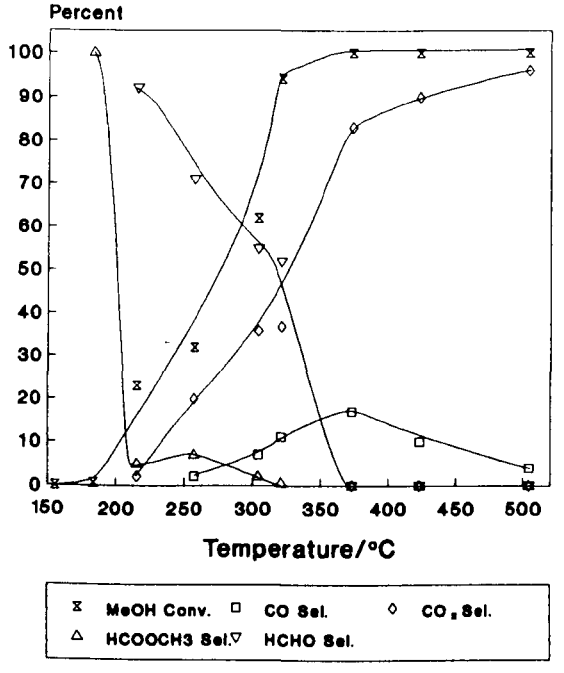

Methanol oxidation over Cr_2O_3

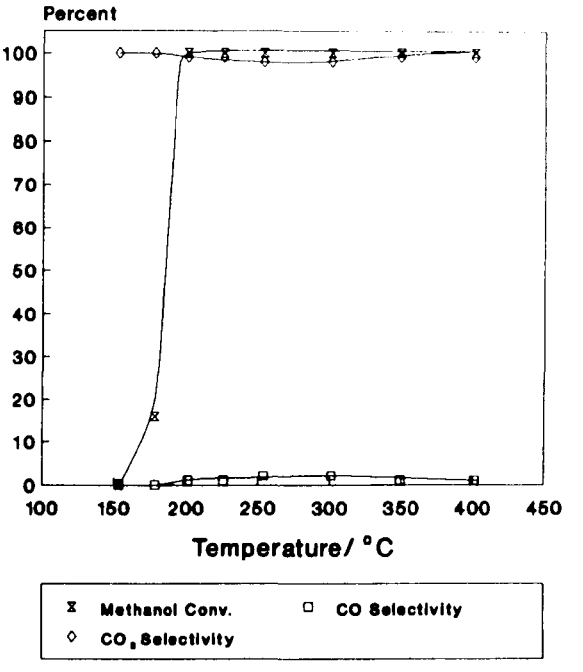

Methanol oxidation over CuO

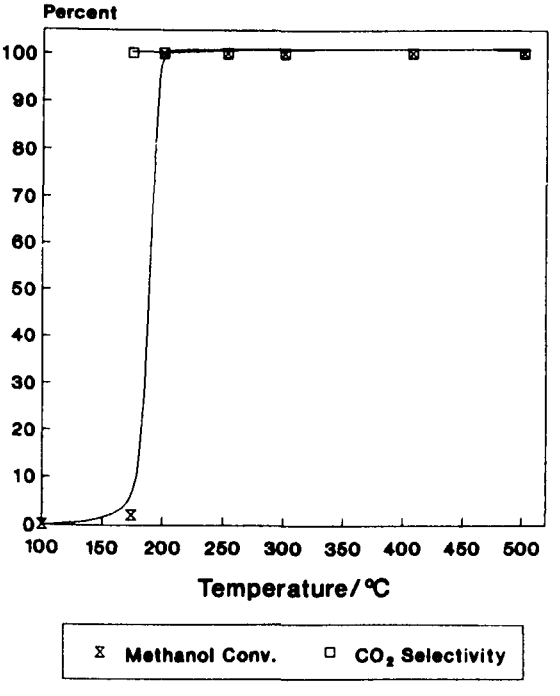

Methanol oxidation over Fe_2O_3

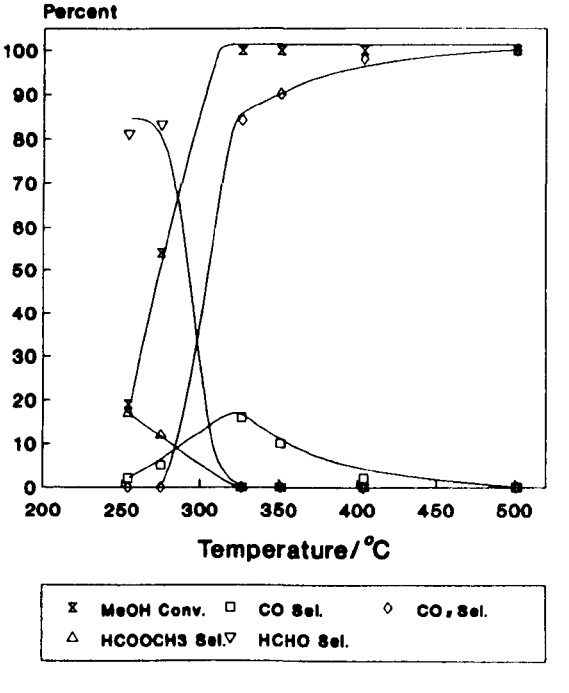

Methanol oxidation over Ga_2O_3

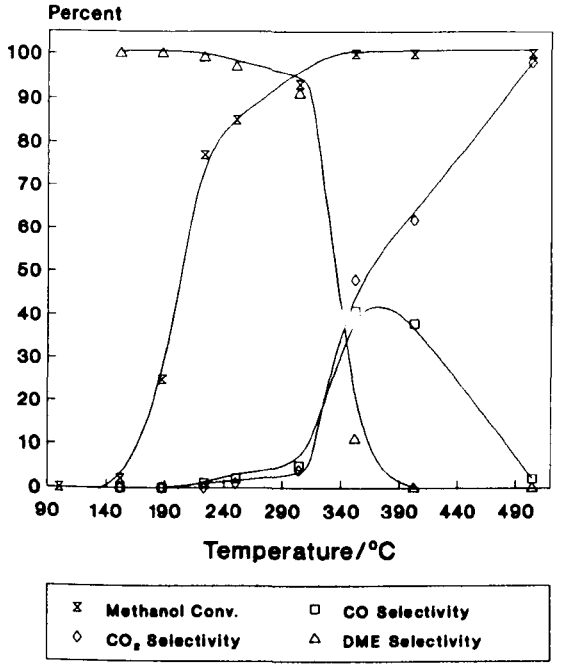

Methanol oxidation over Gd_2O_3

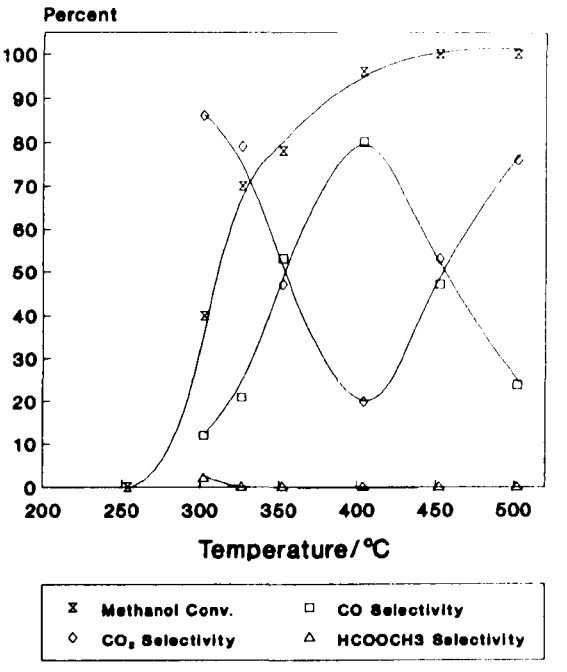

Methanol oxidation over La_2O_3

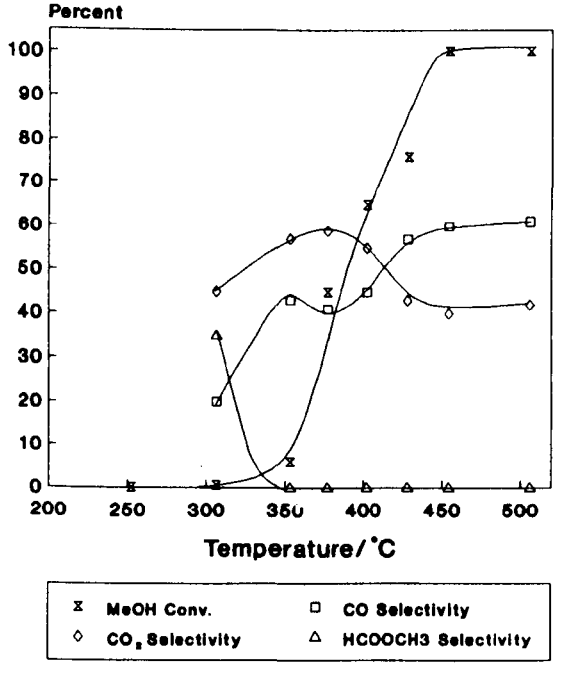

Methanol oxidation over MgO

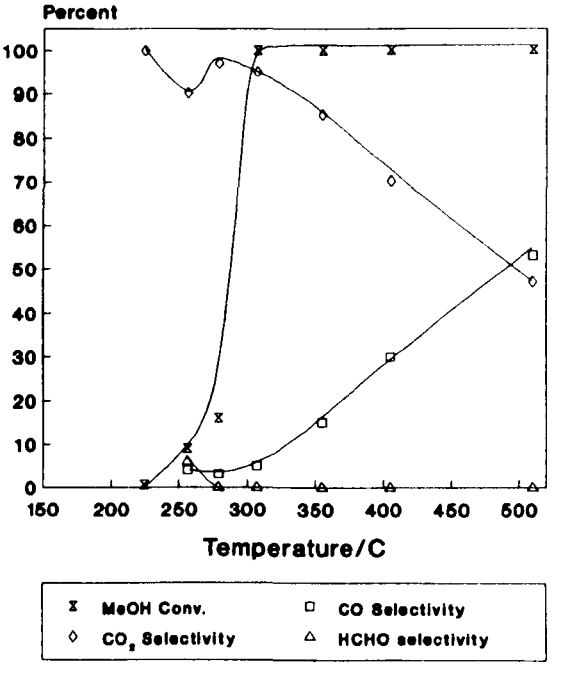

Methanol oxidation over Mn_2O_3

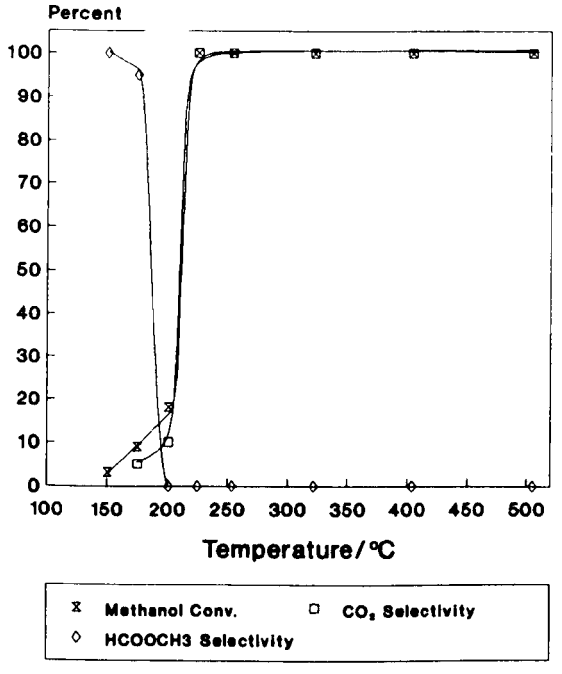

Methanol oxidation over MoO_3

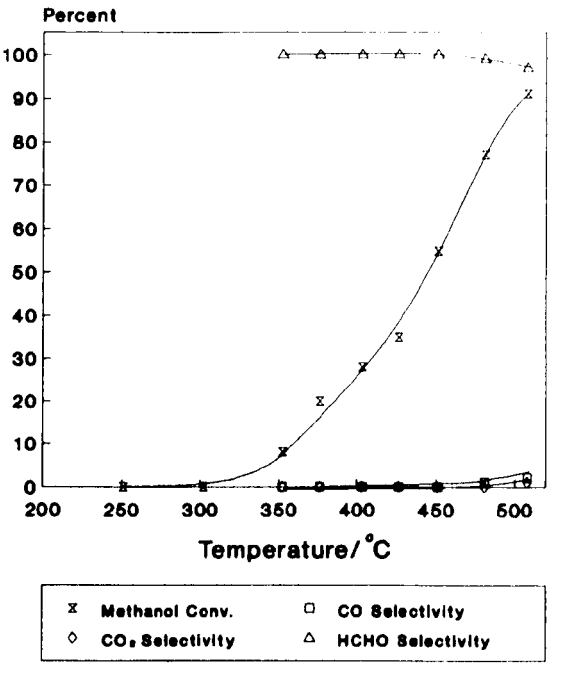

Methanol oxidation over Nb_2O_5

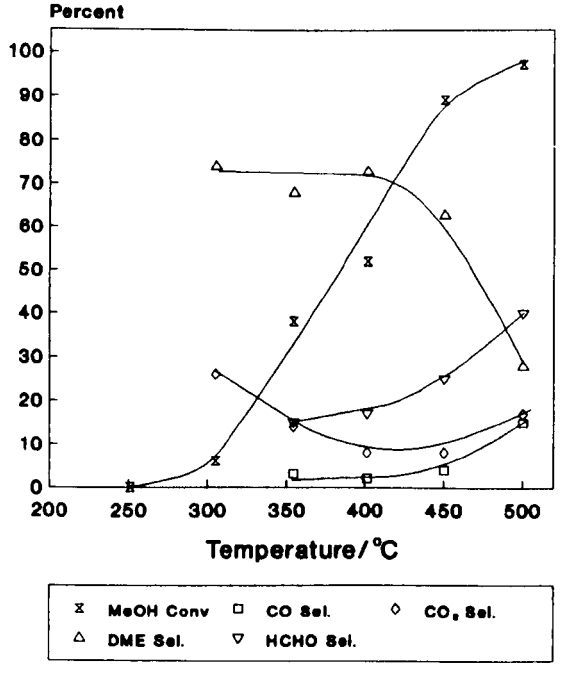

Methanol oxidation over NiO

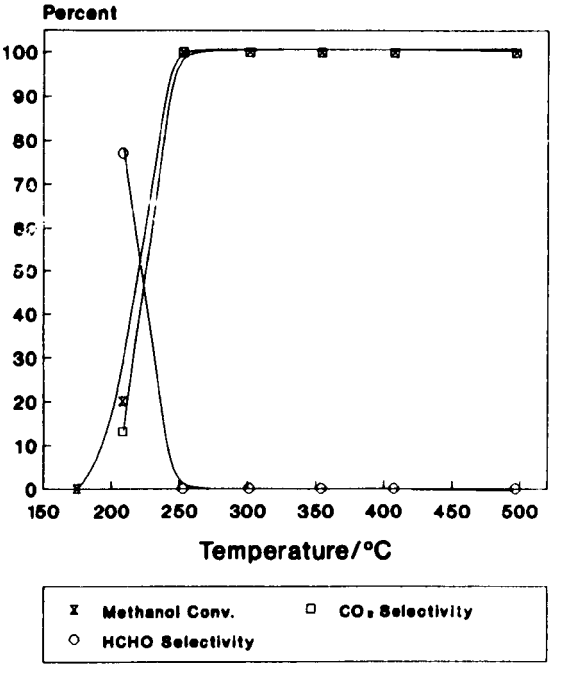

Methanol oxidation over Pr_6O_{11}

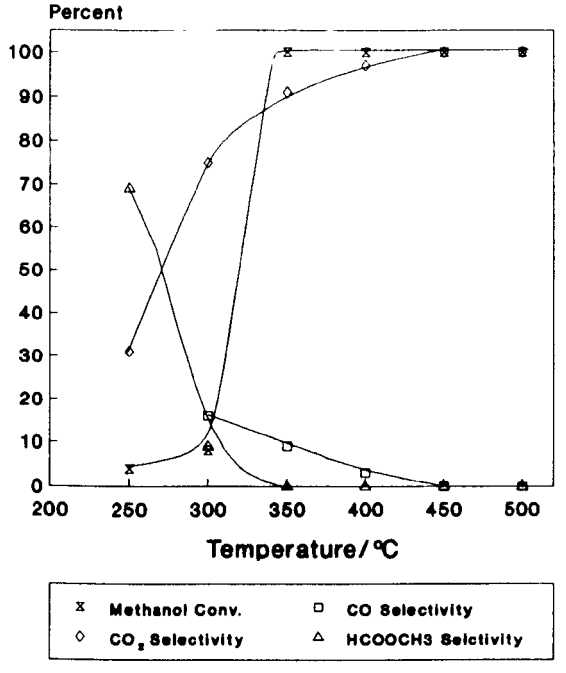

Methanol oxidation over Sb_2O_3

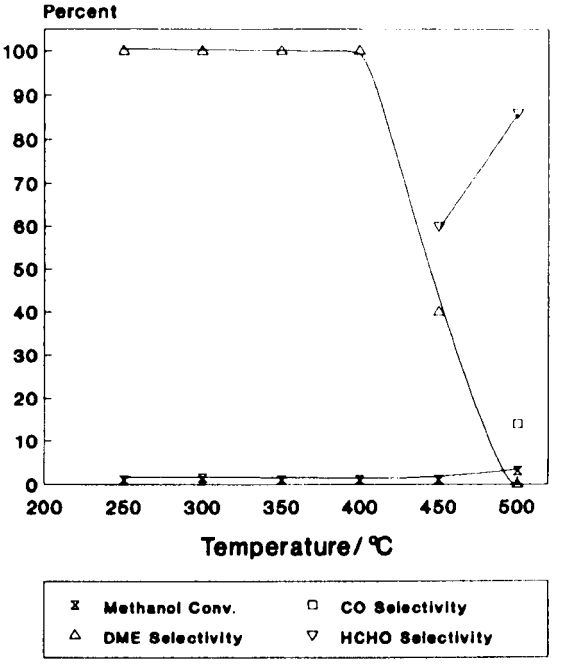

Methanol oxidation over Sm_2O_3

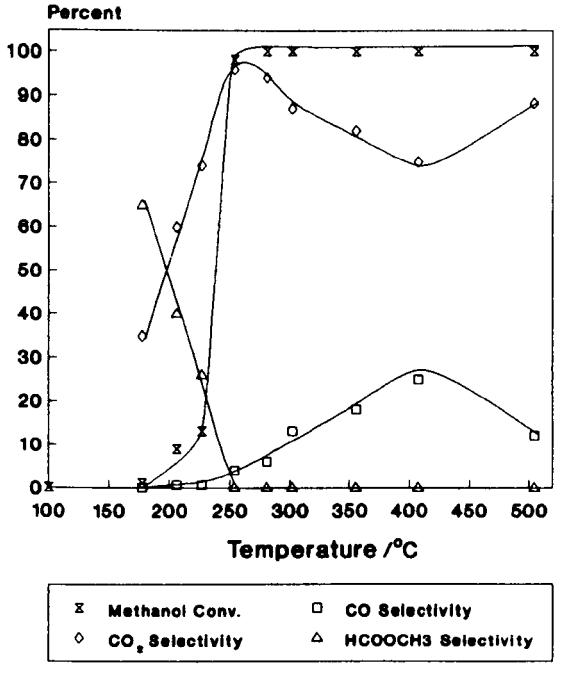

Methanol oxidation over SnO_2

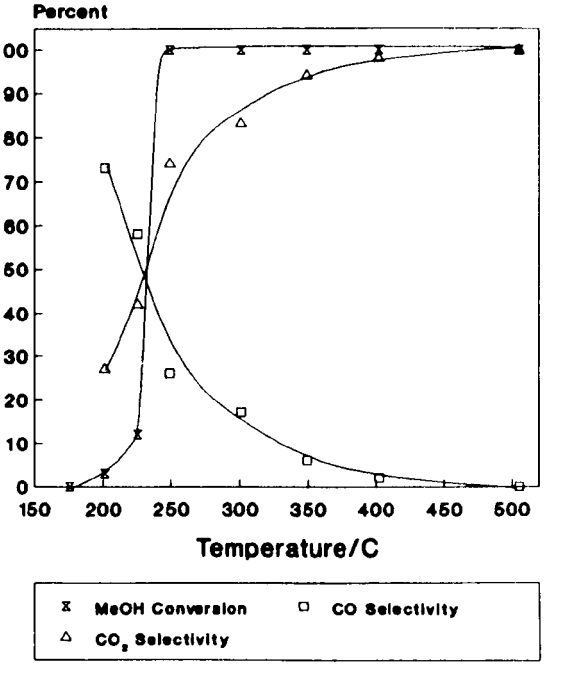

Methanol oxidation over Ta_2O_5

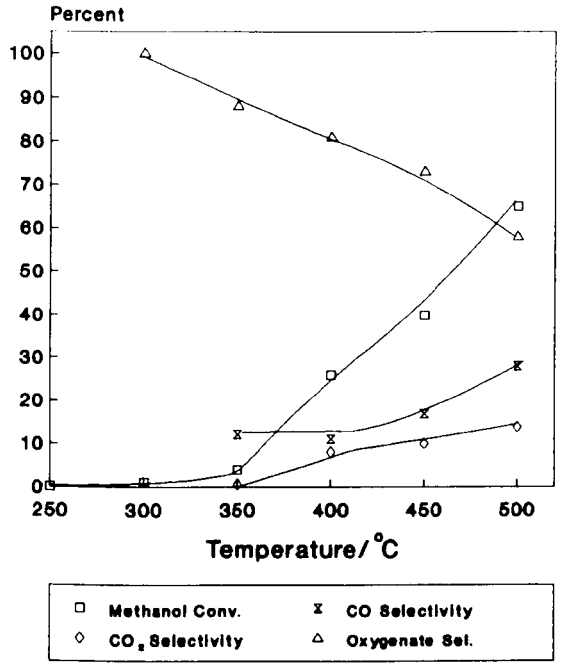

Methanol oxidation over Tb_4O_7

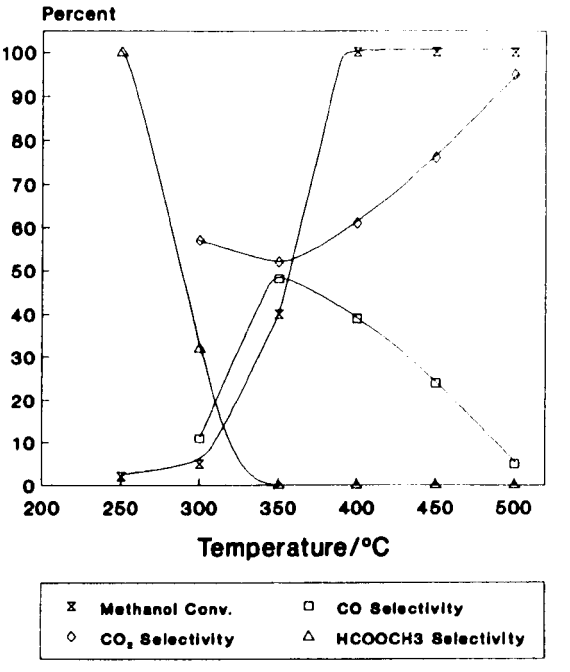

Methanol oxidation over V_2O_5

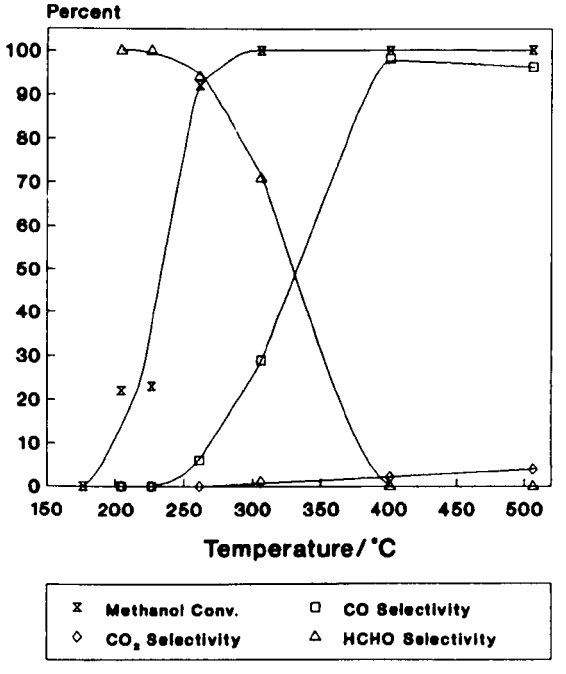

Methanol oxidation over WO_3

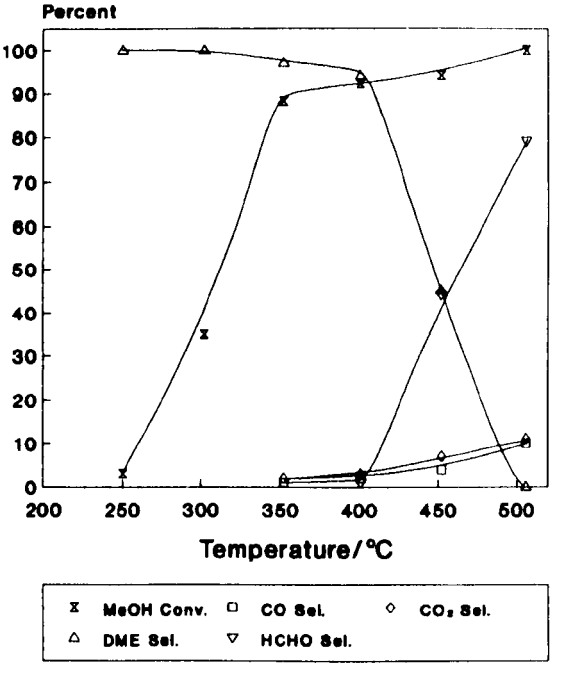

Methanol oxidation over Y_2O_3

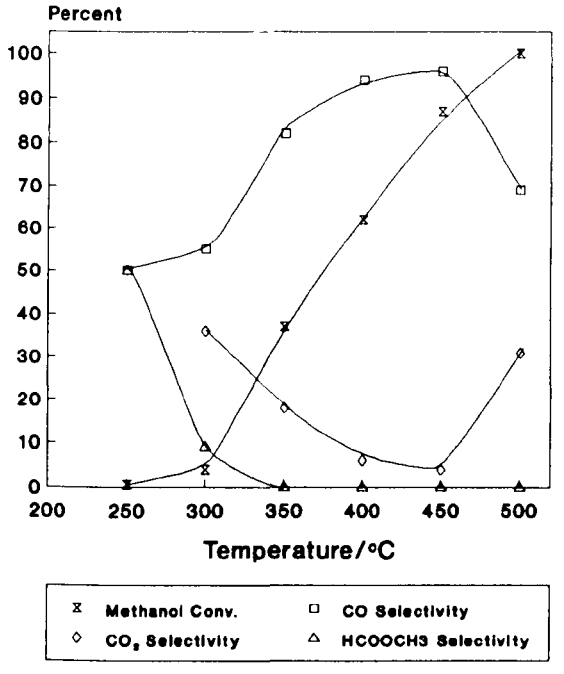

Methanol oxidation over Yb_2O_3

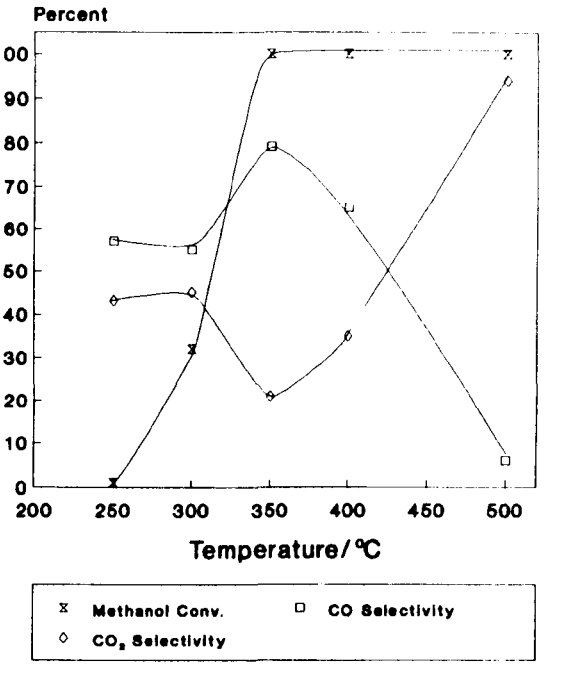

Methanol oxidation over ZnO

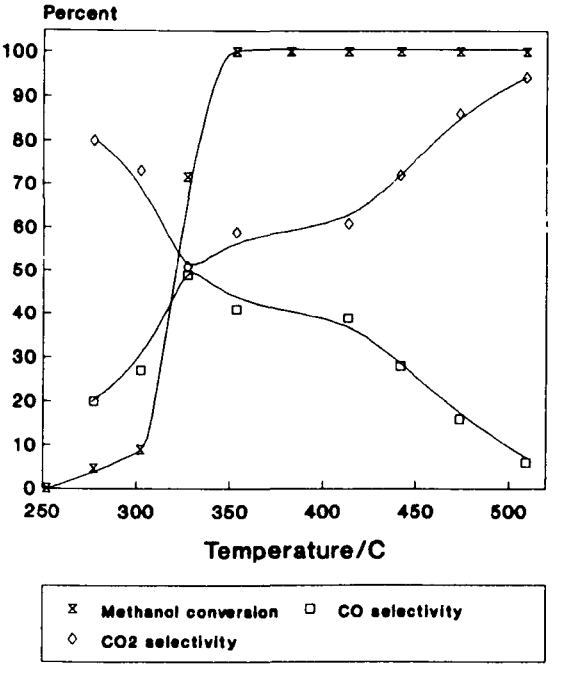

Methanol oxidation over ZrO_2

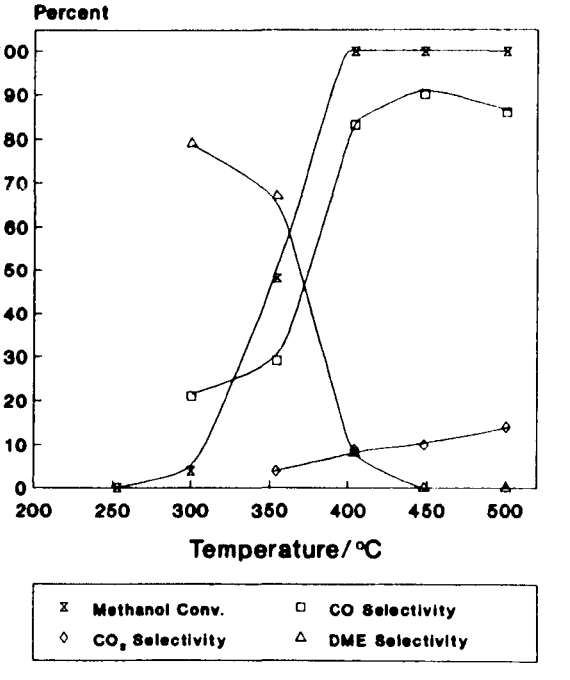

APPENDIX C

FIGURES FOR METHANE DEUTERIUM EXCHANGE

CH4/D2 exchange over Al2O3

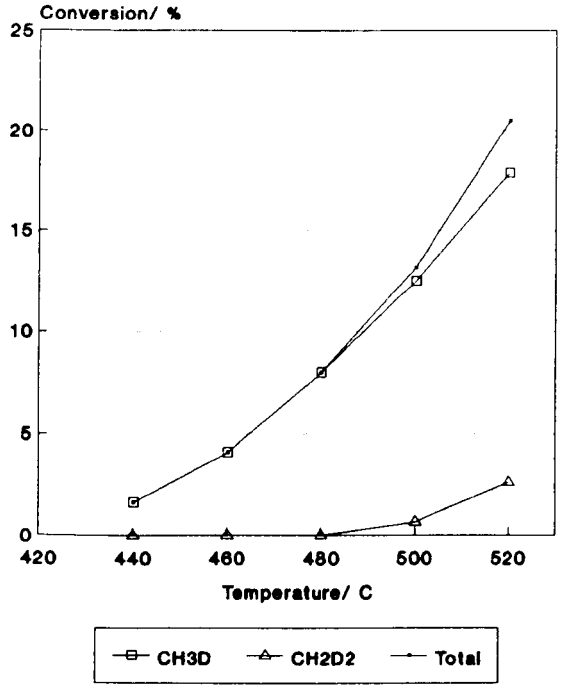

CH4/D2 exchange over CaO

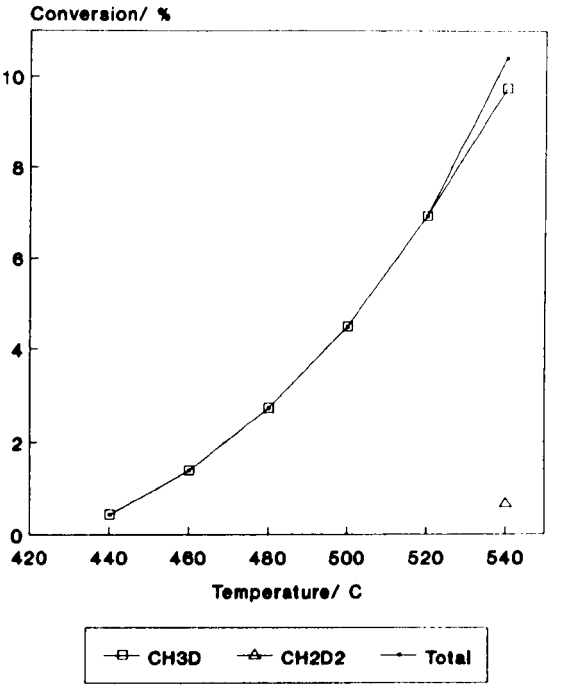

CH4/D2 exchange over CeO2

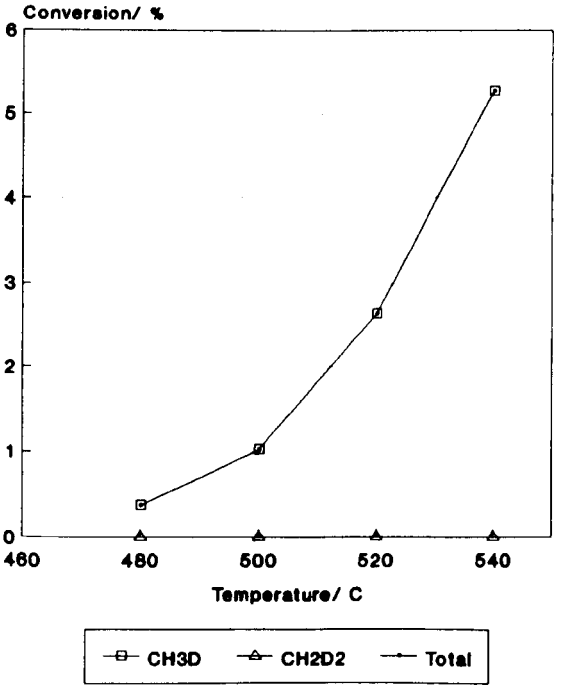

CH4/D2 exchange over Cr2O3

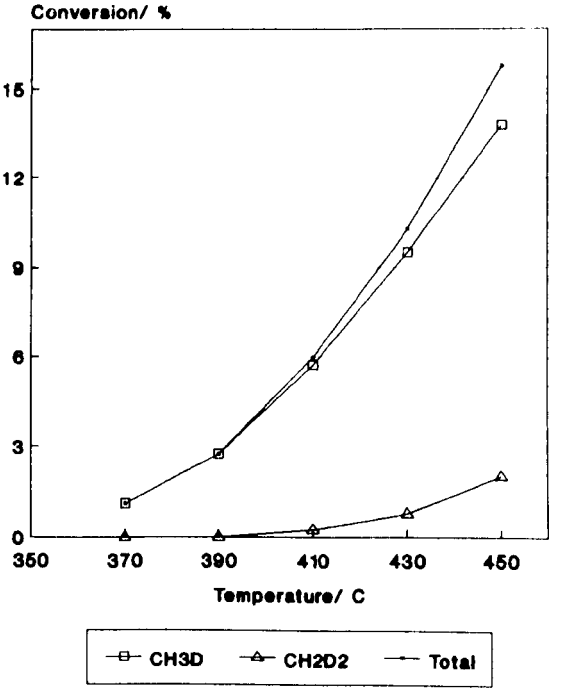

CH4/D2 exchange over Fe2O3

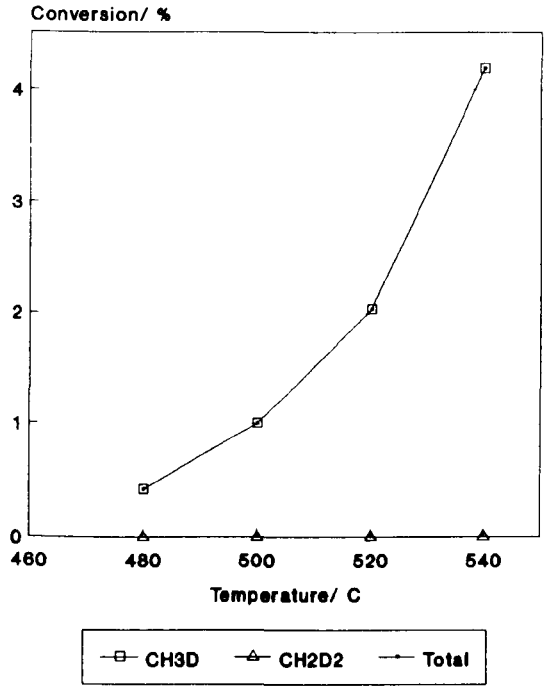

CH4/D2 exchange over Ga2O3

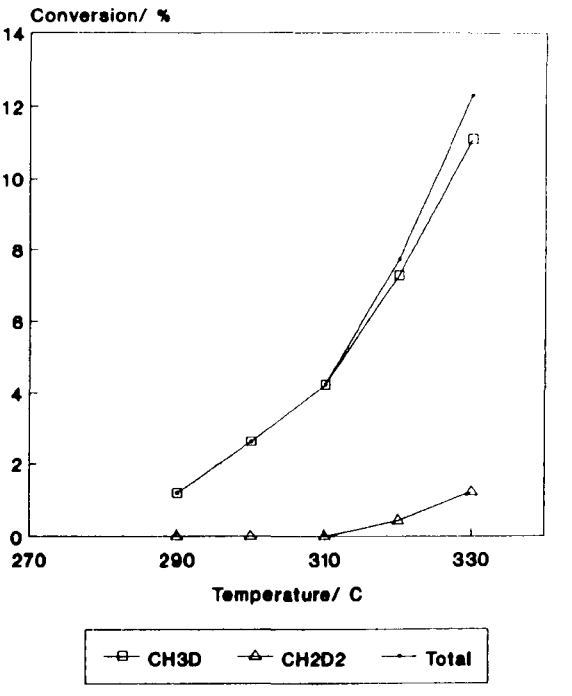

CH4/D2 exchange over Gd2O3

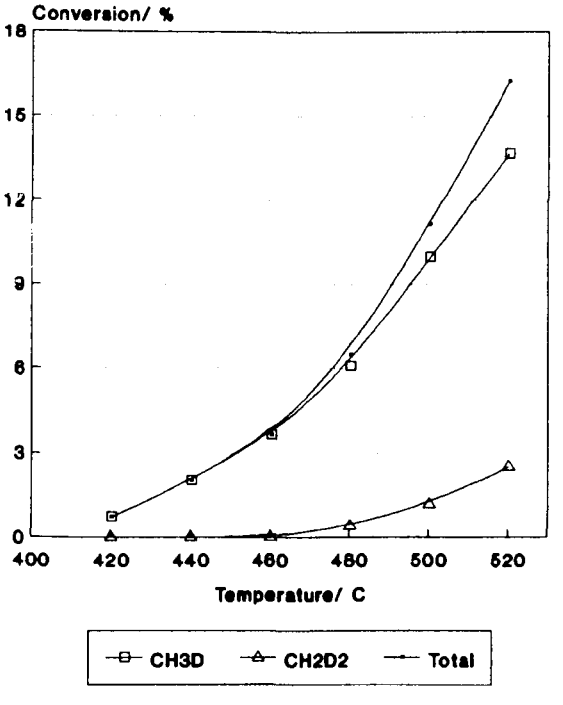

CH4/D2 exchange over La2O3

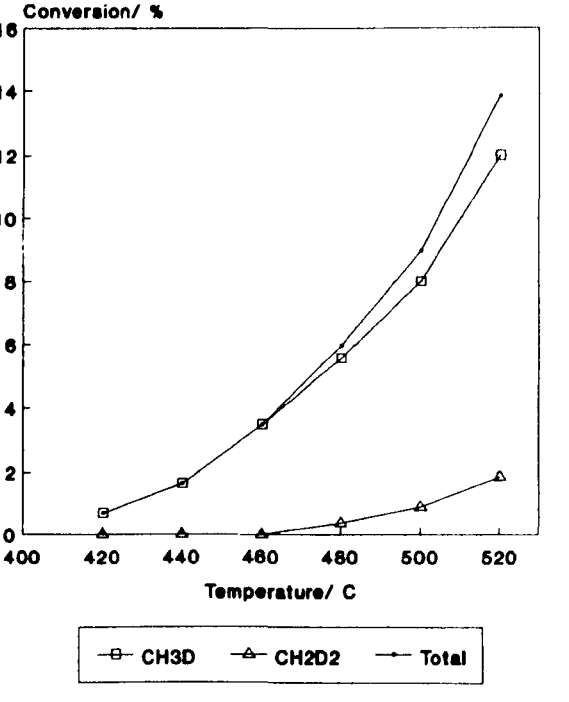

CH4/D2 exchange over MgO

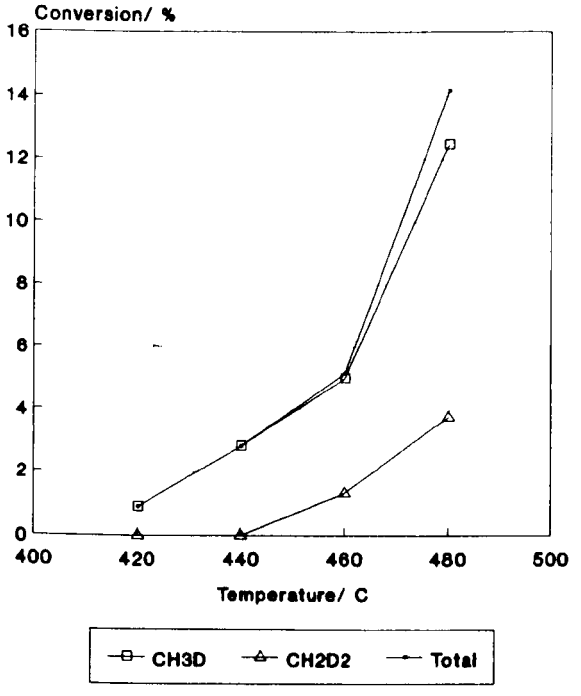

CH4/D2 exchange over MnO

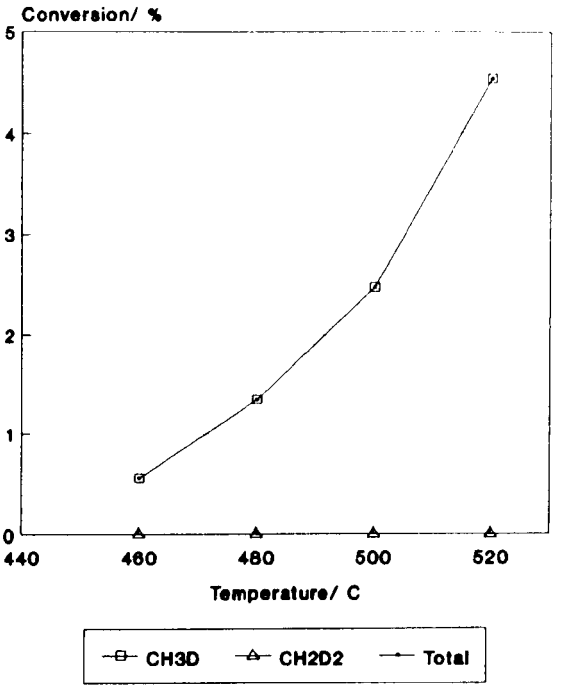

CH4/D2 exchange over Nd2O3

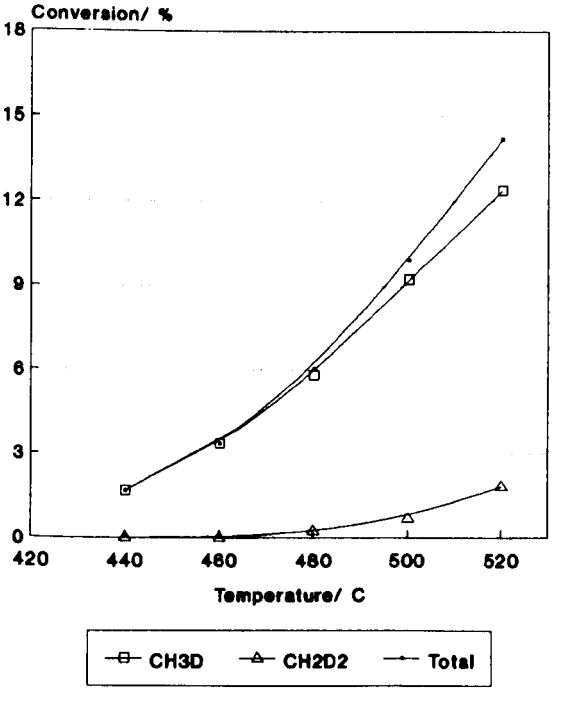

CH4/D2 exchange over Pr6O11

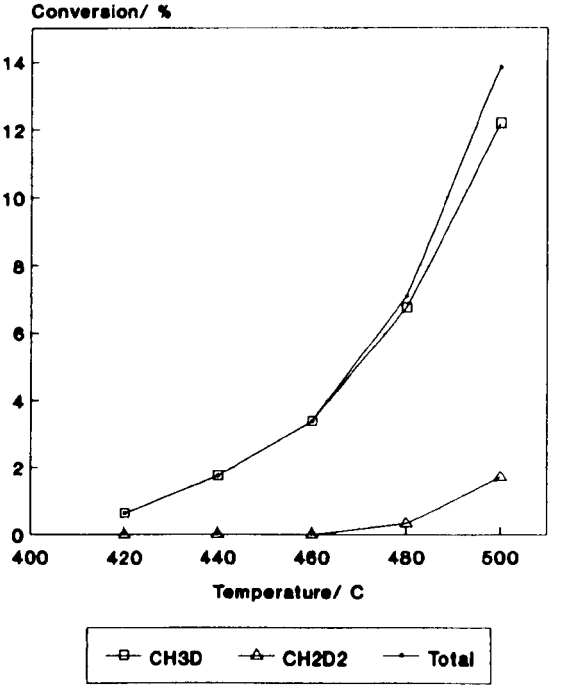

CH4/D2 exchange over Sm2O3

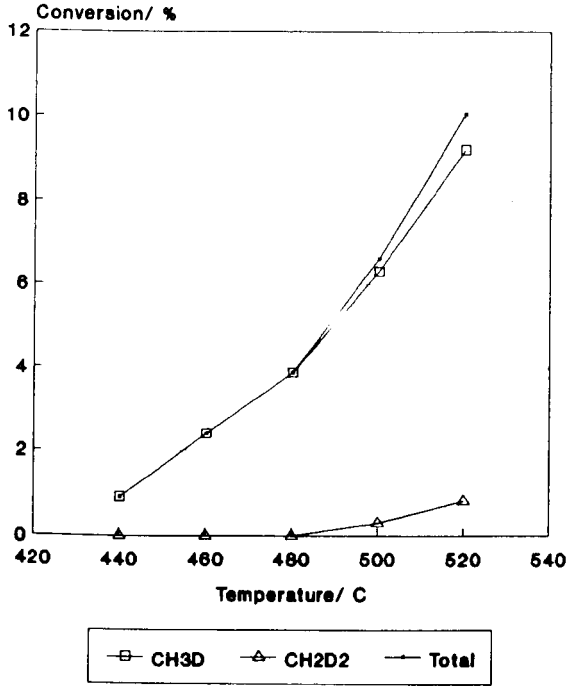

CH4/D2 exchange over TiO2

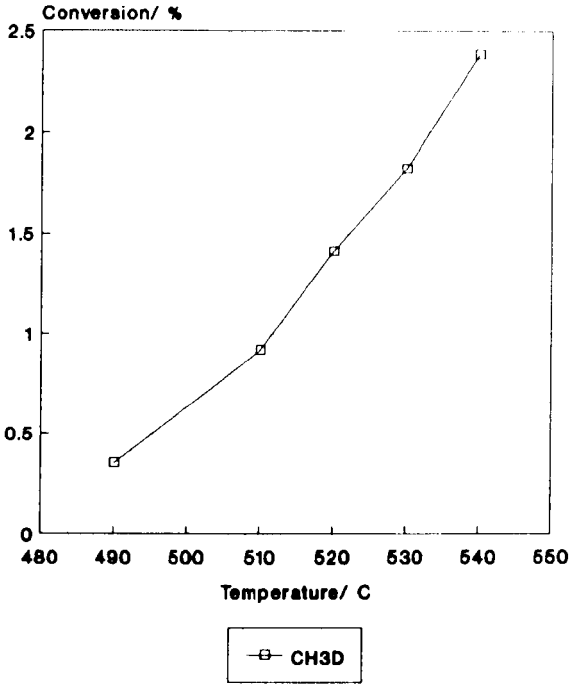

Arrhenius plot for V2O5

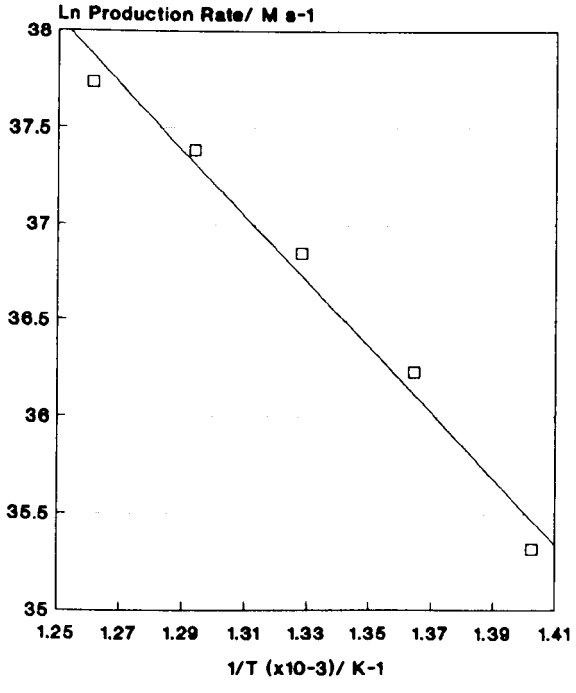

CH4/D2 exchange over Yb2O3

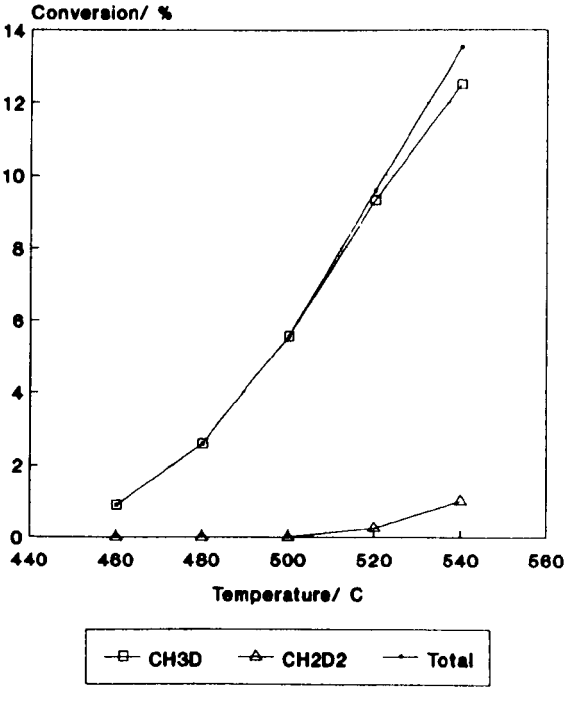

CH4/D2 exchange over ZnO

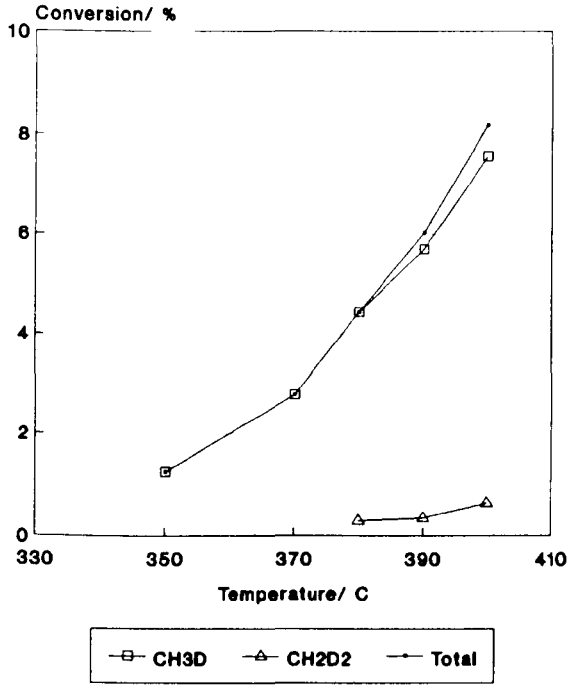

CH4/D2 exchange over ZrO2

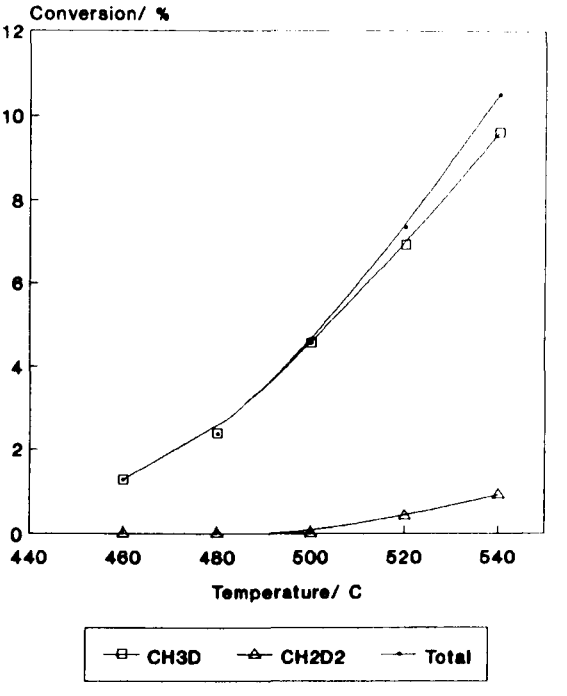

APPENDIX D

RESULTS TABLES FOR METHANE PARTIAL OXIDATION

Table D.1. CH_4 partial oxidation results over MoO_3.

Temp./°C	% Conversion		% Selectivity			
	CH_4	O_2	CH_3OH	CO	CO_2	C_2H_6
350	0	0	-	-	-	-
399	0	0	-	-	-	-
425	0.3	0.4	13	70	17	-
450	1.0	15.9	7	75	18	-
475	1.1	16.1	-	77	23	-
500	1.2	8.5	-	70	25	5

Table D.2. CH_4 partial oxidation results over Ga_2O_3.

Temp./°C	% Conversion		% Selectivity			
	CH_4	O_2	CH_3OH	CO	CO_2	C_2H_6
350	0	0	-	-	-	-
400	0.2	2.8	-	-	100	-
425	0.4	6.1	-	4	96	-
450	1.4	21.0	3	27	68	2
500	3.1	41.0	-	28	70	2
550	3.2	41.0	-	33	64	3

Table D.3. CH_4 partial oxidation results over $ZnMoO_4$.

Temp./°C	% Conversion%					Selectivity
	CH_4	O_2	CH_3OH	CO	CO_2	C_2H_6
350	0	0	-	-	-	-
400	tr	4.9	-	-	100	-
450	0.4	6.3	-	26	74	-
475	2.6	46.3	-	75	25	-
500	3.6	47.3	-	64	44	2
550	4.5	64.1	-	25	72	3

Table D.4. CH_4 partial oxidation results over Ga_2O_3/MoO_3.

Temp./°C	% Conversion		% Selectivity			
	CH_4	O_2	CH_3OH	CO	CO_2	C_2H_6
300	0	0	-	-	-	-
351	tr	1.5	-	-	100	-
402	0.2	4.9	-	14	86	-
460	3.0	47.1	22	50	27	1
502	3.1	43.9	-	62	33	5
552	3.1	42.9	-	28	68	4

Table D.5. CH_4 partial oxidation results in empty tube.

Temp./°C	% Conversion		% Selectivity			
	CH_4	O_2	CH_3OH	CO	CO_2	C_2H_6
350	0	0	-	-	-	-
400	0	0	-	-	-	-
450	8.1	99.6	29	63	7	-
500	8.0	100	19	68	7	6
550	8.3	100	17	69	7	7

Table D.6. CH_4 oxidation results over quartz chips.

Temp./°C	% Conversion		% Selectivity			
	CH_4	O_2	CH_3OH	CO	CO_2	C_2H_6
350	0	0	-	-	-	-
400	tr	0	-	-	100	-
450	0.1	8.5	-	-	100	-
475	3.5	49.1	15	70	13	2
500	3.7	52.8	12	68	17	3
550	4.0	92.7	8	62	26	4

REFERENCES

[1] N.R. Foster, Appl. Catal., 1895, 19, pp1-11.

[2] R. Pitchai, K. Klier, Catal. Rev. Sci. Eng., 1986, 28, pp13-88.

[3] M.J. Brown, N.D. Parkyns, Catal. Today, 1991, 8, pp305-335.

[4] H.D. Gesser, N.R. Hunter, C.B. Prakash, Chem. Rev., 1985, 85, pp235-244.

[5] N.D. Parkyns, C.I. Warburton, J.D. Wilson, Catal. Today, 1993. 18, pp385-442.

[6] T.J. Hall, J.S.J. Hargreaves, G.J. Hutchings, R.W. Joyner, S.H. Taylor, accepted for publication in Fuel Processing Technology.

[7] H.D. Gesser, N.R. Hunter, Methane Conversion by Oxidative Processes - Fundamentals and Engineering Aspects, Ed. E.E. Wolf, Van Nostrand Reinhold Catalysis Series, 1992, pp403-425.

[8] G.C. Bond, Heterogeneous Catalysis Principles and Applications, Clarendon Press, Oxford, 2nd Edition 1987, p101.

[9] C.D. Chang, A.J. Silvestri, Chemtech, 1987, pp624-631.

[10] D.E. Ridler, M.V. Twigg, Catalysis Handbook, Ed. M.V. Twigg, Wolfe Publishing, London, 2nd Edition, 1989, pp225-282.

[11] G.C. Chinchen, K. Mansfield, M.S. Spencer, Chemtech, 1990, pp692-699.

[12] C.N. Satterfield, Heterogeneous Catalysis in Industrial Practice, McGraw Hill, 2nd Edition, 1991, pp286-290.

[13] J.H. Edwards, N.R. Foster, Fuel Sci. and Tech. Int., 1986, 4, pp365-390.

[14] J.W.M.H. Geerts, J.H.B.J. Hoebink, K. Van der Wiele, Catal. Today, 1990, 6, pp613-620.

[15] H.D. Gesser, N.R. Hunter, L. Morton, U.S. Patent 4,618,732, (Oct 1986).

[16] D.A. Dowden, G.T. Walker, U.K. Patent 1,244,001, (Aug 1971).

[17] P.W. Atkins, Physical Chemistry, Oxford University Press, 3rd edition, 1987, p821.

[18] D. Lance, E.G. Elworthy, British Patent 7,297, (Mar 1906).

[19] D.M. Newitt, A.E. Haffner, Proc. Roy. Soc. London, 1932, 134A, pp591-604.

[20] D.M. Newitt, P. Szego, Proc. Roy. Soc. London, 1934, 147A, pp555-571.

[21] W.A. Bone, J.B. Gardener, Proc. Roy. Soc. London, 1936, 154A, pp297-328.

[22] D.M. Newitt, J.B. Gardener, Proc. Roy. Soc. London, 1936, 154A, pp329-335.

[23] R.G.W. Norrish, S.G. Foord, Proc. Roy. Soc. London, 1936, 157A, pp503-525.

[24] P.J. Wiezevich, P.K. Frolich, Ind. Eng. Chem., 1934, 26, pp267-276.

[25] E.H. Boomer, J.W. Broughton, Can. J. Res., 1937, 15B, pp375-400.

[26] E.H. Boomer, V. Thomas, Can. J. Res., 1937, 15B, pp401-413.

[27] E.H. Boomer, V. Thomas, Can. J. Res., 1937, 15B, pp414-433.

[28] M. Yu Smev, V.N. Korshak, O.V. Krylov, Russ. Chem. Rev., 1989, 58, p22.

[29] D.A. Dowden, C.R. Schnell, G.T. Walker, Proc. 4th Int. Congr. Catal., Moscow 1968, Paper 62, pp201-215.

[30] K. Otsuka, M. Hatano, J. Catal., 1987, 108, pp252-255.

[31] V. Amir-Ebrahimi, J.J. Rooney, J. Mol. Catal., 1989, 50, L17-22.

[32] J. Buiten, J. Catal., 1968, 10, pp188-199.

[33] T. Weng, E.E. Wolf, Prepr. Symp. Nat. Gas Upgrading II, 203rd National Meeting of the American Chemical Society, San Francisco, Apr 5-10, 1992, American Chemical Society, Washington D.C., 1992, pp46-50.

[34] T.Weng, E.E. Wolf, Appl. Catal., 1993, 96(A), pp383-396.

[35] V.A Durante, D.W. Walker, W.H. Seitzer, J.E. Lyons, Prepr. 3B Symp. on Methane Activation, Conversion and Utilisation, 1989 Int. Chem. Congr. of Pacific Basin Societies, 1989, pp23-26.

[36] J.E. Lyons, P.E Ellis Jr., V.A. Durante, Stud. Surf. Sci. and Catal., Eds. R.K. Graselli, A.W. Sleight, 1990, 67, pp99-116.

[37] V.A Durante, D.W Walker, S.M. Gussow, J.E. Lyons, U.S. Patent 4,918,249, (Apr. 1989).

[38] J.E. Huheey, Inorganic Chemistry, Principles of Structure and Reactivity, Harper Intenational, 3rd Edition, 1983, p861.

[39] J.G. DeWitt, J.G. Bentsen, A.G. Rosenzweig, B. Hedman, J. Green, S. Pilkington, G.C. Papeafthymiou, H. Dalton, K.O. Hodgson, S.J. Lippard, J. Am. Chem. Soc., 1991, 113, pp9219-9235.

[40] S. Betteridge, C.R.A. Catlow, D.H. Gay, R.W. Grimes, J.S.J. Hargreaves, G.J. Hutchings, R.W. Joyner, Q.A. Pankhurst, S.H. Taylor, Topics in Catalysis, 1994, 1, pp103-110.

[41] L.T. Weng, B. Delmon, Appl. Catal., 1992, 81(A), pp141-213.

[42] J.D. Burrington, C.T. Kartisch, R.K. Grasselli, J. Catal., 1984, 87, pp363-

[43] H.F. Stroud, UK. Patent 1,398,385, (Jun 1975).

[44] G.N. Kastanas, G.A. Tsigdinos, J. Schwank, J. Chem. Soc., Chem Commun., 1988, pp1298-1300.

[45] M.R. Smith, U.S. Ozkan, J. Catal., 1993, 141, pp124-139.

[46] K. Otsuka, Y. Weng, I. Yamanaka, A. Morikawa, J. Chem. Soc. Faraday Trans., 1993, 89, pp4225-4230.

[47] K. Otsuka, Y. Weng, J. Catal., 1994, 24, pp85-94.

[48] R.S. Liu, M. Iwamoto, J.H. Lunsford, J. Chem. Soc. Chem. Commun., 1982, pp78-79.

[49] H.F. Liu, R.S. Liu, K.Y. Liew, R.E. Johnson, J.H. Lunsford, J. Am. Chem. Soc., 1984, 106, pp4117-4121.

[50] M.M. Khan, G.A. Somorjai, J. Catal., 1985, 91, pp263-271.

[51] N.D. Spencer, J. Catal., 1988, 109, pp187-197.

[52] N.D. Spencer, C.J. Pereira, R.K. Grasselli, J. Catal., 1990, 126, pp546-554.

[53] E. MacGiolla Coda, E. Mulhall, R. van Hoek, B.K. Hodnett, Catal. Today, 1989, 4, pp383-387.

[54] E. MacGiolla Coda, M. Kennedy, J.B. McMonagle, B.K Hodnett, Catal. Today, 1990, 6, pp559-566.

[55] M. Kennedy, A. Sexton, B. Kartheuser, E. MacGiolla Coda, J.B. McMonagle, B.K. Hodnett, Catal. Today, 1992, 13, pp447-454.

[56] M.A. Banares, J.L.G. Fierro, J.B. Moffat, J. Catal., 1993, 142, pp406-417.

[57] Y. Barbaux, A.R. Elamrani, E. Payen, L. Gengembre, J.O. Bonnelle, B. Gryzbowska, Appl. Catal., 1988, 44, pp117-132.

[58] S. Kasztelan, E. Payen, J.B. Moffat, J. Catal., 1988, 112, pp320-324.

[59] M.R. Smith, L. Zhang, S.A. Driscoll, U.S. Ozkan, Catal. Lett., 1993, 19, pp1-15.

[60] H.M. Ismail, M.I. Zaki, G.C. Bond, R. Shukri, Appl. Catal., 1991, 72, L1-L12.

[61] M.A. Banares, N.D. Spencer, M.D. Jones, I.E. Wachs, J. Catal., 1994, 146, pp204-210.

[62] M.A. Banares, I. Rodriquez-Ramos, A. Guerrero-Ruiz, J.L.G. Fierro, New Frontiers in Catalysis, Proc. 10th Int. Cong. Catal., Ed. L. Guczi, Budapest 1992, pp1131-1144.

[63] R. Mauti, C.A. Mimms, Catal. Lett., 1993, 21, pp201-207.

[64] K.J. Zhen, M.M. Khan, K.B. Lewis, G.A. Somorjai, J. Catal., 1985, 94, pp501-507.

[65] N.D. Spencer, C.J. Pereira, J. Catal., 1989, 116, pp399-406.

[66] S.Y. Chen, D. Wilcox, Ind. Eng. Chem. Res., 1993, 32, pp584-587.

[67] B. Kartheuser, B.K. Hodnett, J. Chem. Soc., Chem. Commun., 1993, pp1093-1094.

[68] M. Inomato, A. Miyamoto, Y. Murakami, J. Phys. Chem., 1981, 85, pp2372-2377.

[69] B. Kartheuser, B.K. Hodnett, H. Zanthoff, M.A. Baerns, Catal. Lett., 1993, 21, pp209-214.

[70] M.M. Koranne, J.G. Goodwin Jr., G. Marcelin, J. Catal., 1994, 148, pp378-387.

[71] A. Parmaliana, F. Frusteri, A. Mezzapica, M.S. Scurrell, N. Giordano, J. Chem. Soc., Chem. Commun., 1993, pp751-753.

[72] D. Miceli, F. Arena, A. Parmaliana, M.S. Scurrell, V. Sokolovskii, Catal. Lett., 1993, 18, pp283-288.

[73] M.D. Amiridis, J.E. Rekoske, J.A. Dumesic, D.F. Rudd, N.D. Spencer, C.J. Pereira, J. AIChE., 1991, 37, pp87-97.

[74] S. Kasztelan, J.B. Moffat, J. Chem. Soc., Chem Commun., 1987, pp1663-1664.

[75] G.N. Kastanas, G.A. Tsigdinos, J. Schwank, Appl. Catal., 1988, 44, pp33-51.

[76] A. Parmaliana, F. Frusteri, D. Miceli, A. Mezzapica, M.S. Scurrell, Appl. Catal., 1991, 78, L7-L12.

[77] Q. Sun, R.G. Herman, K. Klier, Catal. Lett., 1992, 16, pp251-261.

[78] T. Kobayashi, K. Nakagawa, K. Tabata, M. Haruta, J. Chem. Soc., Chem. Commun., 1994, pp1609-1610.

[79] J.W. Chun, R.G. Anthony, Ind. Eng. Chem. Res., 1993, 32, pp259-263.

[80] J.S.J. Hargreaves, G.J. Hutchings, R.W. Joyner, Nature, 1990, 348, pp428-429.

[81] M. Yu Sinev, S. Setiadi, K. Otsuka, Mendeleev Commun., 1993, pp10-11.

[82] K.J. Zhen, C.W. Teng, Y.L. Bi, React. Kinet. Catal. Lett., 1987, 34, pp295-301.

[83] Z. Sojka, R.G. Herman, K. Klier, J. Chem. Soc., Chem. Commun., 1991, pp185-186.

[84] J.R. Anderson, P. Tsai, J. Chem. Soc., Chem. Commun., 1987, pp1435-1436.

[85] S. Kowalak, J.B. Moffat, Appl. Catal., 1988, 36, pp139-145.

[86] M.A. Banares, B. Pawelec, J.L.G. Fierro, Zeolites, 1992, 12, pp882-888.

[87] K. Otsuka, T. Komatsu, K. Jinno, Proc. 9th Int. Congr. Catal., Eds. M.J. Phillips, M. Ternman, Calgary 1988, 2, pp915-922.

[88] Q. Sun, J.I. Di Cosimo, R.G. Herman, K. Klier, M.M. Bhasin, Catal. Lett., 1992, 15, pp371-376.

[89] T. Suzuki, K. Wada, M. Shima, Y. Watanabe, J. Chem. Soc., Chem. Commun., 1990, pp1059-1060.

[90] K. Wada, K. Yoshida, Y. Watanabe, T. Suzuki, J. Chem. Soc., Chem. Commun., 1991, pp726-727.

[91] C.F.R. Lund, Catal. Lett., 1992, 12, pp395-404.

[92] W.A. Dietz, J. Gas Chromat., 1967, pp68-71.

[93] V.H. Dibeler, F.H. Mohler, J. Res. Natl. Bur. Std., 1950 , 45, pp411-444.

[94] F.H. Mohler, V.H. Dibeler, E. Quinn, J. Res. Natl. Bur. Std., 1958, 61, pp171-172.

[95] L.P. Hill, M.L. Vestal, J.H. Futrell, J. Chem. Phys., 1971, 54, pp3835-3845.

[96] Sample preparation Methods in X-ray Powder Diffraction, JCPDS Data Collection and Analysis Subcommittee, ICDD, Swathmore U.S.A., Ed R. Jenkins, 1989.

[97] Powder Diffraction File, JCPDS International Centre for Diffraction Data, ICDD, Swathmore U.S.A., sets 1-42, 1992.

[98] S. Brunauer, P.H. Emmett, E. Teller, J. Am. Chem. Soc., 1938, 60, pp309-319.

[99] International Union of Pure and Applied Chemistry, Physical Chemistry Division, Commission on Collide and Surface Chemistry, Pure and Appl. Chem., 1985, 57, pp603-619.

[100] C.D. Wagner, W.I. Riggs, L.E. Davis, J.F. Moulder, G.E. Muilenberg, Handbook of photoelectron spectroscopy, Perkin-Elmer Corporation, Minnesota, 1978, p17.

[101] Practical Surface Analysis by Auger and X-ray Photoelectron Spectroscopy, Ed. D. Briggs, M.P. Seah, John Wiley and Sons Ltd., 1983, pp511-514.

[102] K.M. Tawarah, R.S. Hansen, J. Catal., 1984, 87, pp305-318.

[103] J.M. Vohs, M.A. Barteau, Surface Sci., 1986, 76, pp91- .

[104] K. Yamashita, S. Naito, K. Tamaru, J. Catal., 1985, 94, pp353-359.

[105] R.O. Kagel, J. Phys. Chem., 1967, 71, pp844-850.

[106] A. Iimura, Y. Inoue, I. Yasmouri, Bull. Chem. Soc. Jpn., 1983, 56, pp2203-2207.

[107] J. Carrigosa, G. Munuera, S. Castanar, J. Catal., 1977, 44, pp265- .
[108] C.J. Machiels, W.H. Cheng, U. Chowdhry, W.E. Farneth, F. Hong, E.M. McCarron, A.W. Sleight, Appl. Catal, 1986, 25, pp249-256.

[109] S.K. Bhattacharyya, K. Janakiram, N.D. Ganguly, J. Catal., 1967, 8, pp128-136.

[110] R.W. McCabe, P.J. Mitchell, Appl. Catal., 1986, 27, pp83-98.

[111] U.S. Ozkan, R.F. Kueller, E. Moctezuma, Ind. Eng. Chem. Res., 1990, 29, pp1136-1142.

[112] G. Busca, V. Lorenzelli, G. Ramis, R.J. Wiley, Langmuir, 1992, 9, pp1492-1499.

[113] H. Schafer, R. Gruehn, F. Schulte, Agnew. Chem. Internat. Edit., 1966, 5, pp40-52.

[114] B.G. Hyde, E.E. Garver, U.E. Kuntz, L. Eyring, J. Phys. Chem., 1965, 69, pp1667-1675.

[115] F.A. Cotton, G. Wilkinson, Advanced Inorganic Chemistry, John Wiley and Sons, 5th Edition 1988, p654.

[116] N. Abadjieva, J. Pesheva, D. Klissurski, C. Centi, F. Triffiro, Proc. 6th Int. Symp. Heterogeneous Catalysis, Sofia, 1987, Part 1, pp444-449.

[117] K. Tanabe, Catalysis by Acids and Bases, Studies in Surface Science and Catalysis, Eds. B. Imelik, C. Naccache, G. Coudurier, Y. Ben Taarit, J.C. Vedrine, Elsevier Science Publishers BV, 1985, 20, pp1-14.

[118] M. Ai. J. Catal., 1982, 77, pp279-288.

[119] A.I. Vogel, A Textbook of Practical Organic Chemistry, Longman Green and Co., London, 2nd Edition 1951, p316.

[120] T. Moeller, H.E. Kremers, Chem. Rev., 1945, 37, pp97-159.

[121] H. Pines, W.O. Haag, J. Am. Chem. Soc., 1960, 82, pp2471-2483.

[122] M.C. Kung, W.H. Cheng, H.H. Kung, J. Phys. Chem., 1979, 83, pp1737-

[123] H.H. Kung, Transition Metal Oxides: Surface Chemistry and Catalysis, Studies in Surface Science and Catalysis, Elsevier Science Publishers BV, 1989, 45, p176.

[124] J. Edwards, J. Nicoladis, M.B. Cutlip, C.O. Bennett, J. Catal., 1977, 50, pp24-34.

[125] H.H. Kung, Transition Metal Oxides: Surface Chemistry and Catalysis, Studies in Surface Science and Catalysis, Elsevier Science Publishers BV, 1989, 45, pp12-14.

[126] F.A. Cotton, G. Wilkinson, Advanced Inorganic Chemistry, John Wiley and Sons, 5th Edition 1988, p808.

[127] J. Allison, W.A. Goddard, J. Catal., 1985, 92, pp127-135.

[128] R.P. Groff, J. Catal., 1984, 86, pp215-218.

[129] C.J. Machiels, A.W. Sleight, Proc. 4th Int. Conf. Chem. and Uses of Molybdenum, Ed. H.F. Bury, P.C.H. Mitchell, 1982, pp411-414.

[130] M. Ai, J. Catal, 1978, 54, pp426-435.

[131] J.M. Jehng, I.E. Wachs, Catal. Today, 1993, 16, pp417-426.

[132] E.R.S Winter, J. Phys. Chem. (A), 1968, pp2289-2902.

[133] E.R.S. Winter, J. Phys. Chem. (A), 1969, pp1832-1835.

[134] G.K. Boreskov, Disc. of the Faraday Soc., 1966, 41, pp263-276.

[135] D.G. Klissurski, Proc. 4th Int. Congr. on Catalysis, Moscow, 1968, paper 36, pp477-495.

[136] G.K. Boreskov, Adv. Catal., 1964, 15, pp285-339.

[137] A. Maltha, V. Ponec, Catal. Today, 1993, 17, pp419-425.

[138] A. Frennet, Catal. Rev., 1975, 10, pp37-68.

[139] K. Morikawa, W.S. Benedict, H.S. Taylor, J. Am. Chem. Soc., 1936, 58, pp1445-1449.

[140] C. Kemball, Adv. Catalysis, 1959, 11, pp223-262.

[141] P.J. Robertson, M.S. Scurrell, C. Kemball, Trans Faraday Soc., 1975, 71, pp903-912.

[142] J.G. Larson, W.K. Hall, J. Phys. Chem., 1965, 69, pp3080-3089.

[143] R.L. Burwell Jr., A.B. Littlewood, M. Cardew, G. Pass, C.T.H. Stoddart, J. Am. Chem. Soc., 1962, 82, pp6272-6280.

[144] R.L. Burwell Jr. and co workers, papers II-IV, J. Am. Chem. Soc., 1962, 82, pp6281-6291.

[145] M. Utiyama, H. Hattori, K. Tanabe, J. Catal., 1978, 53, pp237-242.

[146] R. Bird, C. Kemball, H.F. Leach, J. Catal., 1987, 107, pp424-433.

[147] P.J. Robertson, M.S. Scurrell, C. Kemball, J. Chem. Res. Miniprints, 1977, 0501-0516.

[148] M.M. Haliday, C. Kemball, H.F. Leach, M.S. Scurrell, Proc. 6th Int. Congr. Catalysis, London, 1976, Vol. 1, pp283-290.

[149] R.C. Hansford, P.G. Waldo, L.C. Drake, R.E. Honig, Ind. Eng. Chem., 1952, 44, pp1108-1113.

[150] H.H. Kung, Transition Metal Oxides: Surface Chemistry and Catalysis, Studies in Surface Science and Catalysis, Elsevier Science Publishers BV, 1989, 45, p55.

[151] G.A. Park, Chem. Rev., 1965, 65, pp177-198.

[152] G.A. Park, Adv. Chem. Series, 1967, 61, p121.

[153] K. Tanabe, Catalysis Science and Technology, Ed. J.R. Anderson, M. Boudart, Springer-Verlag, 1981, 2, pp231-273.

[154] H. Kobayashi, M. Yamaguchi, T. Ito, Acid-Base Catalysis, Eds. K. Tanabe, H. Hattori, T. Yamaguchi, T. Tanaka, Proc. Int. Symp. Acid-Base Catalysis, Sapporo 1988, VCH Publishers (UK), 1989, pp139-146.

[155] T. Ito, T. Watanabe, M. Kawasaki, K. Toi, H. Kobayashi, Acid-Base Catalysis, Eds. K. Tanabe, H. Hattori, T. Yamaguchi, T. Tanaka, Proc. Int. Symp. Acid-Base Catalysis, Sapporo 1988, VCH Publishers (UK), 1989, pp483-490.

[156] V.D. Sokolovskii, S.M. Aliev, O.V. Buyevskaya, A.D.. Davidov, Catal Today, 1989, 4, pp293-300.

[157] T. Ito, W. Ji-Xiang, L. Chiu-Hsun, J.H. Lunsford, J. Am. Chem. Soc., 1985, 107, pp5062-5068.

[158] M. Yu Sinev, V.N. Korchak, O.V. Krylov, Kinet. Katal., 1986, 27, pp1277-

[159] C.R. Adams, T.J. Jennings, J. Catal., 1963, 2, pp63-68.

[160] R. Gonzalez-Luque, I. Nebot-Gil, F. Tomas, Chem. Phys. Let., 1984, 104, pp203-209.

[161] D.L Harrison, D. Nicholls, H. Steiner, J. Catal., 1967, 7, pp359-364.

[162] G. Neumann, Non-Stoichiometric and Defect Structures, in Current Topis in Material Science, Ed. E. Kaldis, New York, 1981, 7, pp153-168.

[163] S.D Robertson, B.D. McNicol, J.H. de Baas, S.C. Kloet, J.W. Jenkins, J. Catal., 1975, 37, pp424-431.

[164] D.A. Dowden, N. McKenzie, B.M.W. Trapnell, Proc. Roy. Soc. London, 1956, A237, pp245-254.

[165] G.M. Dixon, D. Nicholls, H. Steiner, Proc. 3rd Int. Congr. Catalysis, Amsterdam, 1965, 1, pp815-828.

[166] H.H. Kung, Transition Metal Oxides: Surface Chemistry and Catalysis, Studies in Surface Science and Catalysis, Elsevier Science Publishers BV, 1989, 45, p63.

[167] G.B. Peri, J. Phys. Chem., 1965, 69, pp211-219.

[168] R.P. Eischens, W.I. Pliskin, M.J.D. Low, J. Catal., 1962, 1, pp180-191.

[169] G.C. Bond, Heterogeneous Catalysis Principles and Applications, Clarendon Press, Oxford, 2nd Ediiton, 1987, p55.

[170] A.K. Galway, Adv. Catalysis, 1977, 26, pp247-322.

[171] D.W McKee, Trans. Faraday Soc., 1965, 61, pp2273-2283.

[172] D.W McKee, J. Phys. Chem., 1966, 70, pp525-530.

[173] O.V. Krylov, A.A. Firsova, A.A. Bobyshev, V.A. Radtsig, D.P. Shashkin, L.Ya Margolis, Catal. Today, 1992, 13, pp381-390.

[174] L.A. Morton, N.R. Hunter, H.D. Gesser, Morton 1984; reference from The Direct Conversion of Methane to Methanol (DMTM), H.D. Gesser, N.R. Hunter; in Methane Conversion by Oxidative Processes - Fundamentals and Engineering Aspects, Ed. E.E. Wolf, Van Nostrand Reinhold Catalysis Series, 1992, pp403-425.

[175] M.J. Foral, Prepr. Symp. Nat. Gas Upgrading II, 203rd National Meeting of the American Chemical Society, San Francisco, Apr 5-10, 1992, American Chemical Society, Washington D.C., 1992, pp34-39.

[176] P.F. Casey, T. McAllister, K. Foger, Ind. Eng. Chem. Res., 1994, 33, pp1120-1125.

[177] C.S.G. Phillips, R.J.P. Williams, in Inorganic Chemistry Volume 1, Oxford University Press, 1st Edition, 1965, p374.

[178] H.P. Klug, L.E. Alexander, X-ray Diffraction Procedures, John Wiley and Sons Ltd., New York, 1954, p491.

[179] Practical Surface Analysis by Auger and X-ray Photoelectron Spectroscopy, Eds D. Briggs, M.P. Seah, John Wiley and Sons Ltd., 1983, p16.

[180] T.A. Patterson, J.C. Carver, D.E. Leyden, D.M. Hercules, J. Phys. Chem., 1976, 80, pp1700-1708.

[181] S.O. Grim, L.J. Matienzo, Inorg. Chem., 1975, 14, pp1014-1018.

[182] K.S. Kim, J. Electron Spectros., 1974, 5, p362.

[183] W.W. Swartz Jr., D.M. Hercules, Anal. Chem., 1971, 43, p1774.

[184] E.L. Aptekar, M.G. Chadinov, A.M. Alekseev, O.V. Krylov, React. Kinet. Catal. Lett., 1974, 1, pp493-498.

[185] C. Battistoni, J.L Dorman, D Fiorani, E. Paparazzo, S. Viticoli, Solid State Commun., 1981, 39, pp581-585.

[186] J.D. Lee, A New Concise Inorganic Chemistry, Van Nostrand Reinhold (UK), 3rd edition 1987, p31.

[187] T.R. Baldwin, R. Burch, G.D. Squire, S.C. Tsang, Appl. Catal., 1991, 74, pp137-152.

[188] R. Burch, G.D. Squire, S.C. Tsang, J. Chem. Soc., Faraday Trans. 1, 1989, 85, pp3561-3568.

[189] J. Kiwi, K. Ravindranthan Thampi, M. Gratzel, P. Albers, K. Siebold, J. Phys. Chem., 1992, 96, pp1344-1349.

[190] H.H. Kung, Transition Metal Oxides: Surface Chemistry and Catalysis, Studies in Surface Science and Catalysis Vol. 45, Elsevier Science Publishers BV, 1989, Chapter 11, pp169-199.

[191] P. Ruiz, B. Zhou, M. Remy, T. Machej, F. Aoun, B. Doumain, B. Delmon, Catal. Today, 1987, 1, pp181-

[192] V.D. Sokolovskii, Catal. Rev. Sci. Eng., 1990, 32, pp1-49.

[193] I. Matsuura, R. Schuit, K. Hirakwa, J. Catal., 1980, 63, pp152-166.

[194] Y. Tong, J.H. Lunsford, J. Am. Chem. Soc., 1991, 113, pp4741-4746.

[195] G.J. Hutchings, M.S. Scurrell, J.R. Woodhouse, Chem. Soc. Rev., 1989, 18, pp251-283.

[196] E.R.S. Winter, Adv. Catal., 1958, 10, pp196-241.